71-23,780

JONES, Daniel David, 1943-
POTENTIOMETRIC AND COMPUTER STUDIES OF ALBUMIN-ELECTROLYTE INTERACTIONS.

The University of Michigan, Ph.D., 1970
Chemistry, biological

University Microfilms, A XEROX Company, Ann Arbor, Michigan

THIS DISSERTATION HAS BEEN MICROFILMED EXACTLY AS RECEIVED

# POTENTIOMETRIC AND COMPUTER STUDIES OF ALBUMIN-ELECTROLYTE INTERACTIONS

by

Daniel David Jones

A dissertation submitted in partial fulfillment
of the requirements for the degree of
Doctor of Philosophy
(Biological Chemistry)
in The University of Michigan
1970

Doctoral Committee:

Associate Professor Gordon L. Nordby, Chairman
Professor William I. Higuchi
Associate Professor Donald E. Hultquist
Associate Professor Margaret J. Hunter
Professor J. Lawrence Oncley

ABSTRACT

POTENTIOMETRIC AND COMPUTER STUDIES
OF ALBUMIN-ELECTROLYTE INTERACTIONS

by

Daniel David Jones

Chairman: Gordon L. Nordby

One method which has been used for studying the interactions between proteins and electrolytes is the measurement of electromotive force (EMF) between electrodes immersed in solutions which differ in electrolyte activity. The interpretation of such EMF measurements in protein solutions is not straightforward, particularly at low ionic strength and at pH values removed from the isoionic point of the protein. This difficulty is exemplified by the discrepancies between salt binding to bovine plasma albumin inferred from EMF measurements (1) and that inferred from equilibrium dialysis (2) and from osmotic pressure measurements (1).

The present study was undertaken in order to elucidate the constraints imposed upon the design, performance, and interpretation of binding studies based on EMF measurements. The effects of ion-exchange membrane liquid junctions on EMF measurements were studied. An equation is derived which facilitates prediction of the EMF of a concentration cell with liquid junction from electrolyte and solvent transference numbers. Three methods of measuring

transference numbers in ion-exchange membrane cells were investigated: (1) the use of counterion-selective electrodes, (2) a modified Hittorf method, and (3) the EMF method. The transference numbers estimated from the EMF method were close to the limiting values for a liquid junction with ideal transference properties. The effects of several macromolecular solutes on the observed EMF of a KCl concentration cell with Ag-AgCl electrodes were studied. The EMF difference observed in the presence of dissolved dextran was opposite in sign to that observed in the presence of either dextran sulfate or colloidal silica. Amylose dissolved in 0.27 M KCl appeared to have no effect on the observed EMF.

Theoretical and experimental alternatives to the study of protein-electrolyte interaction by EMF measurement were investigated. The distribution of ions around a uniformly charged sphere was simulated with a digital computer. The distribution curves were obtained from a computer program which effects a numerical solution of the unlinearized Poisson-Boltzmann equation. A method is described for obtaining an estimate of the mean free ion concentrations from the ion distribution curves. Using this estimate and a specific definition of the protein component, the value of the ion-binding parameter was estimated for several aqueous mixtures of bovine plasma albumin and NaCl. These estimates agreed reasonably well with the corresponding values calculated from EMF measurements as long as the equivalent protein concentration was not more than about 20 per cent of the ionic strength. Under this condition, the effect of the charged protein on the free ion concentration as

determined by an electrode does not appear to be large. Ultrafiltration was investigated as an independent method of studying protein-electrolyte interactions.

## REFERENCES


1. Scatchard, G., Y.V. Wu, and A.L. Shen, J. Am. Chem. Soc., 81, 6104, (1959).

2. McMenamy, R.H., M.I. Madeja, and F. Watson, J. Biol. Chem., 243, 2328, (1968).

To my parents

and

to my wife

## ACKNOWLEDGEMENTS

I would like to thank Dr. Gordon L. Nordby for his thoughtful counsel and inspiring example during the course of this research. I am grateful to Dr. Margaret J. Hunter for her expert instruction in the techniques of protein chemistry and to Dr. J. L. Oncley for many helpful and illuminating discussions.

The assistance of many individuals at the Computing Center and in the Office of Research Administration is gratefully acknowledged.

Financial support for this research was provided in part by U. S. Public Health Service Predoctoral Fellowship GM-35,584, by National Institutes of Health Training Grant GM-00187, and by the Medical School Fund for Computing.

TABLE OF CONTENTS


Page

ACKNOWLEDGEMENTS . . . . . iii

LIST OF TABLES . . . . . viii

LIST OF ILLUSTRATIONS . . . . . x

ABBREVIATIONS . . . . . xi

I. INTRODUCTION . . . . . 1

Rationale . . . . . 1
Evidence of Protein-Electrolyte Interaction . . . . . 1
History of the Potentiometric Method . . . . . 3
The Teorell-Meyer-Sievers Theory . . . . . 4
Potentiometric Studies by Scatchard and Coworkers . . 4
Calibration Curves . . . . . 5
Non-thermodynamic Assumptions . . . . . 6
$Na^+$ Binding . . . . . 6
Effect of Protein on Ion Activity Coefficients . . . . . 7
Water Transference . . . . . 8
Ion-binding Models . . . . . 9
The Suspension Effect . . . . . 10
Statement of Purpose . . . . . 11

II. POTENTIOMETRIC STUDIES . . . . . 12

Derivation of Equations . . . . . 12
Experimental . . . . . 22
Electrolyte Solutions . . . . . 22
Albumin Solutions . . . . . 22
Amylose . . . . . 23
Dextrans . . . . . 23
Colloidal Silica . . . . . 24
Equilibrium Dialysis . . . . . 24
Carbohydrate Analysis . . . . . 25
Electrochemical Cells . . . . . 25
Ag-AgCl Electrodes . . . . . 30
Electrode Behavior in Albumin Solutions . . . . . 30
Collodion-coated Electrodes . . . . . 31
Ion-Exchange Membranes . . . . . 32
Water Content . . . . . 33

Page


Charge Capacity . . . . . 33
Titration Procedure . . . . . 34
Estimation of Equivalence Point . . . . . 34
Calculation . . . . . 35
EMF Measurements . . . . . 35
Solvent Transference Measurements . . . . . 37
Counterion-selective Electrodes . . . . . 37
Modified Hittorf Method . . . . . 38
Vertical Capillaries . . . . . 38
Horizontal Capillaries . . . . . 39
EMF Method . . . . . 39
Conductivity Measurements . . . . . 40
Results . . . . . 41
Ion-Exchange Membranes . . . . . 41
Water Content . . . . . 41
Charge Capacity . . . . . 41
Symmetry . . . . . 41
Solvent Transference . . . . . 41
Counterion-selective Electrodes . . . . . 41
Membrane in Various Anionic Forms . . . . . 41
Membrane in $NO_3^-$ Form . . . . . 44
Modified Hittorf Method . . . . . 49
Control Experiments Without Current Flow . . . 49
Measurements with Current Flow . . . . . 52
EMF Method . . . . . 52
Time Dependence . . . . . 52
Cation Transference Number . . . . . 57
Water Transference . . . . . 58
Effects of Macromolecular Solutes on Ag-AgCl Electrodes . . . . . 64
Polysaccharides . . . . . 64
Polyelectrolytes . . . . . 66
Discussion . . . . . 70
Solvent Transference . . . . . 70
Comparison with Previous Work . . . . . 70
Reproducibility of EMF Measurements . . . . . 71
Membrane Symmetry . . . . . 71
Membrane Heterogeneity . . . . . 72
Leaching . . . . . 72
Evaporation . . . . . 73
Electrical Heating Effect . . . . . 74
Pressure Variation . . . . . 75
Electrode Surface Strain . . . . . 75
Dissolution at the Electrode Surface . . . . . 75
Collodion Layer . . . . . 76
Solution Agitation . . . . . 77
Effects of Macromolecular Solutes on Ag-AgCl Electrodes . . . . . 81
Polysaccharides . . . . . 81
Polyelectrolytes . . . . . 82

Page

III. COMPUTER SIMULATION OF ION DISTRIBUTIONS AROUND CHARGED MACRO-IONS . . . . . 84

Introduction . . . . . 84
Theory . . . . . 84
The Poisson-Boltzmann Equation . . . . . 84
Transformation of Variables . . . . . 86
Methods . . . . . 89
Numerical Solution of the Poisson-Boltzmann Equation . . . . . 89
Wiersema's Method . . . . . 89
Truncation Error . . . . . 92
Calculation of Ion Distributions . . . . . 92
Interpolation . . . . . 92
Integration . . . . . 93
Calculation of Free Ion Concentrations . . . . . 95
Stoichiometric Estimate . . . . . 95
Estimation from Ion Distributions . . . . . 96
Protein Model . . . . . 96
Averaging Procedure . . . . . 97
Assumptions . . . . . 100
Results . . . . . 101
Computer Solution of Poisson-Boltzmann Equation . . 101
Application to Albumin Solutions . . . . . 101
Discussion . . . . . 111
Definition of the Protein Component . . . . . 111
$Cl^-$ Binding . . . . . 112
Conformational Changes . . . . . 113
Implications for EMF Measurements . . . . . 113

IV. ULTRAFILTRATION STUDY . . . . . 115

Introduction . . . . . 115
Methods . . . . . 116
Ultrafiltration . . . . . 116
Permeability Studies . . . . . 117
KCl Dry Weight Measurements . . . . . 117
Estimation of Protein Concentration . . . . . 118
Results . . . . . 120
Permeability to Water and KCl . . . . . 120
Permeability to Albumin . . . . . 120
Discussion . . . . . 125

Page

V. IMPLICATIONS FOR THE DESIGN OF BINDING STUDIES . . . . . 128

Composition Variables . . . . . 128
pH Range . . . . . 129
Salt and Protein Concentration . . . . . 130
Experimental Method . . . . . 131
Cell Design . . . . . 131
Stirred Solutions . . . . . 132
Flowing Solutions . . . . . 132
Electrodes . . . . . 133
The Transference Method . . . . . 133

VI. SUMMARY AND CONCLUSIONS . . . . . 136

Potentiometric Studies . . . . . 136
Computer Simulation . . . . . 137
Ultrafiltration Study . . . . . 138

REFERENCES . . . . . 140

LIST OF TABLES


| Table | | Page |
|---|---|---|
| 1. | Water Content and Charge Capacity of Cation-Exchange Membranes | 42 |
| 2. | Effect on EMF of Membrane Orientation Compared with That of Different Membranes | 43 |
| 3. | Observed EMF with Membrane Junction in Various Anionic Forms | 45 |
| 4. | Solvent Transport Correction for Anion Membrane | 46 |
| 5. | Solution Resistance Changes in 4.5 ml. Cell with Electrodes Short-Circuited | 50 |
| 6. | Total Resistance Change of 4.5 ml. Cell with Passage of Current | 51 |
| 7. | Solution Resistance Changes on Passing Current Through 4.5 ml. Cell | 53 |
| 8. | Molal Concentrations and Observed EMF | 54 |
| 9. | Calculated Slopes and Intercepts for $E_I - E_0$ vs. $\Delta$(m ln a) | 57 |
| 10. | Concentration, EMF, and Transference Data for Pairs of Solutions in Table 8 | 61 |
| 11. | Effects of Dissolved Polysaccharides on the Potential Difference Between Silver-Silver Chloride Electrodes | 65 |
| 12. | Effects of Colloidal Silica on the Potential Difference Between Silver-Silver Chloride Electrodes | 67 |
| 13. | Summary of Wiersema's Algorithm for Numerical Solution of the Poisson-Boltzmann Equation | 90 |
| 14. | Comparison of the Results of Two Computer Programs for the Numerical Solution of the Poisson-Boltzmann Equation | 102 |
| 15. | Free $Cl^-$ Concentration as a Function of $\nu$ Calculated from Protein Component and from Ion Distribution | 103 |
| 16. | Comparison of $\nu$ Values Estimated from EMF Measurements and from Numerical Solution of Poisson-Boltzmann Equation | 107 |

Table Page

17. Minimum Values of the Ratio $(Na^+ - Cl^-)/(Na^+ + Cl^-)$ for Nine Albumin-NaCl-NaOH Solutions . . . . . 108

18. Chloride Concentrations and Donnan Ratios in a 1 Per Cent Albumin Solution Calculated from Two Different Series Approximations . . . . . 110

19. Concentrations of KCl Ultrafiltrates and Retentates as Determined by Dry Weight Measurement . . . . . 121

20. Ultraviolet Absorbance of Albumin-KCl Solutions Ultrafiltered Through PM-10 Membranes . . . . . 123

21. Analysis of Freeze-Dried Ultrafiltrates by Modified Biuret Method . . . . . 124

22. Calculated Uncertainty in Ion-Binding Parameter $\nu$ as a Function of Albumin Concentration at 0.1 Molal Salt Concentration . . . . . 127

## LIST OF ILLUSTRATIONS


| Figure | | Page |
|---|---|---|
| 1. | Concentration Cell with Transference | 13 |
| 2. | Sectional Views of 0.45 ml. Lucite Cell | 27 |
| 3. | Perspective and Stereographic Views of 4.5 ml. Lucite Cell | 29 |
| 4. | Observed EMF of KCl Concentration Cell with Anion-Membrane Junction in the $NO_3^-$ Form | 48 |
| 5. | Three Representative Time Profiles of the Concentration Cell EMF | 56 |
| 6. | Deviation of Observed EMF from Ideal EMF as a Function of KCl Concentration | 60 |
| 7. | Dependence of Water Transference Number $t_w$ on RMS Molality of KCl Concentration Cell | 63 |
| 8. | EMF Difference Between Colloidal Silica Solutions and Their Dialyzates as a Function of pH | 69 |
| 9. | Flow Chart of Wiersema's Algorithm for Numerical Solution of the Poisson-Boltzmann Equation | 91 |
| 10. | Method for Estimation of Free Ion Concentrations from Ion Distributions | 99 |
| 11. | Calculation of Free $Cl^-$ Concentrations from Protein Component and from Ion Distribution as Functions of $\nu$ | 105 |

## ABBREVIATIONS

BPA - Bovine plasma albumin

EMF - Electromotive force

M - Molar concentration

m - Molal concentration

N - Normal concentration

PVBS - Polyvinylbenzenesulfonate

RMS - Root mean square

TCA - Trichloroacetic acid

# I. INTRODUCTION

## RATIONALE

Interactions between proteins and electrolytes are ubiquitous. Plasma proteins decrease the chemical potential of water (1) and they help to regulate the osmotic and electrolytic balance between plasma and interstitial fluid *in vivo* (2). Albumin, the most abundant plasma protein, appears to interact with a wide variety of charged species *in vitro*. These species can be either anionic (3, 4, 5) or cationic (6, 7). Substances such as salts, buffers, and detergents are often present during physical and chemical studies of protein solutions. These additional components can make significant contributions to the apparent charge, molecular weight, and molal volume of a protein in solution. Rosenberg and Klotz (8), for example, have measured the apparent molal volume changes associated with the interaction between bovine albumin and sodium dodecyl sulfate in aqueous solution.

## EVIDENCE OF PROTEIN-ELECTROLYTE INTERACTION

The most direct evidence of interaction between proteins and electrolytes is the effect of added neutral salt on the pH of an isoionic protein solution. Sandor (9) observed an increase in the pH of an isoionic solution of horse serum albumin when he added alkali metal chlorides or sulfates. These observations have been confirmed by others (5, 10), but different interpretations have been suggested. Sandor (11) postulated the formation of coordinate

covalent complexes between $SO_4^=$ and amino N atoms of the protein. These reactions at the amino groups of the protein were postulated to lower the dissociation constant of nearby carboxyl groups resulting in an increase of the solution pH. Scatchard and coworkers (5, 10) postulated a combination of anions and protein that was largely electrostatic in nature. In their interpretation, the resulting increase in net negative charge of the protein led to a greater electrostatic attraction between the protein and hydrogen ions.

Scatchard and Black (12) calculated the extent of binding of several inorganic ions to albumin from the change of isoionic pH upon addition of various salts. The $\Delta$pH method, as it is sometimes called, has since been used to study the binding of small inorganic ions to myosin (13), $\alpha_s$-casein (14), and $\beta$-lactoglobulin (15). Nagasawa and Holtzer (16) have questioned the validity of individual ion binding as the only interpretation of the $\Delta$pH effect. They suggested that the pH change could be attributed to a shielding effect of the added salt on the electrostatic interactions among discrete charged groups on the protein. Cassel and Steinhardt (17) have recently criticized the use of the $\Delta$pH method in binding studies particularly when applied to high-affinity ligands at low ligand concentration. They attributed the principal limitations of the $\Delta$pH method in such cases to uncertainty in the determination of protein concentration and molecular weight.

This dissertation is divided into three major sections. The first section is concerned with potentiometric studies of protein-

electrolyte interactions. The effects of solvent transference and the effects of macromolecular solutes on potentiometric measurements are emphasized. The second section describes a computer simulation of the distribution of small ions around a macro-ion. The third and final section consists of an ultrafiltration study of protein-electrolyte interactions.

## HISTORY OF THE POTENTIOMETRIC METHOD

The first potentiometric study of the combination of proteins with acids and bases was probably that of Bugarszky and Liebermann in 1898 (18). Since that time a large number of potentiometric titrations of proteins with acids and bases have been performed as well as many studies of protein interactions with neutral salts. One of the major drawbacks to these studies was the relatively small number of ion-specific electrodes. The selection was limited almost exclusively to hydrogen and glass electrodes for $H^+$, Ag-Ag salt electrodes for halides and $SCN^-$, and amalgam electrodes for cations which form stable intermetallic compounds with Hg. Protein interactions with inorganic ions such as $K^+$ and $NO_3^-$ and with buffer ions such as acetate and phosphate could not be studied potentiometrically because of the lack of suitable electrodes. In recent years, a wider variety of ion-selective electrodes has been developed (19). The present study is concerned with ion-selective electrodes fabricated from organic ion-exchange membranes.

## The Teorell-Meyer-Sievers Theory

The earliest theory of the potential difference across a charged membrane separating two electrolyte solutions was developed independently by Teorell (20) and by Meyer and Sievers (21). This theory has been used by subsequent investigators in the interpretation of potentiometric measurements with ion-exchange membrane electrodes (22, 23). Teorell, and Meyer and Sievers divided the total membrane potential into three parts, a diffusion potential within the membrane and two phase boundary potentials at the membrane-solution interfaces. They treated the mobile ions in the membrane as ideal solutes and assumed that no water or non-electrolyte was transferred by the electric current. Scatchard (24) pointed out that these two conditions are not satisfied in a high charge capacity ion-exchange membrane. He derived general equations for the EMF of a membrane-containing cell which included terms expressing the transfer of water through the membrane.

## Potentiometric Studies by Scatchard and Coworkers

The most careful potentiometric studies of protein-electrolyte interactions using ion-exchange membranes are those of Scatchard, Coleman, and Shen (5) and of Scatchard, Wu, and Shen (25). These investigators studied the interactions between bovine serum mercaptalbumin and the fluoride, chloride, iodide, trichloroacetate, and thiocyanate of sodium over the range of pH 2 to 10. Scatchard, Coleman, and Shen (5) employed two kinds of cells. One contained only anion-exchange membranes and was designated by them as the

$\alpha\beta$ cell. The other contained a cation-exchange membrane as well as anion-exchange membranes and was designated the $\alpha\gamma$ cell. Both cells contained saturated calomel electrodes isolated from the cell compartments by saturated KCl bridges. The $\alpha\gamma$ cell contained two flowing liquid junctions and the $\alpha\beta$ cell contained one flowing and one stopcock liquid junction.

Calibration curves

Scatchard, et al. (5, 25) did not use the equations for water and electrolyte transfer which had been derived previously (24). Instead, they constructed calibration curves of $\Delta E$ vs. $\sqrt{m_a m_b}$ where $m_a$ and $m_b$ are the respective salt concentrations on either side of the membrane and $\Delta E$ is the difference between the observed EMF and that calculated from the Nernst equation. The concentration ratio was held constant at a value of 2 over the range 0.00005 to 0.2 m. Using these calibration curves and the observed EMF values in the presence of protein, the authors determined the concentration of free anions in the presence of protein, as described below, and calculated the average number of moles $\bar{\nu}_{x^-}$ of anions bound per mole of protein from

$$\bar{\nu}_{x^-} = (m_3 - (X^-))/m_2 \qquad (1)$$

in which $m_3$ is the total salt molality in the protein solution, $(X^-)$ is the concentration of unbound anion in the protein solution determined from the EMF measurements and the calibration curves,

and $m_2$ is the protein molality. Calibration curves have been used similarly in ion binding studies by Lauffer and coworkers (63) and by Friedberg and coworkers (64).

Non-thermodynamic assumptions

There are several non-thermodynamic assumptions associated with the use of such calibration curves. For the $\alpha\beta$ cell (anion-exchange membranes) the authors (5) assumed that the only effect of protein on the activity of $X^-$ is due to removal of $X^-$ from solution. They further assumed that the anion activity coefficient $\gamma_{X^-}$ in the protein-salt solution was equal to the mean ionic activity coefficient $\gamma_\pm$ of a hypothetical salt solution with the same $Na^+$ concentration. This is equivalent to assuming that the value of the ratio $\gamma_{X^-}/\gamma_\pm$ does not change when the salt concentration changes from $m_3$ to $(X^-)$ in the absence of protein. For the $\alpha\gamma$ cell (cation and anion-exchange membranes) the authors assumed that the only effect of protein on the mean activity of NaX is due to removal of $X^-$ from solution. They calculated the product $(Na^+)$ $(X^-)$ in the protein solution from the observed EMF assuming a mean ionic activity coefficient $\gamma_\pm$ equal to that of a salt solution with the same $Na^+$ concentration in the absence of protein. This assumption is equivalent to assuming that the relation of log $a_\pm$ to the EMF of the $\alpha\gamma$ cell is the same when the activity of $X^-$ is much smaller than that of $Na^+$ as when it is not.

<u>$Na^+$ Binding</u>.--There is some evidence, although indirect, that $Na^+$ is not bound to albumin. Scatchard, Scheinberg, and Armstrong

(26) cited the agreement between their binding curves for albumin based on EMF data and equilibrium dialysis experiments to support this. If EMF experiments measure only the binding of $Cl^-$ and if equilibrium dialysis measures the sum of $Cl^-$ and $Na^+$ bound, agreement between the two methods should indicate that only a small number of Na ions, if any, are bound to the protein. This argument may be vitiated by the fact that the albumin used by Scatchard, Scheinberg, and Armstrong was not completely deionized (27). Tanford has presented an argument for negligible binding of $Na^+$ to albumin based on the effects of different Na salts on the isoionic pH of albumin solutions (ref. 28, p. 563). He pointed out that if Na ions in addition to anions were bound, then the change in isoionic pH on the addition of salt should be plotted against $\bar{\nu}_{X^-} - \bar{\nu}_{Na^+}$ instead of against $\bar{\nu}_{X^-}$ alone. Since different anions are bound with different affinities, the $\bar{\nu}_{X^-}$ for different anions has equal values at different NaX concentrations and therefore at different values of $\bar{\nu}_{Na^+}$. Tanford concluded that the observed distribution of points for different Na salts around the same line on such plots (5, 25) is proof that $\bar{\nu}_{Na^+}$ is negligibly small.

Effect of Protein on Ion Activity Coefficients.--The assumption that the only effect of the protein is due to removal of $X^-$ from solution is common to the interpretation of data from both the $\alpha\beta$ cell and the $\alpha\gamma$ cell (5). If the total salt concentration on each side of the membrane is the same, this is equivalent to assuming that the anion activity coefficients on each side are the same. Edsall and Wyman pointed out that this assumption cannot

be exactly true, but that any error in it is likely to be a second-order correction for a protein which appears to bind anions as extensively as albumin does (ref. 29, p. 597). Because of the experimental inaccessibility of single-ion activities, this assumption or one similar to it is necessary for the interpretation of any kind of activity data on protein-electrolyte interactions.

Water Transference.--The remaining non-thermodynamic assumptions associated with the use of the calibration curves do not have as much support. Scatchard, et al. (5) indicated their belief that the assumption for the $\alpha\beta$ cell that the ratio $\gamma_{X^-}/\gamma_{\pm}$ is constant from $m_3$ to $(X^-)$ is more probable than the assumption that the relation between log $a_{\pm}$ and the EMF in the $\alpha\gamma$ cell remains the same when $a_{X^-}$ is much less than $a_{Na^+}$. The latter assumption, in particular, is strongly influenced by deviations from perfect electrode behavior. Perfect electrode behavior in this context is understood to mean conformity to some variant of the Nernst equation, i.e., the only kind of non-ideality taken into account is that due to ionic interactions in free solution. Scatchard, et al. (5) claimed that their solutions containing protein were so dilute that the EMF measurements were not affected appreciably by the transfer of water through the membrane.

There is evidence from independent measurements with cells containing ion-exchange membranes that water transference does not become negligible as the electrolyte solution becomes more dilute. In most cases, the measured water transference number appears to increase as the electrolyte concentration decreases (30, 31, 32, 33).

In their interpretation of the EMF data, Scatchard, et al. (5) found it necessary to assume the simple relationships outlined above between concentrations, activities, and electric potential differences. The validity of these simple relationships is almost certain to be affected by water transfer and by other deviations from perfect electrode behavior. Although the calibration curves include unknown contributions from factors such as water transfer, the reliability of the EMF method might be improved by explicit incorporation of parameters for water transfer and other sources of deviation into the EMF-activity equations.

## Ion binding models

In addition to the calibration curves for estimating anion activities from EMF measurements, Scatchard, et al. (5) also used a graphical method for fitting a site-class model of ion binding to their data. According to this type of binding model, the total number of binding sites is divided into several classes between which the intrinsic association constants are different but within which they are the same. The choice of the ion-binding model which best fits the data is always somewhat arbitrary. In an independent analysis of Scatchard's data, Saroff chose a site-class model with fewer classes of sites and a different distribution of association constants (34).

The hypothesis of different classes of binding sites is expedient when the binding data, plotted in any of a number of different ways (35), exhibit curvature which is not predicted by the

model. An alternative interpretation to the hypothesis of multiple classes of sites is that of interactions between sites. Arvidsson (36) has developed a statistical mechanical model of protein-small molecule interaction. He considers all the binding sites to have essentially the same intrinsic association constant. The model contains parameters for electrostatic and non-polar interactions between sites and for intra-molecular salt bonding. The model is capable of fitting data on the interaction of proteins with inorganic ions and with fatty acids. Specifically, Arvidsson's model appears to fit the $Cl^-$ and $I^-$ binding data of Scatchard, et al. (5, 25), without recourse to the postulate of multiple classes of binding sites.

The Suspension Effect

A final problem has to do with the interpretation of EMF measurements in solutions of charged macromolecules. The so-called "suspension effect" accompanying the measurement of pH in clay suspensions and in biological fluids has been known for many years (37, 38, 39, 40). The suspension effect has been interpreted as an abnormal junction potential associated with the effect of charged colloids on the relative diffusion rates of $K^+$ and $Cl^-$ (41). McMenamy, et al. (42) have obtained equilibrium dialysis data on the binding of $SCN^-$ to albumin which is not consistent with the EMF data of Scatchard, et al. (5, 25), particularly at pH values removed from the isoionic point. McMenamy (43) has contended that EMF measurements in the presence of charged macromolecules do not

give directly the true mean free concentration of small ions.

It is known that Gibbs-Donnan effects can be appreciable whenever a solution containing charged macromolecules is separated from a solution without charged macromolecules even in the absence of a membrane (ref. 28, p. 238). Macroscopic separations of this kind commonly occur in ultracentrifugation, diffusion, and electrophoresis. McMenamy has suggested that microscopic separations of a similar nature occur in the interfacial region between a protein solution and an electrode or ion-exchange membrane. As a result, the electrode does not respond to the electrochemical potential of an ion in the presence of protein in the same manner as it would in the absence of protein. McMenamy (43) has calculated a correction term for this effect on EMF measurements from the Boltzmann distribution and certain geometrical assumptions.

## STATEMENT OF PURPOSE

The specific goals of the present study, insofar as the potentiometric method is concerned, are as follows:

(1) to derive and test EMF-activity relationships for ion-exchange membrane cells which explicitly take into account the major sources of deviation from perfect electrode behavior and

(2) to calculate the theoretical distribution of small ions in solutions containing charged macromolecules and to average this distribution in such a way as to approximate the mean free ion concentration measured with an electrode.

# II. POTENTIOMETRIC STUDIES

## DERIVATION OF EQUATIONS

The purpose of this section is to present a derivation of equations for the total EMF of a cell containing an ion-exchange membrane. These equations will reflect deviations from perfect electrode behavior, predicted with the Nernst equation (eq. (20), p. 20). Special attention will be given to the contributions of the liquid junction potential and of water transference to the total EMF.

At constant temperature and pressure the condition for thermodynamic equilibrium in a system through which electricity may pass is

$$dF = \sum_i \mu_i dN_i + EdQ = 0 \qquad (2)$$

where F is the Gibbs free energy, $\mu_i$ the chemical potential of species i, $N_i$ the number of moles of species i in the system, E the electric potential, and Q the charge. Eq. (2) is a separable differential equation which can be integrated directly yielding

$$\sum_i \mu_i n_i + n_e fE = 0 \qquad (3)$$

where $n_i$ is the number of moles of species i produced by reaction in a phase in which its chemical potential is $\mu_i$, $n_e$ is the number of faradays of electricity passed through the system, and f is the

Faraday constant. If a mass transference number $t_i$ is defined by $t_i = n_i/n_e$, then eq. (3) can be written

$$Ef = -\sum_i \mu_i t_i \qquad (4)$$

Consider the concentration cell with transference shown in Fig. 1.

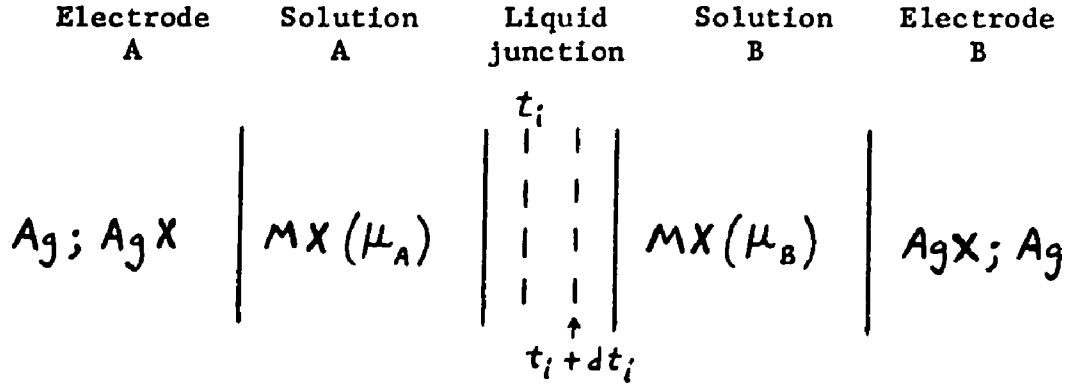



Figure 1. Concentration Cell with Transference

Compartment A contains an Ag-Ag salt electrode and a solution of a completely dissociated, uni-univalent electrolyte MX at a chemical potential $\mu_A$. Compartment B contains a solution of the same electrolyte MX at a chemical potential $\mu_B$ and an Ag-Ag salt electrode. The vertical solid lines represent phase boundaries.

The region between A and B represents a liquid junction of unspecified nature. As pointed out by Lewis and Randall (44), the transference numbers $t_i$ within a liquid junction are in general not constant with distance so there will be a summation of effects at

different points. The contribution to E in an infinitesimal region in which $t_i$ changes by $dt_i$ is $-\mu_i dt_i$ for one species and $-\sum_i \mu_i dt_i$ for all species. The contribution over the entire liquid junction is $-\int_A^B \sum_i \mu_i dt_i$. The total potential given by eq. (4) can then be partitioned into three terms

$$Ef = \sum_i \mu_i t_i (\text{in } A) - \sum_i \mu_i t_i (\text{in } B) + \int_A^B \sum_i \mu_i dt_i \qquad (5)$$

Integrating the last term by parts yields

$$\int_A^B \sum_i \mu_i dt_i = \sum_i t_i \mu_i \Big|_A^B - \int_A^B \sum_i t_i \, d\mu_i$$

$$= \sum_i t_i \mu_i (\text{in } B) - \sum_i t_i \mu_i (\text{in } A) - \int_A^B \sum_i t_i \, d\mu_i \qquad (6)$$

Substituting eq. (6) into eq. (5) gives

$$Ef = -\int_A^B \sum_i t_i \, d\mu_i \qquad (7)$$

The activity $a_i$ of a pure chemical species i is defined in terms of the chemical potential of species i as

$$\mu_i = \mu_i^\circ + RT \ln a_i \qquad (8)$$

in which $\mu_i^\circ$ is a constant equal to the chemical potential of

species i in an arbitrarily chosen standard state, R is the gas constant, and T is the absolute temperature. Substituting eq. (8) into eq. (7)

$$Ef/RT = -\int_A^B \sum_i t_i \, d \ln a_i \tag{9}$$

The sum $(E_A + E_B)$ of the potentials due to the electrodes that are reversible to the $X^-$ ions is given by

$$E_A + E_B = -(RT/f) \ln(a_B^-/a_A^-) \tag{10}$$

In regions of the cell in which transference numbers are not constant with distance, as in the liquid junction, the contribution $E_J$ to the cell EMF has the same form as eq. (9). The total cell EMF is given by $E = E_A + E_B + E_J$. Assuming for the moment that $M^+$ and $X^-$ are the only species contributing to the cell EMF

$$Ef/RT = -\ln(a_B^-/a_A^-) - \int_A^B t^{+\prime} \, d \ln a^+ + \int_A^B t^{-\prime} \, d \ln a^- \tag{11}$$

in which the primes indicate transference numbers measured with respect to the solvent as a stationary frame of reference.

Eq. (11) is useful for examining the effects of the nature of the liquid junction on the cell EMF. Consider first a connection

between the two solution compartments via an ideal salt bridge in which the cation and anion constituents have equal mobilities. Make the provisional assumption that the sum of the liquid junction potentials at either end of the bridge is negligible so that attention may be focused on the transference properties of the bridge as a whole. The transference numbers $t^+$ and $t^-$ within the bridge will be constant with distance and both equal to 0.5. Under these conditions, eq. (11) becomes

$$Ef/RT = -\ln(a_B^-/a_A^-) - (0.5)\ln(a_B^+/a_A^+) + (0.5)\ln(a_B^-/a_A^-) \qquad (11a)$$

Adding the terms in $\ln(a_B^-/a_A^-)$ and converting single-ion activities to mean ionic activities with the relation $a^-a^+ = (a^\pm)^2$ gives

$$Ef/RT = -\ln(a_B^\pm/a_A^\pm) \qquad (11b)$$

For a ten-fold mean ionic activity ratio at 25° C this results in an EMF of 59.158 mv.

If the ideal salt bridge is replaced by an ion-exchange membrane, the membrane can be regarded as a single liquid junction with highly altered transference properties. For a perfect anion-exchange membrane (fixed positive charges), $t^+$ would be zero and $t^-$ would be unity. Eq. (11) for this system would be

$$Ef/RT = -\ln(a_B^-/a_A^-) + \ln(a_B^-/a_A^-) \qquad (11c)$$

and the EMF would be zero at all activity ratios. The null EMF can be intuitively regarded as the sum of the potential difference between the bulk solutions and an equal but opposite potential difference across the membrane junction. For a perfect cation-exchange membrane (fixed negative charges), $t^+$ would be one and $t^-$ would be zero. Eq. (11) for this system is

$$Ef/RT = -\ln(a_B^-/a_A^-) - \ln(a_B^+/a_A^+) \qquad (11d)$$

Converting to mean ionic activities gives

$$Ef/RT = -2\ \ln(a_B^{\pm}/a_A^{\pm}) \qquad (11e)$$

and the EMF for a ten-fold mean ionic activity ratio at 25° would be 118.32 mv. In this case the potential difference between the bulk solutions and that across the membrane junction have the same sign and the maximum EMF for a given activity ratio is obtained.

The transference numbers $t^{+'}$ and $t^{-'}$ in eq. (11) are defined relative to the solvent as a stationary frame of reference. In the case of cells containing ion-exchange membranes, transference numbers are experimentally determined by physical measurements or chemical analysis relative to the membrane as a frame of reference. An equation of the same from as eq. (11) would not be valid for transference numbers measured relative to the membrane unless the transference of solvent relative to the membrane were zero. A number of factors suggest that zero water transference relative to

an ion-exchange membrane would be extremely fortuitous. Among these factors are the weak-electrolytic nature of water, the larger mobility of $H^+$ and $OH^-$ relative to other ions (ref. 45, p. 231), the apparent hydration of salt ions (ref. 45, p. 525), and the postulated transfer of momentum to the solvent by mobile ions in the membrane (ref. 46, p. 327). For these reasons, equations containing transference numbers measured relative to the membrane should in general contain a term for water transference.

Writing eq. (9) for the EMF of the cell in Fig. 1 and including a term for water transference

$$\frac{Ef}{RT} = -\ln \frac{a^-_B}{a^-_A} - \int_A^B t^+ d\ln a^+ + \int_A^B t^- d\ln a^- - \int_A^B t_w d\ln a_w \qquad (12)$$

in which $a_w$ is the water activity and $t_w$, the transference number of water, is equal to the number of moles of water which cross a reference plane when one faraday of electricity passes through the cell. The transference numbers in eq. (12) are measured relative to the ion-exchange membrane as a frame of reference. If we specify a cation-exchange membrane at the liquid junction, $t^-$ can be expressed in terms of $t^+$ from the relation $t^+ + t^- = 1$.

$$\frac{Ef}{RT} = -\ln \frac{a^-_B}{a^-_A} - \int_A^B t^+ d\ln a^+ + \int_A^B (1-t^+) d\ln a^- - \int_A^B t_w d\ln a_w$$

$$= -\ln \frac{a^-_B}{a^-_A} - \int_A^B t^+ d\ln a^+ + \int_A^B d\ln a^- - \int_A^B t^+ d\ln a^- - \int_A^B t_w d\ln a_w \qquad (13)$$

The third term on the right in eq. (13) is equal to $+\ln (a^-_B/a^-_A)$ so

that

$$\frac{Ef}{RT} = -\int_A^B t^+ d\ln a^+ - \int_A^B t^+ d\ln a^- - \int_A^B t_w d\ln a_w \qquad (14)$$

Converting from single-ion activities to mean ionic activity gives

$$\frac{Ef}{RT} = -2\int_A^B t^+ d\ln a^{\pm} - \int_A^B t_w d\ln a_w \qquad (15)$$

The water activity $a_w$ in eq. (15) can be expressed in terms of the mean ionic activity $a^{\pm}$. Harned and Owen (45) have derived the relation

$$d \ln a_w = -2 \times 10^{-3} m^{\pm} M_1 \, d \ln a^{\pm} \qquad (16)$$

where $m^{\pm}$ is the mean ionic molality and $M_1$ is the solvent molecular weight.

Substituting eq. (16) into eq. (15) gives

$$\frac{Ef}{2RT} = -\int_A^B (t^+ - 10^{-3} m^{\pm} M_1 t_w) d\ln a^{\pm} \qquad (17)$$

Eq. (17) has been derived by Hills, Jacobs, and Lakshminarayanaiah (47), though not in as detailed a form as given here. Scatchard (24) has pointed out that all thermodynamic treatments of voltaic cells require the assumption that the laws of reversible thermodynamics apply to instantaneous values of concentrations and activities although these are changing due to the irreversible

process of diffusion. Eq. (17) has also been derived using irreversible thermodynamics (47, 48). Experimental tests of eq. (17) have been carried out for only a few types of ion-exchange membranes (32, 49). In one case (49), the predictions of eq. (17) agreed with the observed EMF to within 1 per cent whereas the predictions of the Teorell-Meyer-Sievers theory (20, 21) did not.

If the substitution $\beta = 10^{-3} M_1 t_w$ is made and if the superscript $\pm$ is dropped, the definite integral in eq. (17) can be written

$$E_o = -\frac{2RT}{f}\left[(t^+ - \beta m_B)\ln a_B - (t^+ - \beta m_A)\ln a_A\right] \qquad (18)$$

where $E_0$ is the observed EMF. Eq. (18) can be rearranged to

$$E_o = -\frac{2RT}{f}\left[t^+ \ln \frac{a_B}{a_A} - \beta(m_B \ln a_B - m_A \ln a_A)\right] \qquad (19)$$

If the liquid junction has ideal transference properties i.e., if $t^+ = 1.0$ and $t^- = t_w = 0.0$, eq. (19) reduces to the well-known Nernst equation

$$E_I = -(2RT/f)\ \ln(a_B/a_A) \qquad (20)$$

where $E_I$ is the EMF observed when the liquid junction has ideal transference properties. If eq. (19) is subtracted from eq. (20), the result is

$$E_I - E_o = -\frac{2RT}{f}\left[(1-t^+)\ln\frac{a_B}{a_A} + \beta(m_B \ln a_B - m_A \ln a_A)\right] \qquad (21)$$

Eq. (21) will be used in a later section for the estimation of transference numbers.

## EXPERIMENTAL

### Electrolyte Solutions

Electrolyte solutions for the EMF measurements were prepared by weight using Mettler balances Model H16 (80 g. capacity, $\pm$ 0.01 mg. sensitivity) and Model K7 (800 g. capacity, $\pm$ 0.02 g. sensitivity). Sodium and potassium salts were "Baker Analyzed" reagents and were used without further purification. KCl was dried in air at 110° C for at least 24 hours and cooled in a desiccator over "Drierite" prior to weighing. $KNO_3$ was dried in a desiccator over activated alumina for several days prior to weighing. Water for most solutions was collected from a Barnstead still and passed through a Bantam 802 deionizing cartridge. A typical water sample deionized in this manner had a specific conductance of 0.980 $\mu$mhos in a conductivity cell with a constant of 0.0825. A sample of glass-distilled water from a Corning still (model AG-10a) had a specific conductance of 3.87 $\mu$mhos under similar conditions. Solutions of HCl and KOH for volumetric determinations were prepared from Harleco concentrates sealed in glass.

### Albumin Solutions

Crystallized BPA was supplied by Armour Pharmaceutical Co., Kankakee, Ill. The dry powder was dissolved in water with mild agitation at room temperature. Freshly prepared solutions were placed in pre-rinsed Visking dialysis bags and dialyzed at 4° C against several changes of glass-distilled water for at least 48 hours. These dialyzed solutions were then passed successively

through a HAWP 01300, 0.45 μ Millipore filter, a mixed-bed deionizing column (50), a second Millipore filter, and stored as a frozen solution at -40° C. When stored in this manner for periods of up to 6 months, BPA has shown excellent stability with respect to the criterion of constant sulfhydryl content (51). The concentration of BPA solutions prior to cold storage was determined with an accuracy of 1 per cent by measurement of ultraviolet absorption in a Zeiss PMQ II spectrophotometer. The hypothetical absorbance of a 1 per cent BPA solution in a 1.0 cm. cuvette was taken to be 6.67 at 279 nm. (52). The concentration of BPA solutions following cold storage was determined with an accuracy of 0.1 per cent by the method of dry weight measurement described by Hunter (53).

Amylose

A sample of potato amylose labelled "Superlose" was obtained from Corn Products Co., New York. The sample did not dissolve appreciably in 0.3 M KCl even when heated to near boiling. The sample dissolved slowly in 0.5 N KOH at room temperature. After neutralizing with 2.0 N HCl and centrifuging to remove any precipitate, enough amylose remained dissolved to give a 0.43 per cent solution as determined by dry weight measurement.

Dextrans

A sample of partially fractionated dextran was obtained from Pharmacia, Uppsala, Sweden. According to the manufacturer, the

number-average molecular weight from end-group analysis was 80,000 and the weight-average molecular weight from light scattering was 113,000. A sample of dextran sulfate of molecular weight 500,000 was obtained from the same company. Both samples dissolved in 0.1 M KCl at room temperature.

## Colloidal Silica

A turbid, aqueous suspension of colloidal silica "Ludox SM-30" was obtained from E. I. duPont de Nemours and Co., Wilmington, Del. According to the manufacturer (97), the approximate diameter of the colloidal particles in the suspension was 7 to 8 nm. The pH of a 1:10 dilution of the suspension in 0.01 M KCl was about 10. Another aliquot of the suspension was diluted by a factor of 10 in distilled water and was dialyzed exhaustively against distilled water. At the end of the dialysis the pH of the Ludox solution was about 6. Dialysis of the 1:10 Ludox dilution did not appear to result in any gelation or precipitation. Dry weight measurement of the dialyzed solution indicated a weight concentration of 2.46 per cent.

## Equilibrium Dialysis

Solutions of amylose, dextran, dextran sulfate, and colloidal silica in aqueous KCl were dialyzed in the following manner. The solutions were placed in pre-rinsed Visking dialysis bags and dialyzed with stirring against an equal volume of water in glass-stoppered test tubes for at least 48 hours at room temperature.

The amylose solution and the more acidic colloidal silica solutions became slightly opalescent during the dialysis.

## Carbohydrate Analysis

The phenol-$H_2SO_4$ method (54) was used as a general test for monosaccharides. One ml. of 5 per cent redistilled phenol and 5 ml. of concentrated $H_2SO_4$ were added to 2 ml. each of the sample to be analyzed and a suitable blank. The solutions were thoroughly mixed and allowed to stand at room temperature for one hour. The absorbance of the solutions was read in a Bausch and Lomb "Spectronic 20" spectrophotometer at 490 nm. The monosaccharide content was estimated from a previously-determined calibration curve for glucose.

## Electrochemical Cells

Cells of two different designs were constructed from Lucite blocks. The half cells are illustrated in Figures 2 and 3. The two cells will be distinguished by the volume of their respective solution compartments, 0.45 ml. for one cell and 4.5 ml. for the other. The luer fittings were made of Kel-F. The gaskets which fit around the edges of the membrane were made of Neoprene. The cells were filled from 5 ml. gas-tight Hamilton syringes. The solutions were agitated by continuous-flow injection from a Sage syringe pump (Model 237-2) in the case of the 0.45 ml. cell and by a tiny magnetic stirring bar in the case of the 4.5 ml. cell. The luer fittings of the 4.5 ml. cell could accommodate Hamilton 3-way

FIGURE 2

SECTIONAL VIEWS OF 0.45 ML. LUCITE CELL

Dimensions are in inches.

E - electrode opening

F - press-fitted Kel-F luer fittings

H - holes for screws which hold cell together
Holes are omitted from side and top views.

I - inlet opening

O - outlet opening

M - membrane

# FIGURE 2

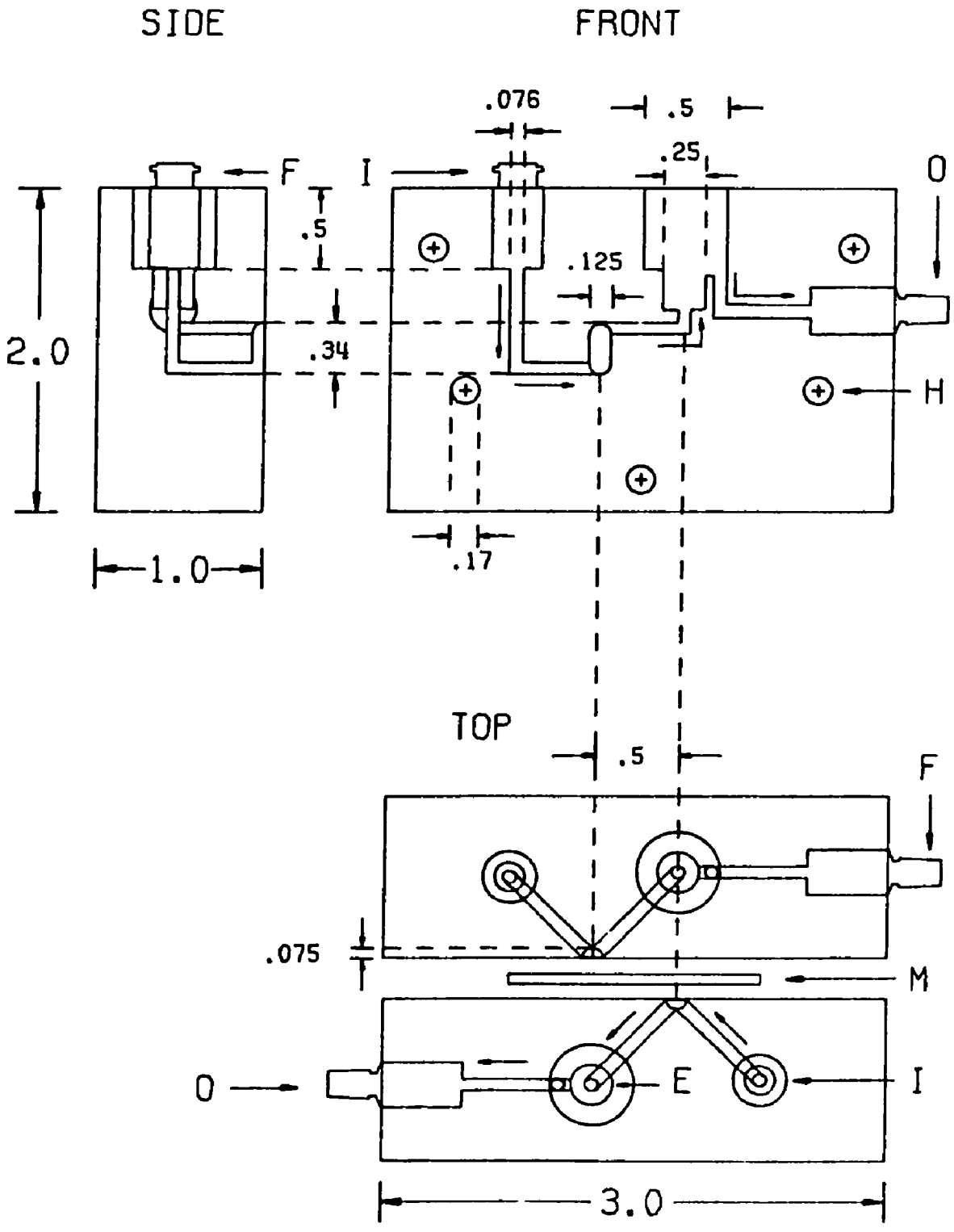


FIGURE 3

PERSPECTIVE AND STEREOGRAPHIC VIEWS

OF 4.5 ML. LUCITE CELL

Dimensions are in inches.

E - electrode opening

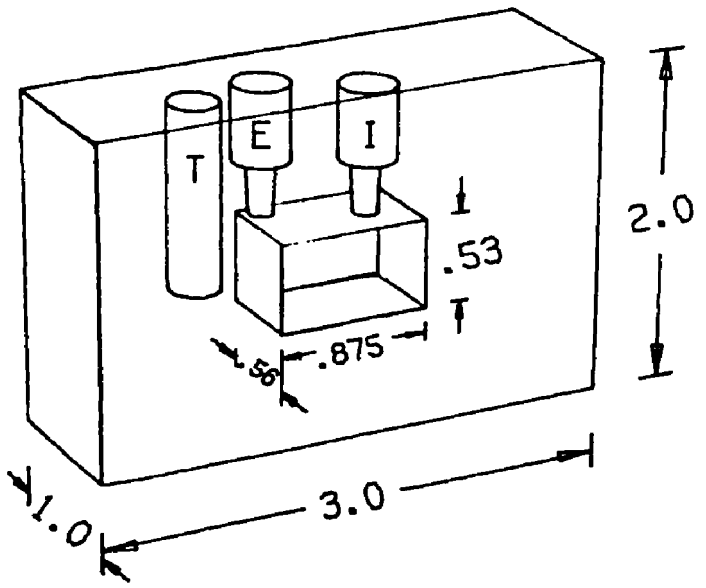
I - inlet opening

T - thermometer opening

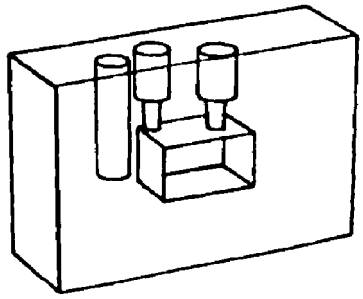
The electrode and inlet openings accommodate standard luer fittings.

# FIGURE 3

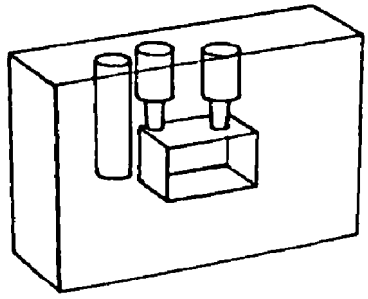
PERSPECTIVE




STEREO



STEREO



valves which in turn could accommodate male luer-tipped capillaries and polyethylene tubes with luer locks. A Teflon mask with a circular hole 9 mm. in diameter was placed on each side of the membrane in the 4.5 ml. cell. The two half-cells were held together by brass screws which are not shown in Figures 2 and 3. Ag-AgCl electrodes were inserted into the solution compartments through holes in the top of the cell.

Ag-AgCl Electrodes

Ag-AgCl electrodes for the 0.45 ml. cell were constructed from optical grade AgCl by the method of Greyson (55). A bead of molten AgCl was applied to the tip of a 24 gauge Pt wire. The AgCl bead was then cooled and cathodized in dilute HCl. Electrodes for the 4.5 ml. cell were constructed according to the method described by Bates (40). A coat of AgO paste was applied to a piece of 20 gauge Pt wire and heated at 250° C in a muffle furnace until the coating was completely white. The Ag residue was then cooled and anodized in dilute HCl. HCl solutions for electrolyzing Ag and AgCl were prepared by diluting an azeotropic mixture of water and HCl. Any two electrodes whose potentials differed by more than 0.10 mv. were not used together. Between experiments all electrodes were short-circuited and stored in 0.01 M KCl.

Electrode behavior in albumin solutions

The effect of dissolved albumin on the Ag-AgCl electrodes was

examined in the following manner. Two electrodes were immersed in 0.01 M KCl. One electrode was removed, immersed in a 1 per cent albumin solution for several minutes, rinsed with water, and re-immersed in the KCl solution. The usual result of this treatment was an erratic drift in EMF, sometimes covering a range of 15 mv. or more. If the electrode was soaked in 8 M urea prior to re-immersion in the KCl solution, the excursion of the drift was usually smaller, but the electrode did not attain a constant potential without overnight soaking in 8 M urea and extensive re-conditioning in dilute KCl.

Collodion-coated electrodes

The behavior of electrodes coated with a thin layer of collodion was examined. An electrode was coated by dipping it into a methanol-ether solution of collodion and drying it in air. When the coated electrode was re-immersed in 0.01 M KCl, the EMF differed from its original value by as much as 0.5 mv., but it usually returned to the original value with continued soaking in 0.01 M KCl. When collodion-coated electrodes were immersed in a 1 per cent albumin solution, rinsed with water, and re-immersed in 0.01 M KCl, the EMF usually drifted slowly. The drift was always in one direction and the rate varied from about 0.01 mv. per min. to 0.20 mv. per min. Some of the drift rates of the coated electrodes appeared to be small enough for the electrodes to be analytically useful in protein solutions.

Ion-Exchange Membranes

Ion-exchange membranes, supplied by Ionics Inc., Watertown, Mass., were used in the experiments. The anion-exchange membrane (no. 111EZL219) was of the quaternary ammonium type and the cation-exchange membrane (no. 61DZL183) was of the sulfonic acid type. Both membranes had an organic matrix of polystyrene cross-linked with divinylbenzene and both were strengthened with a reticulate backing of Dynel, a copolymer of vinyl chloride and acrylonitrile. According to the manufacturer (58), the water content of the membranes was 34 per cent of the weight of the wet resin and the Dynel backing constituted 43 per cent of the weight of the dry membranes. The membranes were 0.06 cm. thick and were cut into rectangular pieces 2.54 cm. by 3.81 cm. for insertion into the cell. The freshly-cut edges of the membranes were briefly pressed with a hot soldering gun to retard leakage and evaporation. Preliminary treatment of the membranes consisted of alternate rinsing with dilute HCl and KOH solutions and concluded with rinsing in concentrated salt solutions. The cation membranes were converted to the $K^+$ form by soaking them in saturated KCl solutions. The anion membranes were converted to any of several different anionic forms by soaking in solutions of the corresponding Na or K salt. Prior to an experiment, the membrane was usually soaked for not less than 4 hours in several aliquots of a 1:1 mixture of the two solutions to which it was to be exposed. Several hours appeared to be sufficient time for equilibration. This was confirmed by titration of an anion membrane in the $OH^-$ form with HCl. The initial rate of change in

pH was about 0.1 pH unit per min. After 30 min. the rate of change was about 0.01 pH unit per min. and after 90 min. the rate had fallen to about 0.0008 pH unit per min. Between experiments the membranes were stored in concentrated salt solutions.

Water content

The water content of the cation-exchange membrane was estimated by weighing each of two membranes in the wet and dry forms. The membranes were converted to the $H^+$ form by soaking in several changes of 0.02 N HCl for 3 days. The membranes were blotted dry with lens paper, placed in two clean, dry, glass-stoppered weighing bottles and weighed in the wet form. The stoppers were placed at right angles on top of the bottles and the wet membranes were heated in a vacuum oven at 110° C for 48 hours. At the conclusion of the heating period, air was not let into the oven until it had cooled to less than 70° C. After cooling to room temperature in a desiccator over "Drierite", the membranes were reweighed in the dry form. The water content was calculated by dividing the weight loss on heating by the weight of the membrane in both the wet and dry forms.

Charge capacity

The charge capacity of the cation-exchange membrane was estimated by an indirect titration method described by Helfferich (ref. 46, p. 91). A cation-exchange membrane was soaked in several changes of 0.01 N HCl for 3 days in a Dubnoff metabolic shaking

incubator at room temperature. The membrane was then soaked in several changes of deionized water for 7 hours to remove any HCl not associated with charged groups. The membrane was placed in a stirred, closed rinsing vessel through which liquid could be circulated. The membrane was rinsed for 65 hours with 1 M KCl and the rinsings were collected.

Titration Procedure.--Three 50 ml. aliquots of the rinsings were titrated potentiometrically under $N_2$ gas with a tenfold dilution of Harleco 0.10 N KOH. The titrant was delivered from a 5.00 ml. Manostat burette graduated in 0.01 ml. intervals. A Beckman Research pH Meter was used with a Beckman Ag-AgCl reference electrode (no. 39070) and a Beckman glass electrode (no. 41263). The titration assembly was standardized with Harleco buffers of pH 6.86 and 4.01. The buffer adjustment dial and the temperature control dial of the pH meter were adjusted until the instrument indicated the correct pH with both buffers. At a given temperature, this procedure establishes a unique slope for the variation of EMF with pH given by the equation

$$EMF = \sum_i E_i^0 + (2.303RT/f)pH \qquad (22)$$

where $\sum_i E_i^0$ is the sum of the standard potentials of the electrodes.

Estimation of the Equivalence Point.--The titration curves of the HCl-KCl membrane rinsings appeared to be symmetrical about the equivalence point (ca. pH 6.0). The volume of the titrant corresponding to the equivalence point was estimated graphically according

to the procedure described by Blaedel and Meloche (ref. 56, p. 351). The respective values for the 3 aliquots were 3.945, 3.960, and 3.950 ml. The 3 values agreed to within 4 parts in 1000.

Calculation.--The membrane whose rinsings were titrated was converted to the $H^+$ form and dried in a vacuum oven at 110° C for 48 hours. The charge capacity c in meq. per g. of dry $H^+$ form was calculated from

$$c = (v_e \; N \; V_t)/(v_a \; W) \tag{23}$$

where $v_e$ is the average volume of titrant corresponding to the equivalence point, N is the normality of the titrant, $V_t$ is the total volume of the rinsings, $v_a$ is the volume of a single aliquot, and W is the weight of the dry membrane in the $H^+$ form. Since the Dynel backing constituted 43 per cent of the weight of the dry membrane, the charge capacity of the dry, unbacked resin is given by c/(1.00-0.43).

EMF Measurements

EMF measurements with KCl solutions were most frequently performed with a membrane clamped between the two halves of the 4.5 ml. cell. The electrode leads were connected to the input terminals of a Beckman Research pH Meter (Model 101900) which was used as a potentiometer. Some EMF measurements were performed with a Radiometer pH meter, Type PHM4c. The pH meter was connected via a shielded cable to a Hewlett-Packard strip chart recorder (Model

7101B). The metal stand which supported the cell, the shielded connecting cords, and the potentiometer and recorder instrument cases were connected via a single wire to a grounded #2 copper cable. For some measurements the EMF cell was enclosed in a Faraday cage, but this did not seem to be invariably necessary.

EMF measurements with polymer solutions and their dialyzates were performed in a cell with two Ag-AgCl electrodes but without a membrane junction. Part of the sample solution was siphoned into a polyethylene tube connected to a tapered capillary dipping into saturated aqueous KCl in which the reference electrode was immersed. The liquid junction formed in this way was stabilized by the density difference between the two solutions. The EMF of the cell containing the polymer solution was measured and recorded and the process was then repeated with the dialyzate. The liquid junction was broken and reformed at least 3 times with each solution and the capillary and polyethylene tube were rinsed successively with water and methanol and dried with air between different solution fillings.

The above procedure gave stable and reproducible EMF readings with the amylose and fractionated dextran solutions. With the dextran sulfate and colloidal silica solutions the Ag-AgCl electrodes had to be coated with a thin layer of collodion before stable readings were observed. In spite of this precaution, the EMF showed a tendency to drift at times. In the case of the dextran sulfate solution, the EMF drifted over a range of 0.4 mv. and then became unstable.

## Solvent Transference Measurements

Three methods of estimating solvent transference are described in this section. They are (1) measurements with counterion-selective electrodes, (2) a modified Hittorf method and (3) the EMF method.

### Counterion-selective electrodes

Greyson (57) has studied the solvent contribution to the EMF of ion-exchange membrane cells containing water and heavy water. He suggested a special method of estimating water transference from EMF measurements with concentration cells. The method requires that the cell contain an ion-exchange membrane junction permeable to the same ions to which the electrodes respond. Eq. (11c) on p. 16 gives the ideal EMF of such a cell containing Ag-Ag salt electrodes. The EMF of a cell containing a membrane junction with $t^- = 1.0$ and all other $t_i = 0$ is predicted from eq. (11c) to be zero irrespective of the salt concentration ratio. Deviations of the EMF from zero were attributed by Greyson primarily to water transference (57) although there may be a small contribution from co-ion transference. In the present study, an empirical water transference correction curve for a concentration cell containing an anion-exchange membrane and Ag-AgCl electrodes was constructed by plotting the deviation of the EMF from zero as a function of the RMS salt concentration.

Modified Hittorf method

One of the most direct methods of measuring transference numbers is the classical Hittorf method (59). A known amount of current is passed through a cell for a measured length of time and aliquots of solution are withdrawn for chemical analysis. Solution volume changes as well as solution composition changes may be associated with the passage of current. Modifications of this method for estimating electrolyte and solvent transference numbers of ion-exchange membranes have been developed (49, 60).

Vertical Capillaries.--Transference measurements were performed with the 4.5 ml. cell. One of the openings in the top of each half-cell contained an Ag-AgCl electrode sealed into the male luer tip of a 1 cc. Becton-Dickinson syringe. The other opening contained a Hamilton 3-way valve with a "T" configuration. The top opening of the valve accommodated a vertical, luer-tipped precision bore capillary supplied by the Fischer and Porter Co., Warminster, Pa. According to the manufacturer's specifications (61), the inside diameter of the capillary was 0.500 mm. with a tolerance of 0.005 mm. The side opening of the 3-way valve was connected to a 5 cc. Hamilton syringe by means of which the compartment was filled with solution. When the cell was assembled and filled, the solution-air menisci were adjusted to convenient levels in the vertical capillaries by manipulation of the syringes and valves. The electrodes were connected to a 22.5 v. "C" battery and a measured current was passed for a measured length of time. The current could be varied by varying the total resistance of the circuit and it was

measured with a Simpson 260 milliammeter. Movement of the menisci in the capillaries could be measured with a small movable telescope coupled via a worm gear to a millimeter scale. Changes in salt concentration were estimated by measurement of solution conductivity. With knowledge of the salt concentration changes, the solution volume changes, and the total number of coulombs passed through the cell, estimates of the cation and water transference numbers can be calculated (49, 60).

Horizontal Capillaries.--An alternative to the vertical capillary arrangement was tried. Two polyethylene tubes from the outlet valves above the solution compartments were cemented to the ends of a 3 in. long capillary which was clamped in a horizontal position. This arrangement is similar to that used by Lakshminarayanaiah and Subrahmanyan (62). A tiny bubble could be positioned in the horizontal capillary by manipulation of the valves and syringes. With this arrangement it was much easier than with the vertical capillaries to stabilize the menisci prior to the passage of current.

EMF method

In eq. (21), p. 21, the cation transference number $t^+$ appears as a coefficient of $\ln(a_B/a_A)$ and the water transference number $t_w$ appears as a coefficient of $(m_B \ln a_B - m_A \ln a_A)$. If $\ln (a_B/a_A)$ and $(m_B \ln a_B - m_A \ln a_A)$ are each varied over a finite range, it should be possible to estimate $t^+$ and $t_w$ from the resulting variation in $E_I - E_0$. In the present study, $E_I - E_0$ for a concentration

cell containing a cation-exchange membrane was calculated as a function of salt concentration ratio and of RMS salt concentration.

Conductivity Measurements

Two conductivity bridges were used, a Model 3216B supplied by LKB Produckter, Stockholm, and a Model RC-18A supplied by Beckman Instruments, Cedar Grove, N. J. Five conductivity cells of the Jones and Bollinger design (65) supplied by LKB were available. The cells had nominal cell constants of 0.1, 2, 5, 10, and 50 and sample volumes ranging from 2 to 10 ml. The cell constant of each cell on both bridges was determined with the conductivity standards of Jones and Bradshaw (66). The concentrations of the standard solutions made up in the laboratory differed from those of the Jones and Bradshaw standards by 1 part in 2000 after buoyancy corrections. The specific conductance of the solutions made up was calculated by linear extrapolation from the specific conductance of the Jones and Bradshaw standards. The conductivity measurements for the cell constant determinations were performed in a Fisher Isotemp waterbath at 25.000 $\pm$ 0.005° C. The thermometer, manufactured by the Brooklyn Thermometer Co., had a range of 19 to 35° C. It was graduated in 0.01° C intervals and it had been calibrated by the U. S. National Bureau of Standards. A less accurate thermometer with a range of 0 to 50° C graduated in 0.05° C intervals was used for routine conductivity measurements. The conductivities of standard KCl solutions with molal concentrations close to that of the sample were usually measured along with the sample.

# RESULTS

## Ion-Exchange Membranes

### Water content

The water content of the cation-exchange membrane was estimated by weighing each of two membranes in the wet and dry H form. The results are shown in Table 1. The mean water content is 0.3176 g. of $H_2O$ per g. of wet membrane. This is about 6 per cent less than the value of 0.34 given by the manufacturer (58).

### Charge capacity

The charge capacity of the cation-exchange membrane was estimated by the indirect titration method described in the Experimental Section. The result, shown in Table 1, is 1.86 meq. per g. of dry resin in the H form. The manufacturer reported a charge capacity of 2.3 meq. per g. of dry resin for this membrane (58), but he did not specify the method used in the determination.

### Symmetry

In order to test the membranes for structural asymmetry, the effect on the cell EMF of turning a membrane over was compared to that of replacing one membrane with another in the same cell. The results for two orientations and two membranes are shown in Table 2.

## Solvent Transference

### Counterion-selective electrodes

Membrane in Various Anionic Forms.--It had been observed in

TABLE 1

WATER CONTENT AND CHARGE CAPACITY OF CATION-EXCHANGE MEMBRANE[a]

| | Wt. of wet membrane (g., H form) | Wt. of dry membrane (g., H form) | Wt. loss on drying (g.) | Mean no. of meq. from titration | WATER CONTENT | | CHARGE CAPACITY | |
|---|---|---|---|---|---|---|---|---|
| | | | | | g. $H_2O$/g. dry H form | g. $H_2O$/g. wet memb. | meq./g. dry H form | meq./g. wet memb. |
| #1 | 0.64305 | 0.43946 | 0.20359 | | 0.46327 | 0.31660 | | |
| #2 | 0.62860 | 0.42833 | 0.20027 | | 0.46756 | 0.31860 | | |
| #3 | | 0.43460 | | 0.46120 | | backed[b] | 1.06 | 0.724 |
| | | | | | | unbacked[c] | 1.86 | 1.02 |

a. Membranes 1, 2, and 3 were cut from the same sheet of cation-exchange membrane 61DZL183 supplied by Ionics, Inc., Watertown, Mass.

b. Calculated from eq. (23).

c. According to manufacturer (58), dry membrane contained 43 wt. per cent Dynel backing. Properties of dry, unbacked resin were calculated by dividing corresponding property of dry, backed membrane by (1.00-0.43); properties of wet, unbacked resin were calculated by dividing corresponding property of wet, backed membrane by (1.00 - (0.43)(1.00 - 0.32)).

TABLE 2

EFFECT ON EMF OF MEMBRANE ORIENTATION COMPARED WITH THAT OF DIFFERENT MEMBRANES

Cell: Ag;AgCl/$KNO_3$ (0.01 m) / A / [a] $KNO_3$ (0.001 m) / $KNO_3$ (0.02 m) / $KNO_3$ (0.029 m) / AgCl;Ag

| Membrane | ELECTROMOTIVE FORCE (mv.) Orientation[b] I | | II | Difference between orientation means | Membrane mean |
|---|---|---|---|---|---|
| #1 | 70.15[c] | | 70.15 | | |
| | 69.85 | | 70.50 | | |
| | 69.90 | | 70.60 | | |
| | 69.97 | mean | 70.42 | 0.45 | 70.19 |
| #2 | 71.00 | | 70.80 | | |
| | 71.40 | | 71.80 | | |
| | 71.20 | | 72.15 | | |
| | 71.20 | mean | 71.58 | 0.38 | 71.39 |
| | | Difference between membrane means | | | 1.20 |
| | | Overall standard deviation | | | 0.39 |

a. Anion-exchange membrane pre-soaked overnight in 1 M $KNO_3$.

b. Membrane was rotated 180° around a horizontal axis between orientations. Orientation I arbitrarily chosen as that which gave lower EMF.

c. Each of the triplicate measurements corresponds to a fresh injection of solutions into the 0.45 ml. cell.

this laboratory that concentration cells containing two Ag-AgCl electrodes and one anion-exchange membrane exhibited highly transient EMF readings when the membrane was in the $Cl^-$ form. The same was true with the membrane in the $I^-$, $SCN^-$, and $OH^-$ forms. The most stable EMF readings were obtained with the anion membrane in the $NO_3^-$, $F^-$, $ClO_4^=$ forms. These anions form readily soluble Ag salts and therefore they do not react appreciably at the Ag-AgCl electrodes. The results are summarized in Table 3 which also gives the solubilities of the corresponding Ag salts.

Membrane in $NO_3^-$ Form.--With the anion membrane in the $NO_3^-$ form, the EMF of the cell shown in Table 4 was measured as a function of KCl concentration. The results are listed in Table 4 and illustrated in Fig. 4. The tabulated EMF values are the arithmetic means of from 4 to 10 readings. Ninety-nine per cent confidence limits for the population means were estimated from the sample size n and from the sample standard deviation s (67), assuming that the observed EMF readings were samples from a normally distributed population. The regression curve in Fig. 4 corresponds to the logarithmic model: $y = B \log (x + C)$. Estimates of the parameters B and C were determined graphically and refined by a systematic search procedure on an IBM 360/67 computer. The parameter combination which appeared to minimize the sum of squared deviations from the regression curve was $B = 15.6$ and $C = 0.089$. The horizontal line at EMF = 0.0 represents the EMF across an ideal liquid junction saturated with the ions to which the electrodes respond. The difference between this line and the regression curve

TABLE 3

OBSERVED EMF WITH MEMBRANE JUNCTION IN VARIOUS ANIONIC FORMS

Cell: Ag;AgCl/KCl + MX /A/[a] KCl + MX /AgCl;Ag

| ANION X | IONIC STRENGTH[b] | EMF (mv.) | Solubility of Ag Salt[c] (g./100 ml. $H_2O$) |
|---|---|---|---|
| $Cl^-$ | 0.03 | unstable | $8.9 \times 10^{-5}$ ($10^o$) |
| $I^-$ | .03 | unstable | $3 \times 10^{-7}$ |
| $SCN^-$ | .03 | unstable | $2.1 \times 10^{-5}$ ($25^o$) |
| $OH^-$ | .01/.001 | unstable | 0.0013 ($20^o$) (AgO) |
| $NO_3^-$ | .03 | 72.5 | 122 ($0^o$) |
| $F^-$ | .15 | 59.0 | 182 ($15.5^o$) |
| $ClO_4^-$ | .10 | 60.1 | 525 ($25^o$) |
| $SO_4^=$ | .28/.30 | 57.4 | 0.57 ($0^o$) |

a. Anion-exchange membrane pre-soaked in concentrated solution of MX.

b. KCl concentration ratio was 0.01/0.001 in all cases. Ionic strength was equalized with salt in which membrane was soaked except for KCl, KI, and KSCN in which cases it was adjusted with $KNO_3$.

c. Ref. 96.

TABLE 4

SOLVENT TRANSPORT CORRECTION FOR ANION MEMBRANE

Cell: Ag;AgCl/KCl($m_i$)/A/$^{a}$KCl($m_r$)/AgCl;Ag

| $m_i \times 10^2$ | $\gamma_i$ [b] | $\sqrt{m_i m_r} \times 10^2$ | -E(mv.)[c] | n | s | 99% confidence interval, E (mv.)[d] |
|---|---|---|---|---|---|---|
| 0.09995 | 0.9653 | 0.31615 | 5.77 | 4 | 0.510 | ±1.489 |
| 0.3001 | 0.9423 | 0.5479 | 3.19 | 6 | 0.288 | ±0.474 |
| 1.000[e] | 0.9021 | 1.000 | -0.387 | 6 | 0.172 | ±0.283 |
| 3.000 | 0.8481 | 1.7320 | -3.31 | 8 | 0.301 | ±0.372 |
| 9.999 | 0.7696 | 3.1622 | -8.21 | 10 | 0.314 | ±0.323 |
| 19.998 | 0.719 | 4.4719 | -10.59 | 6 | 0.656 | ±1.08 |
| 1.000 | 0.9021 | 1.000 | -0.353 | 8 | 0.545 | ±0.674 |

a. Anion-exchange membrane in nitrate form.

b. Molal activity coefficients calculated from eqn. 12-1-9, ref. 45, p. 490.

c. Observed EMF corrected to 25° C.

d. Confidence intervals calculated from sample size n and sample standard deviation s (ref. 67, p. 540).

e. Reference solution for all 6 experiments.

FIGURE 4

OBSERVED EMF OF KCl CONCENTRATION CELL WITH ANION-MEMBRANE JUNCTION IN THE $NO_3^-$ FORM

Cell: $Ag;AgCl/KCl(m_i)/A/KCl(m_r)/AgCl;Ag$

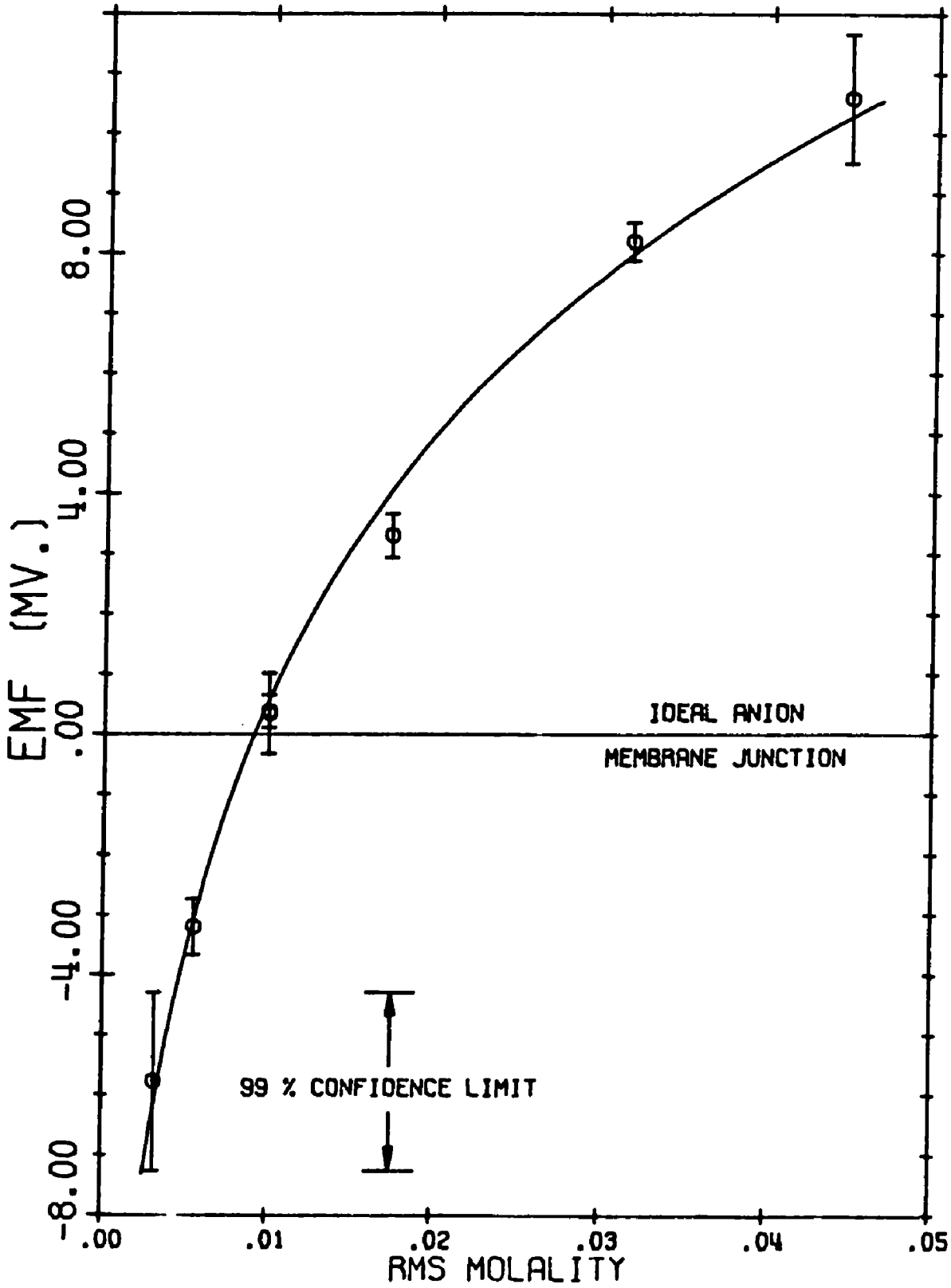
The data are shown in Table 4.

Abscissa - RMS molality, $\sqrt{m_i m_r}$

Ordinate - observed EMF with $m_r = 0.01$

The error bars represent 99 per cent confidence limits. The horizontal line at EMF = 0.0 represents the EMF across an ideal liquid junction saturated with the ions to which the electrodes are reversible.

# FIGURE 4


EMF (MV.)
8.00
4.00
.00
-4.00
-8.00
.00
.01
.02
.03
.04
.05
RMS MOLALITY
IDEAL ANION
MEMBRANE JUNCTION
99 % CONFIDENCE LIMIT

represents an empirical solvent transport correction that could be subtracted from the total EMF observed for a specific kind of concentration cell. The corrections determined from Fig. 4 would be applicable to a concentration cell containing cation-selective electrodes and the same kind of liquid junction, i.e., an anion-exchange membrane in the $NO_3^-$ form.

Modified Hittorf method

Control Experiments Without Current Flow.--In preparation for the measurement of transference numbers by this method, two control experiments were performed. The first consisted of measurement of the solution resistance changes on both sides of a cation-exchange membrane when no current was passed. The Ag-AgCl electrodes were short-circuited and the cell was left to stand with stirring for an hour at three different KCl concentrations. The results are shown in Table 5. At the highest concentration the resistance changes in the two solutions nearly complement each other. At the lower concentrations the resistance decreased on both sides and was a larger fraction of the total resistance. In a second control experiment, the change in total resistance of the transference cell was measured at three different KCl concentrations. The results are shown in Table 6. The total resistance decreased over a period of 20 to 30 min. even before the passage of current. After the current was turned on, the total resistance continued its downward trend but there were occasional increases probably due to temperature fluctuations. These results demonstrate that control experiments are

TABLE 5

SOLUTION RESISTANCE CHANGES IN 4.5 ML. CELL
WITH ELECTRODES SHORT-CIRCUITED[a]

Cell: $Ag;AgCl/KCl(m_1)/C/^{b}KCl(m_1)/AgCl;Ag$

| KCl $m_1$ | RESISTANCE (ohms)[c] Original solution | Side A[f] | Side B[f] | % change A | % change B |
|---|---|---|---|---|---|
| 0.0022 | 14,477.5[d] | 14,343.0 | 14,209.0 | -0.93 | -1.85 |
| 0.010 | 3274.2[d] | 3262.3 | 3236.1 | -0.36 | -1.16 |
| 0.100 | 728.30[e] | 727.50 | 728.85 | -0.11 | +0.08 |

a. Electrodes short-circuited for one hour with stirring.

b. Cation-exchange membrane soaked overnight in KCl solution of concentration $m_1$.

c. Resistance measured with Beckman RC-18A Conductivity Bridge with conductivity cell immersed in water bath at 25.00° C.

d. Conductivity cell had cell constant of 4.62.

e. Conductivity cell had cell constant of 9.37.

f. "A" and "B" designate respectively the left and right sides of the cell which was oriented the same way in all experiments.

TABLE 6

TOTAL RESISTANCE CHANGE OF 4.5 ML. CELL
WITH PASSAGE OF CURRENT

Cell: $Ag;AgCl/KCl(m_1)/C/^{a}KCl(m_1)AgCl;Ag$

| KCl $m_1$ | Current (ma.) | RESISTANCE (ohms)[b] Initial | Final | Duration (min.) | % change |
|---|---|---|---|---|---|
| 0.0019 | 0.025 | 26,920 | 25,632 | 70 | -4.78 |
| 0.03 | 0.020 | 3675 | 3471 | 86 | -5.55 |
| 0.10 | 0.025 | 2510 | 2413 | 45 | -3.86 |

a. Cation-exchange membrane soaked overnight in KCl solution of concentration $m_1$.

b. Resistance measured with Beckman RC-18A conductivity bridge with 4.5 ml. cell at ambient temperature.

necessary to estimate the solution composition changes that are not due to current flow and electrolyte transference.

Measurements with Current Flow.--Preliminary measurements of the resistance changes associated with the passage of current through the 4.5 ml. cell are shown in Table 7. The resistance changes shown in the last two columns clearly do not complement each other. With the capillaries in the vertical position, there was no detectable movement of the menisci. During several hour-long runs with the horizontal capillary arrangement, the meniscus did not appear to move when current was passed. During other runs the meniscus moved but it did not change direction when the current was reversed.

EMF method

Eq. (21) on p. 21 was used to estimate cation and water transference numbers from the EMF of several KCl concentration cells. The KCl concentration ratio was varied from 1 to 8 and the RMS molality was varied from 0.005 to 0.10. The composition and observed EMF, $E_o$, for 36 concentration cells are shown in Table 8.

Time Dependence.--Some of the EMF measurements with the 4.5 ml. cell exhibited a time dependence. Three typical time profiles of the EMF measurements are illustrated in Fig. 5. The dashed lines indicate the type of extrapolation employed for each profile. The "zero time" was arbitrarily but consistently defined as the mid-point of the cell filling process. Ideally, the extrapolation procedure should yield the EMF corresponding to the minimum diffusion

TABLE 7

SOLUTION RESISTANCE CHANGES ON PASSING CURRENT THROUGH 4.5 ML. CELL

Cell: $Ag;AgCl/KCl(m_1)/C/^{a}KCl(m_1)/AgCl;Ag$

| Experiment | KCl molality | Initial current $\mu$a. | Final current[b] $\mu$a. | Number of coulombs passed | RESISTANCE (ohms)[c] Original solution | Side A | Side B | Change side A | Change side B |
|---|---|---|---|---|---|---|---|---|---|
| 1 | 0.01 | 20 | 20 | 0.0378 | 3432 | 3394 | 3555 | -38 | +123 |
| 2 | 0.01 | 100 | 150 | 0.225[d] | 3275 | 3208 | 3470 | -67 | +195 |
| 3[e] | 0.01 | 25 | 25 | 0.045 | 3393 | 3339 | 3340 | -54 | -53 |

a. Cation-exchange membrane soaked overnight in 0.01 molal KCl.

b. Current was passed for 30 minutes and was measured with a Simpson 260 milliammeter.

c. Solution resistance was measured with LKB 3216B Conductivity Bridge and conductivity cell with cell constant of 4.62.

d. Assuming a linear variation of current between initial and final values.

e. Different membrane with a coarser Dynel backing.

TABLE 8

MOLAL CONCENTRATIONS AND OBSERVED EMF

Cell: Ag;AgCl/KCl($m_1$)/C/[a]KCl($m_2$)/AgCl;Ag

| No. | $m_1$ x 100 | $m_2$ x 100 | $E_0$(mv.)[b] | No. | $m_1$ x 100 | $m_2$ x 100 | $E_0$(mv.)[b] |
|---|---|---|---|---|---|---|---|
| 1 | 0.4985 | 0.4985 | 0.03 | 19 | 3.478 | 7.106 | 33.43 |
| 2 | 4.071 | 4.071 | -0.03 | 20 | 7.106 | 14.16 | 31.67 |
| 3 | 0.3761 | 0.6983 | 30.38 | 21 | 7.108 | 14.21 | 31.77 |
| 4 | 0.3761 | 0.6983 | 30.57 | 22 | 7.108 | 14.21 | 31.43 |
| 5 | 0.3582 | 0.7172 | 34.33 | 23 | 7.114 | 14.27 | 31.83 |
| 6 | 0.3582 | 0.7172 | 34.28 | 24 | 2.551 | 10.06 | 64.18 |
| 7 | 0.3571 | 0.7303 | 35.03 | 25 | 2.551 | 10.06 | 64.38 |
| 8 | 0.3571 | 0.7303 | 34.99 | 26 | 2.379 | 9.837 | 66.75 |
| 9 | 0.2593 | 1.012 | 67.24 | 27 | 5.773 | 20.68 | 58.43 |
| 10 | 0.2617 | 1.034 | 67.85 | 28 | 5.043 | 19.63 | 62.45 |
| 11 | 0.2617 | 1.034 | 67.87 | 29 | 5.043 | 20.14 | 63.22 |
| 12 | 0.1813 | 1.414 | 101.32 | 30 | 1.778 | 14.10 | 97.03 |
| 13 | 0.1813 | 1.414 | 101.45 | 31 | 1.785 | 14.25 | 96.86 |
| 14 | 0.1723 | 1.479 | 106.16 | 32 | 1.785 | 14.25 | 97.11 |
| 15 | 3.082 | 5.433 | 26.66 | 33 | 1.786 | 14.31 | 97.47 |
| 16 | 3.649 | 7.129 | 31.30 | 34 | 3.498 | 28.68 | 95.98 |
| 17 | 3.649 | 7.129 | 32.32 | 35 | 3.478 | 28.70 | 96.30 |
| 18 | 3.539 | 7.062 | 31.77 | 36 | 3.605 | 29.29 | 96.21 |

a. Cation-exchange membrane pre-soaked overnight in 1:1 mixture of molality $m_1$ and $m_2$.

b. $E_0$ = observed EMF corrected to 25° C.

FIGURE 5

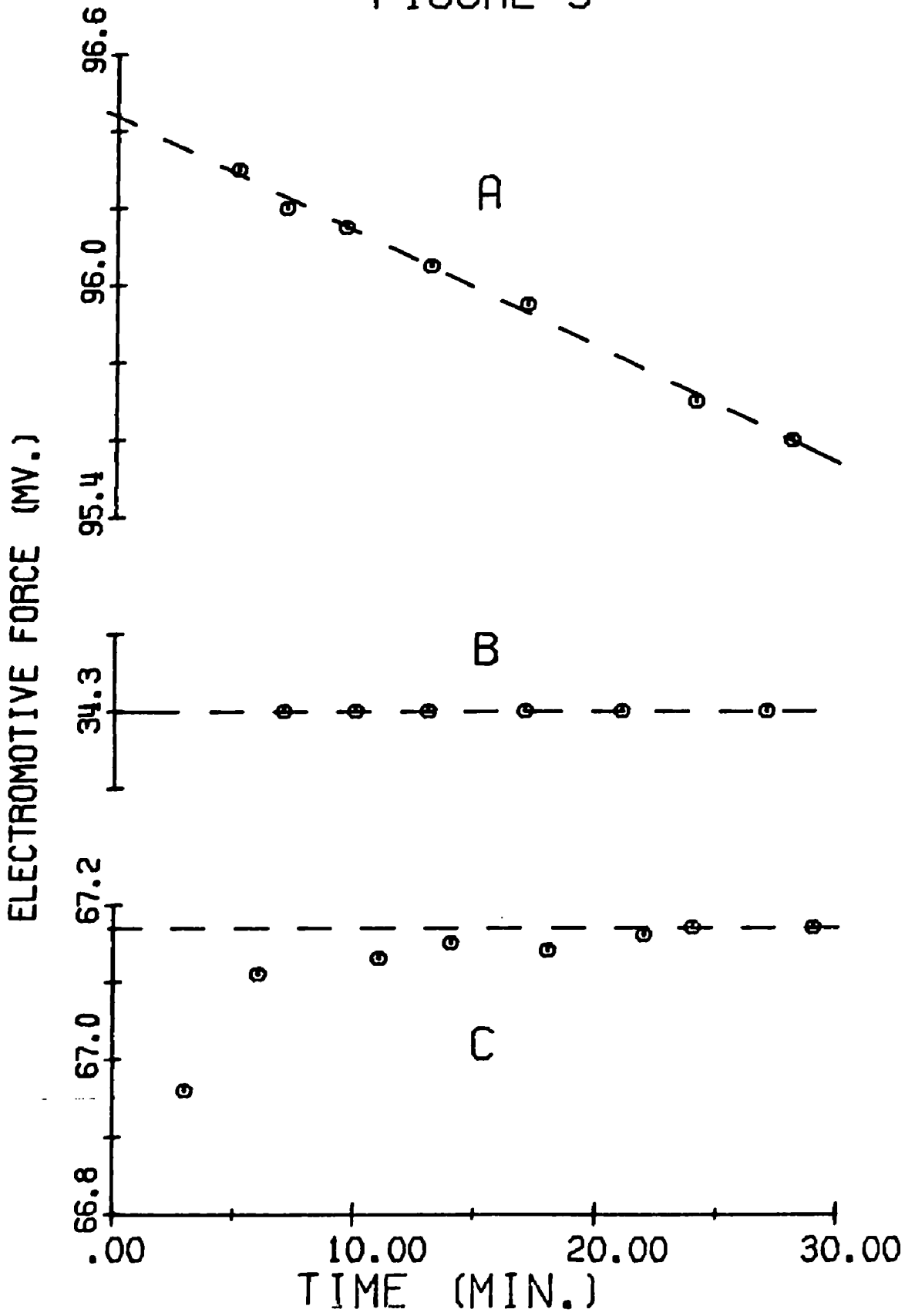
THREE REPRESENTATIVE TIME PROFILES

OF THE CONCENTRATION CELL EMF

Cell: Ag;AgCl/KCl($m_1$)/C/KCl($m_2$)/AgCl;Ag

EMF measurements were made in 4.5 ml. cell with magnetic stirring bars. Cation-exchange membrane C had been pre-soaked overnight in a 1:1 mixture of solutions of concentrations $m_1$ and $m_2$. Membrane-solution interface was circular with a diameter of 9 mm.

FIGURE 5


96.6
96.0
95.4
A
34.3
B
67.2
67.0
66.8
C
ELECTROMOTIVE FORCE (MV.)
.00
10.00
20.00
30.00
TIME (MIN.)

film thickness at the membrane-solution interface. About 50 per cent of the time profiles were of type A. These occurred almost exclusively at concentrations of 0.05 m and higher. The slopes varied from -0.02 mv. per min. to -0.2 mv. per min. with the steeper slopes occurring at the higher concentration ratios. About 25 per cent of the profiles were of type B. These occurred exclusively at concentrations of 0.05 and lower. The remaining 25 per cent of the profiles were of type C. The type C profiles appeared to be uniformly distributed with respect to RMS concentration and concentration ratio. There were 3 EMF-time profiles which did not exhibit the unimodality of types A, B, or C and they were therefore discarded.

Cation Transference Number.--For a cell with an ideal membrane junction, the first term on the right in eq. (21) is zero since $t^+ = 1.00$. The magnitude of this term for the data in Table 8 was examined. The ideal EMF, $E_I$, was calculated from eq. (20), and the difference $E_I - E_0$ was plotted against the quantity ($m_B \ln a_B - m_A \ln a_A$) which will be abbreviated $\Delta$(m ln a). Three least-squares regression lines were calculated for the data sets corresponding to concentration ratios of 2, 4, and 8. The results of the least-squares regressions are shown in Table 9.

TABLE 9

CALCULATED SLOPES AND INTERCEPTS FOR $E_I$-$E_0$ vs. $\Delta$(m ln a)

| Conc. ratio | No. of points | $E_I$-$E_0$ intercept (mv.) | Slope (mv.) |
|---|---|---|---|
| 2 | 17 | 0.153 | 4.047 |
| 4 | 9 | 0.087 | 3.807 |
| 8 | 10 | 0.133 | 4.663 |

The individual points and the 3 regression lines are shown in Fig. 6. The values of $t^+$ estimated from eq. (21) and the intercepts of the regression lines in Table 9 were greater than unity, but they differed from unity by less than 0.5 per cent. Comparison of the three regression lines in pairs (ref. 67, p. 571) indicated that the variances, slopes, and intercepts did not differ significantly at the 5 per cent level. On this basis, the regression lines corresponding to the concentration ratios 2, 4, and 8 appear to be identical.

Water Transference.--A separate estimate of the slope $2RTM_1 t_w / 1000f$ for each of the 36 concentration cells was computed. In order to balance the weighting effect of points located far from the origin, the point corresponding to the mean abscissa and mean ordinate in Fig. 6 was selected as the computing origin. The value of the slope for each point was multiplied by $1000f/2RTM_1 = 1.08$ moles per (mv. faraday) to obtain an estimate of the water transference number $t_w$. The values of the physical constants used in the above calculation were f = 96,487 coulombs per mole and R = 8.3143 joules per (deg. mole) (72). The values of $\Delta$(m ln a), $E_I - E_0$, and $t_w$ for each concentration cell are shown in Table 10. The value of $t_w$ is plotted against the RMS molality $\sqrt{m_1 m_2}$ for each point in Fig. 7. The dashed line in Fig. 7 is a least-squares regression line through the points. Application of the t-test described by Hald (ref. 67, p. 540) indicated that the slope of the regression line in Fig. 7 does not differ significantly from zero. On this basis, the water transference number appears to be constant

FIGURE 6

DEVIATION OF OBSERVED EMF FROM IDEAL EMF

AS A FUNCTION OF KCl CONCENTRATION

Cell: $Ag;AgCl/KCl(m_1)/C/KCl(m_2)/AgCl;Ag$

Same conditions as in Figure 5. Data from Table 8.

Abscissa - $(m_2 \log a_2 - m_1 \log a_1)$ where

$m_i$ is KCl molality and $a_i$ is

KCl activity calculated with activity coefficients from ref. (45), p. 490.

Ordinate - difference in mv. between ideal EMF calculated with eq. (20) and observed EMF.

Solid lines represent least-squares regression lines through data points corresponding to concentration ratios, CR = 2, 4, and 8, respectively.

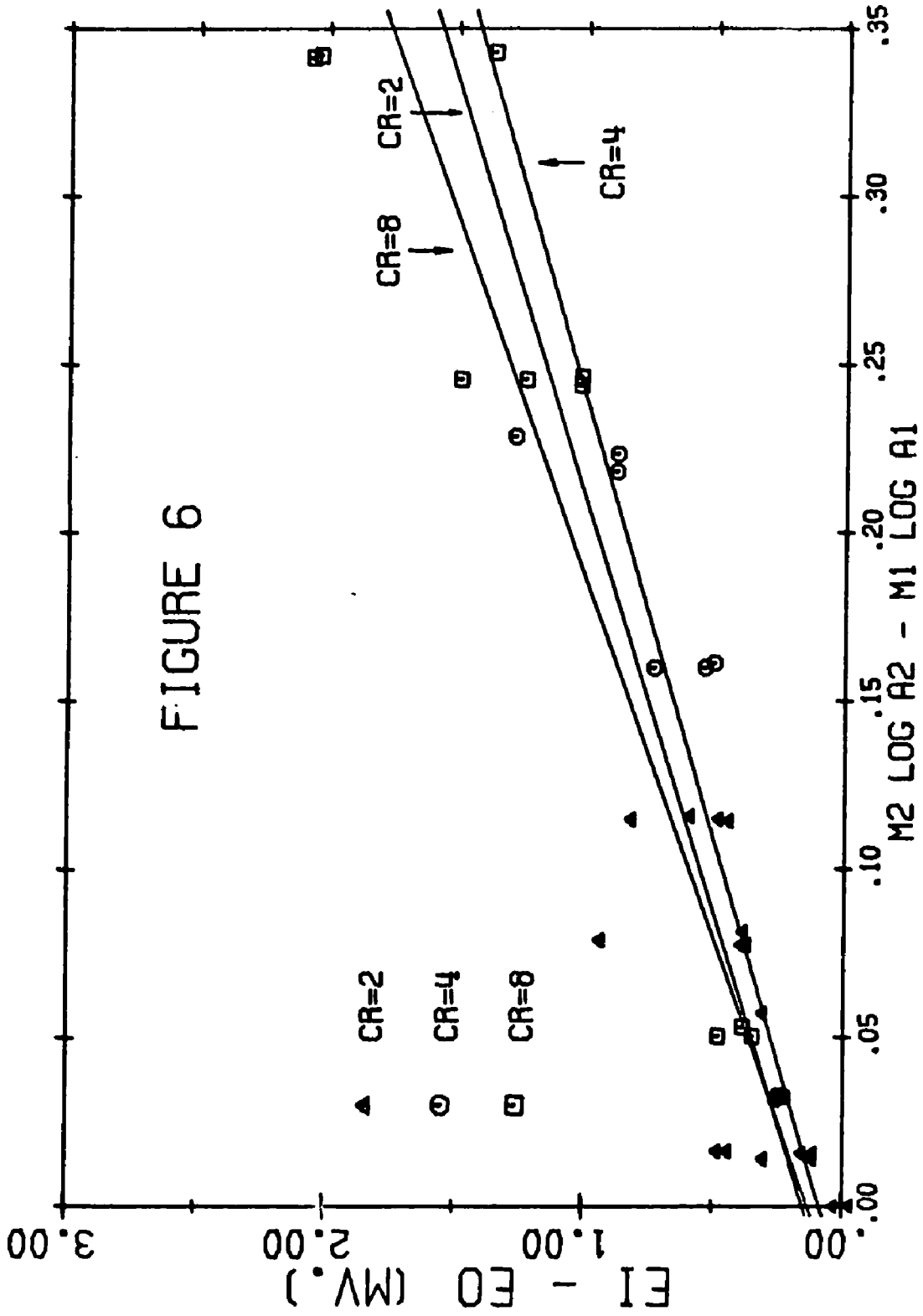

FIGURE 6
EI - EO (MV.)
3.00
2.00
1.00
.00
M2 LOG A2 - M1 LOG A1
.00
.05
.10
.15
.20
.25
.30
.35
CR=2
CR=4
CR=8
CR=2
CR=4
CR=8

TABLE 10

CONCENTRATION, EMF, AND TRANSFERENCE DATA FOR PAIRS OF SOLUTIONS IN TABLE 8

| No. | CD x 100[a] | $E_I - E_O$[b] | $t_w$[c] | No. | CD x 100 | $E_I - E_O$ | $t_w$ |
|---|---|---|---|---|---|---|---|
| 1 | 0.000 | 0.030 | 6.08 | 19 | 8.140 | 0.386 | 7.25 |
| 2 | 0.000 | -0.030 | 5.54 | 20 | 11.44 | 0.444 | 36.6 |
| 3 | 1.403 | 0.304 | 3.50 | 21 | 11.49 | 0.481 | 33.1 |
| 4 | 1.403 | 0.114 | 5.43 | 22 | 11.49 | 0.818 | -33.5 |
| 5 | 1.565 | 0.111 | 5.54 | 23 | 11.57 | 0.591 | 13.1 |
| 6 | 1.565 | 0.153 | 5.10 | 24 | 15.99 | 0.734 | 2.35 |
| 7 | 1.622 | 0.442 | 2.13 | 25 | 15.99 | 0.537 | -3.03 |
| 8 | 1.622 | 0.482 | 1.73 | 26 | 16.12 | 0.501 | -3.89 |
| 9 | 3.193 | 0.255 | 4.80 | 27 | 21.82 | 0.883 | 2.59 |
| 10 | 3.265 | 0.248 | 4.93 | 28 | 22.35 | 0.880 | 2.43 |
| 11 | 3.265 | 0.227 | 5.19 | 29 | 22.88 | 1.274 | 6.24 |
| 12 | 5.039 | 0.481 | 2.57 | 30 | 24.39 | 1.023 | 3.28 |
| 13 | 5.039 | 0.350 | 4.60 | 31 | 24.57 | 1.486 | 7.23 |
| 14 | 5.308 | 0.388 | 4.18 | 32 | 24.57 | 1.235 | 5.06 |
| 15 | 5.721 | 0.309 | 5.79 | 33 | 24.64 | 1.022 | 3.21 |
| 16 | 7.746 | 0.395 | 6.36 | 34 | 34.13 | 2.066 | 6.94 |
| 17 | 7.746 | 0.372 | 6.94 | 35 | 34.19 | 2.037 | 6.78 |
| 18 | 7.897 | 0.937 | -7.53 | 36 | 34.29 | 1.362 | 3.47 |

a. $CD = m_2 \log a_2 - m_1 \log a_1$. Activity coefficients calculated with eq. 12-1-9, ref. 45, p. 490.

b. $E_I$ = ideal EMF calculated from eq. (20). $E_O$ = observed EMF. $E_I$ and $E_O$ are in mv.

c. $t_w$ = water transference number in moles/faraday calculated from eq. (21).

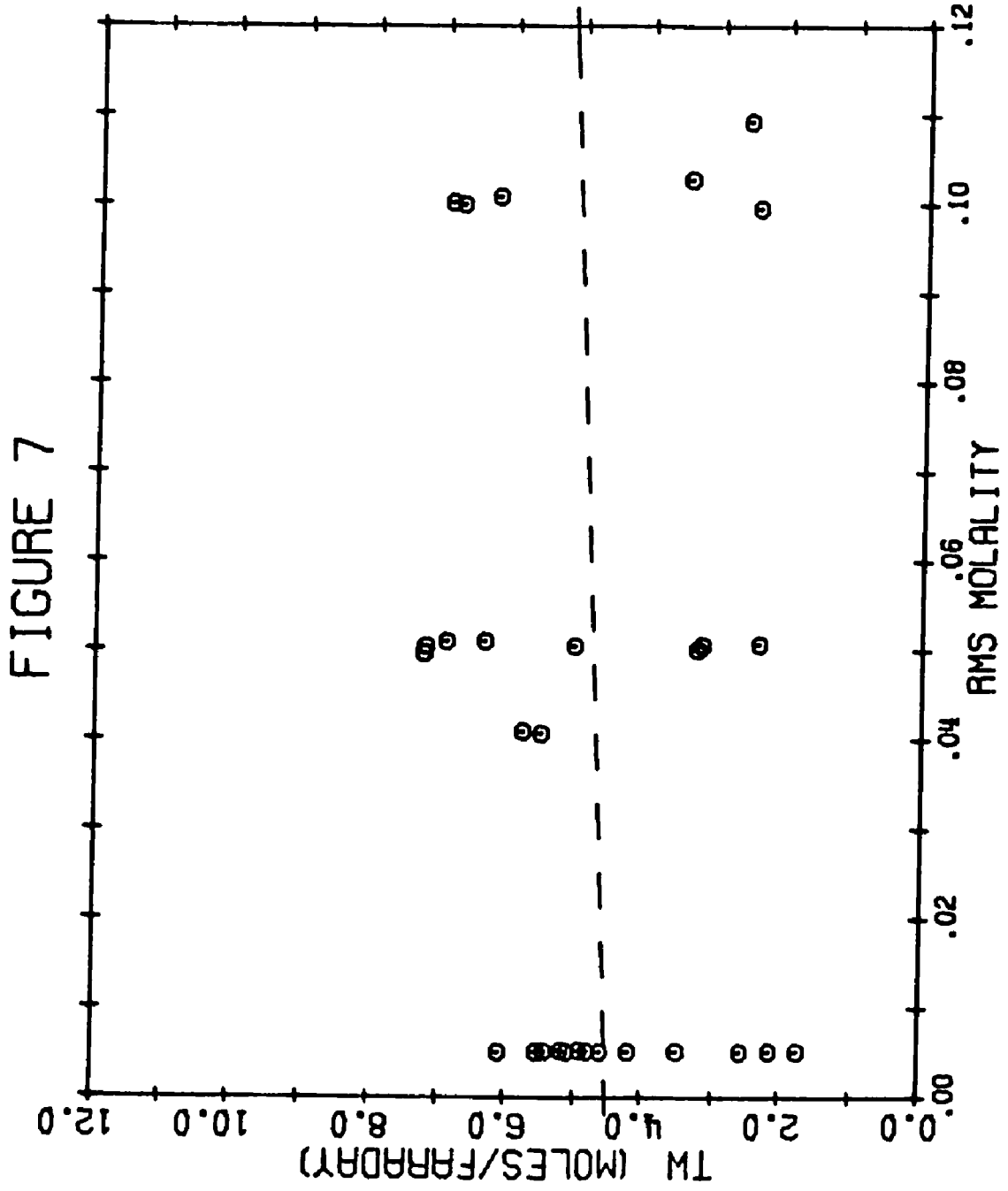
FIGURE 7

DEPENDENCE OF WATER TRANSFERENCE NUMBER $t_w$

ON RMS MOLALITY OF KCl CONCENTRATION CELL

Data from Table 10.

The dashed line represents a least-squares regression line through the points.


FIGURE 7
RMS MOLALITY
.00
.02
.04
.06
.08
.10
.12
TW (MOLES/FARADAY)
0.0
2.0
4.0
6.0
8.0
10.0
12.0

over the RMS molality range 0.005 to 0.10. The overall mean of $t_w$ is 4.50 $\pm$ 0.67 moles per faraday.

## Effects of Macromolecular Solutes on Ag-AgCl Electrodes

The effects of dissolved dextran, dextran sulfate, amylose, and colloidal silica on the potential difference between Ag-AgCl electrodes were studied. In these experiments ion-exchange membranes were not present at the liquid junction between half-cells. Instead, cells with capillary liquid junctions were used.

### Polysaccharides

The results of the EMF measurements in solutions of dextran and amylose are shown in Table 11. The EMF observed with the fractionated dextran solution was lower than that of its dialyzate. When the potentials of the potato amylose solution and its dialyzate were compared, no difference between the two could be detected. The amylose solution was slightly turbid but its dialyzate was clear. In order to determine if any hydrolysis of the amylose had occurred, the dialyzate was analyzed spectrophotometrically for the presence of monosaccharides by the phenol-$H_2SO_4$ method (54). A 0.3 M KCl solution was used as the blank. After addition of the reagents, the dialyzate had an absorbance of 0.20 at 490 nm. On a glucose calibration curve, this absorbance value corresponded approximately to a concentration of 12 $\mu$g. per ml. as glucose in the dialyzate. The amylose had apparently been hydrolyzed to a small extent by the 0.5 N KOH which was used to dissolve it.

TABLE 11

EFFECTS OF DISSOLVED POLYSACCHARIDES ON THE POTENTIAL DIFFERENCE BETWEEN SILVER-SILVER CHLORIDE ELECTRODES

Cell: $Ag;AgCl/\frac{KCl\ (sat.)}{+\ AgCl\ (sat.)}$ [a] //KCl (sat.)// [b] KCl solution with or without polysaccharide /AgCl;Ag [c]

| Polysaccharide | $M_w$ [d] | Weight % | KCl molality | ELECTROMOTIVE FORCE (mv.) Outer solution [e] | Inner solution [e] | Difference |
|---|---|---|---|---|---|---|
| Dextran | 113,000 | 1.76 [f] | 0.05 | 104.83 | 104.47 | -0.36 |
| | | | 0.05 | 106.12 | 105.48 | -0.64 |
| Dextran sulfate | 500,000 | 1.61 [f] | 0.05 | 105.55 | 108.44 | 2.89 [h] |
| Amylose | | 0.43 [g] | 0.27 | 66.90 | 66.90 | 0.00 |

a. Asbestos fiber liquid junction.
b. Density-stabilized capillary liquid junction.
c. Electrode was coated with collodion for dextran sulfate measurements.
d. Values of weight-average molecular weight furnished by Pharmacia, Uppsala, Sweden.
e. Inner and outer solutions from a 48-hour dialysis against an equal volume of water.
f. Determined by weighing polysaccharides as supplied by Pharmacia.
g. Determined by dry weight measurement after dissolving amylose.
h. Drifted over 0.4 mv. range, then became unstable.

Polyelectrolytes

The results of EMF measurements in solutions of dextran sulfate and colloidal silica are shown in Tables 11 and 12, respectively. The EMF values observed with both polyelectrolyte solutions appeared to be higher than those of their dialyzates. The EMF difference between the various colloidal silica solutions and their corresponding dialyzates exhibited a pH dependence. The EMF difference was smallest near pH 6.6 and largest near 9.7. The experimental points are shown in Fig. 8 along with an exponential regression curve of the form $y = A \exp(B(x-\bar{x}))$. The calculated values of the coefficients were A = 0.781, B = 0.493, and the residual variance of fit was 0.00011.

TABLE 12

EFFECTS OF COLLOIDAL SILICA ON THE POTENTIAL DIFFERENCE BETWEEN SILVER-SILVER CHLORIDE ELECTRODES

Cell: Ag;AgCl/ KCl (sat.) + AgCl (sat.) a //KCl (sat.)// b KCl solution with or without colloidal silica[c] /AgCl;Ag[d]

| Meq. HCl added[e] | pH[f] Before dialysis | pH[f] After dialysis[g] | KCl molality | ELECTROMOTIVE FORCE (mv.) Outer solution | Inner solution | Difference |
|---|---|---|---|---|---|---|
| 0.0 | 9.72 | 9.73 (outer)<br>9.70 (inner) | 0.05 | 106.90 | 108.50 | 1.60 |
| 0.1635 | 8.03 | 8.21<br>8.41 | 0.05 | 104.05 | 104.90 | 0.85 |
| 0.2641 | 6.01 | 6.56<br>6.65 (turbid) | 0.05 | 104.27 | 104.62 | 0.35 |

a. Asbestos fiber liquid junction.
b. Density-stabilized capillary liquid junction.
c. "Ludox SM-30" supplied by DuPont Co., Wilmington, Del. Approximate particle diameter was 7-8 nm., according to supplier. Sample was diluted to a weight concentration of 2.2%.
d. Electrode coated with collodion.
e. 0.610 N HCl delivered from 5.00 ml. Manostat buret graduated in 0.01 ml.
f. pH measured with glass electrode, Ag-AgCl reference electrode, and Beckman Research pH Meter standardized at pH 6.86 and pH 9.18 with Harleco buffer salt mixtures.
g. 52-hour dialysis against an equal volume of water.

FIGURE 8

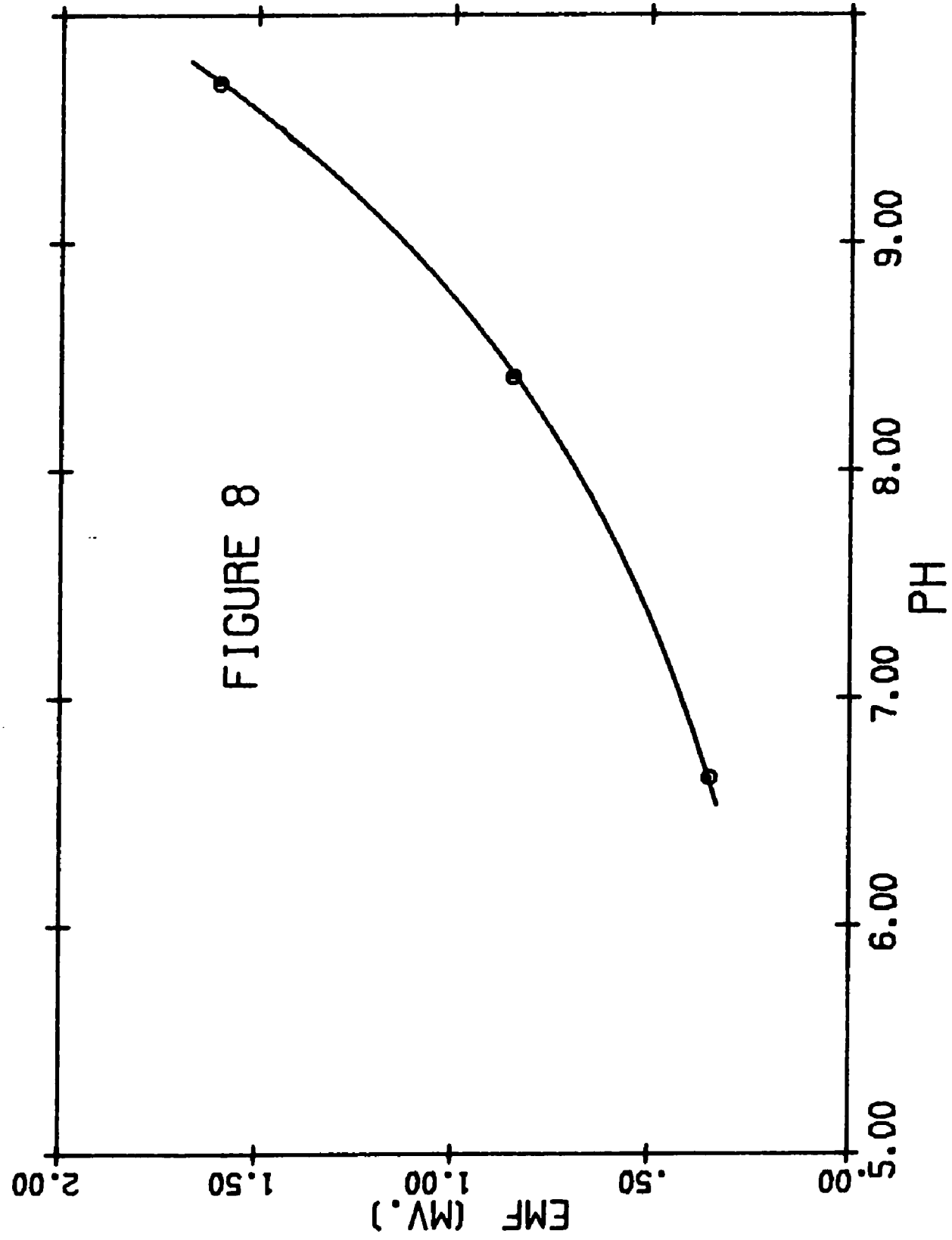
EMF DIFFERENCE BETWEEN COLLOIDAL SILICA SOLUTIONS AND THEIR DIALYZATES AS A FUNCTION OF pH

Data from Table 12.

The abscissa is the pH of a colloidal silica solution in 0.05 M KCl after 48 hour dialysis at room temperature. The curve represents the exponential regression model

$$y = A \exp(B(x - \bar{x}))$$

where $y = \Delta$ EMF, $x$ = pH, $A = 0.781$, and $B = 0.493$.


FIGURE 8
EMF (MV.)
2.00
1.50
1.00
.50
.00
5.00
6.00
7.00
8.00
9.00
PH

# DISCUSSION

## Solvent Transference

### Comparison with previous work

Brydges determined the solvent transference number of PVBS membranes by measuring the solution volume changes associated with the passage of electrical current (60). He reported difficulties similar to those of this study in stabilizing the menisci in the capillaries prior to the passage of current. Brydges attributed the instability of the menisci to uncontrollable movements of the gaskets. This did not affect the reliability of his results because he measured the solution volume changes by weighing the cell before and after draining out the solutions. This could not have been done accurately in the present study since the solutions constituted only 2.3 per cent of the weight of the entire cell (ca. 390 g.).

For PVBS membranes of the type used in this study, Brydges reported a water transference number of $8.42 \pm 0.40$ moles per faraday over the concentration range 0.01 to 0.10 molal (60). If Brydges' value is used to estimate the expected volume change in the transference experiments of Table 7, the result is $3.5 \times 10^{-4}$ cc. In the capillary used for the transference experiments, this volume change should result in a meniscus displacement of 1.8 mm., a change easily detectable in the viewing telescope. However, meniscus displacement consistent with the flow of current was not observed in the transference experiments of the present study. This led to the conclusion that occluded bubbles or other mechanical

problems were interfering with proper connection between the solutions and the solution limbs in the valves and capillaries.

In the present study, the water transference number $t_w$ was estimated from the EMF of KCl concentration cells containing cation-exchange membranes. The result was 4.50 $\pm$ 0.67 moles per faraday over the RMS concentration range 0.005 to 0.10 m. This value is about half the value obtained by Brydges using a modified Hittorf method (60). Hills (68) has pointed out that the near-equilibrium conditions of an EMF measurement are considerably different from those associated with the ionic and electro-osmotic fluxes set up during a Hittorf experiment. Transference numbers determined from EMF measurements might therefore be expected to be closer to the ideal, limiting values than those determined by the Hittorf method. Rosenberg, et al. (31) measured cation transference numbers by both methods and found this to be the case. The value of $t_w$ determined in the present study is in good agreement with the minimum hydration number of the $K^+$ ion (ref. 45, p. 546).

Reproducibility of EMF measurements

Membrane Symmetry.--There are two kinds of membrane structural effects which could contribute to marginal reproducibility of the EMF measurements. The first is the possibility of directional asymmetry in the membranes. The relative effects on the mean EMF of reversing a membrane and of replacing one membrane with another in the same cell were shown in Table 2. The differences between the orientation means were approximately the same as the overall

standard deviation of the EMF measurements (0.39 mv.). In contrast, the difference between the membrane means was greater than the overall standard deviation by a factor of 3. The relative contributions of the orientation effect and of the membrane effect to the total variation of the EMF were examined by a two-factor analysis of variance described by Bowker and Lieberman (ref. 120, p. 928). The value of the variance ratio corresponding to the membrane effect was significant at the 5 per cent level, but that corresponding to the orientation effect was not. Given an overall standard deviation of 0.39 mv., the observed EMF variation between different orientations could have occurred by chance. On the other hand, the variation between membranes was sufficiently great that it is not likely to have occurred by chance. The effect on the EMF of reversing a membrane does not appear to be greater than that of replacing one membrane with another.

Membrane heterogeneity.--A second possible membrane structural effect is the physical heterogeneity of the membranes. The ion-exchange resin was cast on a 20-mesh Dynel screen. Since the junction cross-section of the 0.45 ml. cell was about twice as wide as the Dynel mesh (see Fig. 2), small misalignments of the membrane could alter appreciably the nature of the liquid junction.

Leaching.--There are two possible leaching effects involving the ion-exchange membranes. The first is the possible presence of residual plasticizer in the membranes. Before the membranes were used as liquid junctions, they were extensively leached with HCl, KOH, and KCl solutions and rinsed with distilled water until the

rinsings had an absorbance less than 0.01 in the wavelength range 210 to 350 nm. A second factor which could have contributed to the resistance changes in Table 5 is the leaching of salt from the membrane into the solution. This is plausible because the solution in which the membrane was soaked prior to an experiment was usually not stirred. The formation of an appreciable salt concentration gradient near the membrane surface could offer a very different ionic environment than a well-stirred salt solution. When the presoak solution was stirred, results similar to those of Table 5 were obtained. Brydges (60) measured the resistance changes of salt solutions containing membranes which had been used in transference experiments. He observed the same resistance changes in the soaking solution whether or not a current had been passed through the membrane. On this basis Brydges discounted the leaching of salt from the membrane as a source of variation in solution resistance.

Evaporation.--Brydges (60) observed that when the membrane area was reduced by a factor of four, the resistance change in the soaking solution was reduced by a factor of two. He interpreted this as evidence for evaporation from the circumference of the membrane resulting in the uptake of water from the solution. In the present study, the circumference of the membrane was invariant with the area of the membrane-solution interface. The freshly-cut edges of the membranes in the present study were usually sealed with a hot soldering gun to retard evaporation. In order to determine the importance of evaporation, the solution resistance changes using membranes with sealed and unsealed edges were compared. When the

rectangular gasket which fit around the edges of the membrane was omitted, the resistance changes using the membrane with unsealed edges were about 25 per cent larger than when using the membrane with sealed edges. When the gasket was in place there was no appreciable difference between the two. This demonstrates that evaporation from the edges of the membrane is not a likely source of EMF variation as long as the rectangular gasket is in place.

Electrical Heating Effect.--The amount of heat generated in the transference cell due to the passage of current can be estimated from

$$H = RI^2t/4.18 \qquad (24)$$

where H is the amount of heat in calories, R is the resistance in ohms, I is the current in amperes, and t is the duration of current flow in seconds. The total resistance of the transference cell containing 0.01 m KCl was 2595 ohms with the membrane and 2382 ohms without the membrane. At this salt concentration the solution resistance appears to be about ten times greater than the membrane resistance. If the membrane resistance is assumed to be 200 ohms and if a current of $10^{-4}$ ampere is passed for 30 min., as in Table 7, the calculated value of H is about 0.001 calorie. If this amount of heat is confined to the disc of membrane (9 mm. in diameter, 0.6 mm. thick) adjoining the two solutions, the temperature change as estimated from the definition of specific heat is 0.07° C. The corresponding calculation for the salt solutions results in an

estimated temperature change of 0.001° C. The amount of heat generated in the transference cell by the passage of current appears to be small relative to other sources of temperature variation such as convection and conduction.

Pressure Variation.--The two half-cells were held together with brass nuts and bolts. There was no observable effect on the cell EMF over the range of pressures attainable with screwdriver and wrench tightening.

Electrode Surface Strain.--Electrodes for the EMF studies were prepared by the method of Greyson (55) in which Ag is electrolytically deposited on an AgCl surface. MacFarlane and Hartley (73) reported a difference of 1.7 mv. between electrolytic Ag electrodes and granular Ag electrodes. It has been suggested that electrolytically deposited Ag may be subject to surface strain which affects the electrode potential (74, 75). Thermally-deposited granular Ag, on the other hand, is nearly strain-free since it has been annealed during the process of deposition. If appreciable surface strain exists in electrolytically deposited Ag electrodes, such as those used in this study, it would be very difficult to either control or evaluate its effect on the observed EMF.

Dissolution at the Electrode Surface.--Janz and Ives (76) have pointed out that the electrolytic chloridation method may leave a slowly-dispersing excess of $Cl^-$ on the electrode surface. In addition, proper functioning of an Ag-AgCl electrode requires that the solution in the immediate vicinity of the electrode be saturated with AgCl. If this condition is not met, the electrode may become

stripped of its AgCl coating (119). It is known that Ag is capable of forming stable complexes with amino and sulfhydryl functional groups (77). Brush, et al. (78), have reported the results of a study of the binding of $Ag^{110}$ to albumin. Janz and Ives (76) have suggested that if such Ag complexes are sufficiently stable, the solubility equilibrium of AgCl could be irreversibly shifted in the direction of dissolution from the electrode surface resulting in ultimate electrode failure. It should be possible to test this hypothesis by using albumin in which the sulfhydryl group(s) and the $\epsilon$-amino groups have been chemically modified.

Collodion Layer.--It was found in the present study that the performance of Ag-AgCl electrodes in protein solutions could usually be improved by coating the electrodes with a thin layer of collodion. This treatment did not always leave the electrode unchanged in comparison to its behavior in dilute salt solutions. There are at least two problems introduced by the collodion treatment. The first has to do with the collodion itself. The improvement in electrode performance in protein solutions is presumably due to a significant difference between the diffusion rate of the protein in the collodion and in free solution. If this difference is significant for the electrolytes as well, a phenomenon analogous to concentration polarization may develop. Concentration polarization is described as the inability of ions to diffuse toward or away from an electrode as rapidly as they are being consumed or produced (79). It is also associated with an EMF opposed to the electrode EMF. The presence of concentration polarization at an electrode can be

detected by a test for reversibility, such as a cyclic micropolarization test (76, 80). The second problem raised by the collodion treatment involves the organic solvent. In the present study, the electrode was briefly dipped into a methanol-ether solution of collodion. There is evidence that organic solvents may be selectively adsorbed to the electrode surface resulting in electrode poisoning. One of the few documented cases is that of acetone, which in low concentrations, has been reported to have an adverse effect on the Ag-AgCl electrode (76).

Solution Agitation.--Solution agitation appears to be one of the most important factors affecting the accuracy and reproducibility of EMF measurements with ion-exchange membranes. Scatchard and Helfferich observed changes on the order of 5 mv. across solution-equilibrated membranes when the stirring was alternately started and stopped (81). When the membrane was not in ion-exchange equilibrium with the solutions, changes as large as 90 mv. could be produced by starting and stopping the stirring.

Such EMF variations have been interpreted in terms of time-dependent changes in the activity gradients between membrane and solution (82). In the bulk solution the concentrations of cations and anions are equal and their transference numbers are of the same order of magnitude. In a high charge capacity, ion-exchange membrane, the concentration and transference number of one ion are very much larger than those of the other ion (24). Between the bulk solution and the membrane there is presumably a region in which these quantities vary. If terms for the membrane-solution activity

gradients are included, eq. (11d), p. 17, can be written

$$\frac{Ef}{RT} = -\ln\frac{\bar{a}_B}{\bar{a}_A} - \bar{t}^+ \ln\frac{a_B^{+\prime}}{a_A^{+\prime}} + t^+ \ln\frac{a_B^+}{a_B^{+\prime}} + t^+ \ln\frac{a_A^{+\prime}}{a_A^+} \qquad (25)$$

where $\bar{t}^+$ is the cation transference number within the membrane, $t^+$ is the corresponding value in the bulk solution, the unprimed activities $a_A^+$ and $a_B^+$ are the cation activities in the two bulk solutions, and the primed activities $a_A^{+\prime}$ and $a_B^{+\prime}$ are the corresponding values at the membrane surfaces. The transference numbers in eq. (25) refer to the solvent as a stationary frame of reference. The first term corresponds to the difference between the electrode potentials, the second term to the membrane potential, and the third and fourth terms to the contribution of the transition layers to the cell EMF.

One of the assumptions required for the integration of eq. (17) for any cell is that the differences $(a_A^+ - a_A^{+\prime})$ and $(a_B^+ - a_B^{+\prime})$ are negligible relative to the difference $(a_B^+ - a_A^+)$. If this assumption is valid, the contribution of the third and fourth terms of eq. (25) to the total EMF will be negligible compared to that of the first two terms. If the assumption is not valid, the observed EMF will be less by an amount proportional to the logarithm of the total activity gradient which is not localized in the membrane.

If the bulk solution is undergoing forced convection or agitation, the flow rate decreases continuously into the interfacial region (83). At sufficiently low solution velocities and in regions of small enough dimensions, solute diffusion predominates over convective transport (ref. 84, p. 52). Some years ago, Nernst (85)

postulated the existence of a layer of defined thickness at the solid-liquid interface in which solute transport occurs exclusively by diffusion. This concept is clearly an idealization, but it has proven useful for the description of many diffusion phenomena at solid-liquid interfaces (83, 86).

A number of investigators have attempted to estimate the thickness of the Nernst diffusion layers between ion-exchange membranes and the bulk solution (60, 87). Brydges, in particular, has estimated the diffusion film thickness as a function of stirring rate in PVBS membrane cells (60). He concluded that the thickness of the diffusion film depended on the stirring rate, the solution viscosity, and the solute diffusion coefficient. The estimated thickness of the diffusion film decreased from 500 microns to about 50 microns as the stirring rate was increased from 0 to 800 r.p.m. It appears that the thickness of the diffusion layers can be reduced by increasing the stirring rate, but it is apparently not possible to do away with them entirely by stirring alone. Glueckauf and Watts were able to detect a diffusion layer of finite thickness even after blotting an equilibrated membrane with filter paper (88).

The existence of an interfacial region between membrane and solution in which activity gradients are localized has important consequences for the observed EMF of a cell. If the thickness of the interfacial regions can be reduced only to a finite minimum by vigorous stirring, then the contribution of the third and fourth terms of eq. (25) to the total EMF may not be negligible. This imples that there is a limiting EMF value which would not change

with an increase in solution agitation (81). The accuracy and reproducibility of any EMF less than the limiting value would depend on the effectiveness and reproducibility of the solution agitation.

Scatchard and Orttung (82) studied the behavior of the EMF of a cation-membrane cell in which the solutions were either flowing or agitated by squeezing a Saran bulb. They observed a difference of 1 mv. in the EMF extrapolated to zero time for the two cases. They interpreted this to mean that stirring with a Saran bulb was not as efficient as agitation with flowing solutions (82). With a method of agitation that is not efficient enough to insure a limiting EMF value, as defined above, the validity of comparisons between different sets of measurements (e.g., with and without protein) may be impaired.

Evidently, the most reproducible EMF value is the limiting value which does not change when the stirring rate is increased. Attainment of the limiting EMF value requires vigorous, efficient solution agitation. This is best achieved by directing a jet of solution at high velocity either obliquely against the face of the membrane or normal to the face of the membrane (89). The glass turbine cell used by Scatchard and Helfferich appears to be a satisfactory means for accomplishing this (81). Neither syringe injection nor magnetic stirring as employed in the present study were sufficiently vigorous to give a limiting EMF value. In the absence of a limiting EMF value, the reproducibility of the EMF would depend strongly on the reproducibility of the solution agitation. It is likely that the difficulty of maintaining uniform solution agitation

throughout a series of experiments is a major reason for the marginal reproducibility of the EMF measurements in the present study.

## Effects of Macromolecular Solutes on Ag-AgCl Electrodes

### Polysaccharides

The results of EMF measurements in solutions of several polysaccharides were shown in Table 11. The smaller EMF observed with the dextran solution relative to its dialyzate indicates that the KCl activity was higher in the dextran solution than in the dialyzate. This does not necessarily indicate a preferential interaction between dextran and KCl. Aqueous dextran solutions have an appreciable colloid osmotic pressure (90, 91) and there is physical evidence that dissolved dextran is extensively hydrated (92). It is likely that the effect of dextran on the KCl activity ratio is a secondary consequence of the interaction between dextran and water.

A concept which is sometimes useful in the interpretation of phenomena in polymer solutions is that of the θ-temperature or θ-solvent. Tanford (28) has expressed the chemical potential $\mu_1$ of the solvent in a two-component solution as

$$\mu_1 - \mu_1^{\circ} = -RTKx_2(1 + Bx_2 + Cx_2^2 \ldots) \qquad (26)$$

where $\mu_1^{\circ}$, R, and K are constants and $x_2$ is the solute concentration. The θ-temperature or θ-solvent for a given polymer-solvent pair will be defined for the purposes of the present discussion as

the set of conditions under which B = 0 and the higher-order terms are negligible. The phenomenon of the θ-temperature or θ-solvent is usually conceived in terms of a balance between the physical excluded volume of a polymer molecule and the intra-molecular attractive forces (28). Different segments of the same polymer molecule physically exclude each other from the volume elements which they occupy. In a θ-solvent the preference for segment-segment interactions over segment-solvent interactions is sufficient to cancel the effect of the physical exlcuded volume.

Everett and Foster have reported that 0.33 M KCl is a θ-solvent for potato amylose at 25° C (93). In the present study, when the EMF of a 0.43 per cent potato amylose solution in 0.27 M KCl was compared to that of its dialyzate, no difference could be observed (see Table 11). In principle, the EMF should assume a non-zero value if either the temperature or composition is varied relative to that of the θ-solvent. This could not be tested experimentally because the second virial coefficient B does not change very rapidly with changes in temperature or composition (93).

## Polyelectrolytes

The effects of macro-ions on the potential of Ag-AgCl electrodes were also studied. The results for dextran sulfate were shown in Table 11 and those for colloidal silica were shown in Table 12. The EMF observed with solutions of dextran sulfate and colloidal silica was greater than that of their respective dialyzates. This indicates that the activity of KCl in the macro-ion

solution was lower than in the dialyzates. This observation agrees qualitatively with predictions of the theory of the Donnan equilibrium (94).

A notable feature of the effect of colloidal silica on the EMF was its pH dependence (see Table 12). The pH of a 1:10 dilution of the commercial sample of colloidal silica in 0.1 M KCl was 9.72. As the pH was decreased by the addition of HCl, the EMF difference between solution and dialyzate appeared to decrease exponentially over the pH range 9.7 to 6.5. Iler (95) has estimated that the isoelectric point of colloidal silica is between pH 4 and 5. While the regression curve in Fig. 8 is not inconsistent with Iler's estimate, the available data points do not offer a firm basis for extrapolation below pH 6.5. Data points at pH values less than 6.0 cannot be obtained at this ionic strength (ca. 0.05) because of the tendency of the colloidal silica to precipitate.

# III. COMPUTER SIMULATION OF ION DISTRIBUTION AROUND MACRO-IONS

## INTRODUCTION

Much of the preceding sections has been concerned with the comparison of theoretical and experimental EMF values. The calculation of theoretical EMF values requires either independent information or a priori assumptions about the variation of transference numbers and chemical potentials. The interpretation of experimental EMF values is frequently complicated by unknown liquid junction potentials. The purpose of this section is to examine protein-electrolyte interactions by the computer simulation of small-ion distributions around a macro-ion.

## THEORY

### The Poisson-Boltzmann Equation

The theory of the radial dependence of the electrostatic potential and of the charge distribution around a charged sphere has been rigorously treated elsewhere (28). For the purpose of the present study, it will be sufficient to outline the development of the Poisson-Boltzmann equation and the numerical method for its solution.

The electrostatic potential $\psi$ at any point is defined as the work required to bring a unit positive charge from an infinite distance, where the electrostatic forces are assumed to the zero, up to the specified point. In a volume element containing both positive and negative ions, the net charge per unit volume or the

net charge density $\rho$ is given by

$$\rho = e(z_+ n_+ - z_- n_-) \tag{27}$$

where e is the electronic charge, $n_+$ and $n_-$ are the local concentrations of the respective ions in number of ions per $cm.^3$, and $z_+$ and $z_-$ are their respective valences. In the space surrounding a given reference ion, one relationship between $\psi$ and $\rho$ is provided by Poisson's equation

$$\rho = -\frac{D}{4\pi}\left[\frac{1}{r^2}\frac{d}{dr}\left(r^2\frac{d\psi}{dr}\right)\right] \tag{28}$$

where D is the dielectric constant of the medium and r is the radial distance from the center of the reference ion. The local concentrations $n_+$ and $n_-$ are related to the corresponding bulk concentrations $n_+^o$ and $n_-^o$ by the Boltzmann distribution law

$$n_\pm = n_\pm^o \exp\left(\mp\frac{z_\pm e\psi}{kT}\right) \tag{29}$$

If equations (28) and (29) are substituted into eq. (27), a form of the Poisson-Boltzmann equation is obtained.

$$\frac{1}{r^2}\frac{d}{dr}\left(r^2\frac{d\psi}{dr}\right) = -\frac{4\pi e}{D}\left[z_+ n_+^o \exp\left(-\frac{z_+ e\psi}{kT}\right) - z_- n_-^o \exp\left(\frac{z_- e\psi}{kT}\right)\right] \tag{30}$$

Transformation of Variables

In order to facilitate the numerical solution of eq. (30), several transformations of variables are made. First, a dimensionless distance variable x is defined by

$$x = 1/\varkappa\, r \tag{31}$$

where $\varkappa$ is the Debye-Hückel reciprocal length which for a uni-univalent electrolyte is defined as

$$\varkappa^2 = 8\pi e^2 cN/1000\ DkT \tag{32}$$

In eq. (32) N is Avogadro's number and c is the electrolyte concentration in equivalents per 1000 cm.$^3$ The transformation indicated in eq. (31) was introduced by Müller (98) and has the advantage that integrations can be performed on the finite interval $0 < x < x_o$ where $x_o = 1/\varkappa\, a$ in which "a" is the radius of a sphere around the reference ion from which other ions are excluded. A dimensionless potential variable is defined as

$$y = e\Psi/kT \tag{33}$$

In the bulk solution, the different concentration variables are related by

$$z_+ n_+^o = z_- n_-^o = cN/1000 \tag{34}$$

If equations (31), (32), (33), and (34) are substituted into equation (30), the Poisson-Boltzmann equation in terms of the dimensionless variables x and y becomes

$$d^2y/dx^2 = (e^y - e^{-y})/2x^4 \tag{35}$$

for a solution of a uni-univalent electrolyte.

Eq. (35) relates the potential y at a point to the distance x of the point from the reference ion. In addition to this relation, it is necessary to have a function which characterizes the cumulative charge distribution in the space surrounding the reference ion. Wiersema (102) has defined a surface charge density function $\sigma(r)$ as

$$\sigma(r) = -\frac{1}{4\pi r^2}\int_r^\infty \rho(4\pi r^2)\,dr \tag{36}$$

where $\sigma(r)$ has the dimensions esu/cm.$^2$ If equations (27) and (29) are substituted into eq. (36)

$$\sigma(r) = -\frac{e}{r^2}\int_r^\infty \left[z_+ n_+^\circ \exp\left(-\frac{e\Psi}{kT}\right) - z_- n_-^\circ \exp\left(\frac{e\Psi}{kT}\right)\right] r^2\,dr \tag{37}$$

Substituting equations (32), (33), (34), and $q = \varkappa r$ into eq. (37) results in

$$\sigma(q) = \frac{DkT\varkappa}{4\pi e}\, I(q) \tag{38}$$

where

$$I(q) = \frac{1}{q^2} \int_{q}^{\infty} \frac{e^{y} - e^{-y}}{2} q^2 \, dq \tag{39}$$

Making the transformation q = 1/x gives the result

$$I(x) = x^2 \int_{0}^{x} \frac{e^{y} - e^{-y}}{2x^4} \, dx \tag{40}$$

Of particular importance for the numerical computations is the relationship between the value of the function I and the surface charge density $\sigma$ at the exclusion radius. Substituting the value of $\chi$ from eq. (32) into eq. (38) gives the result

$$\sigma(a) = \left( \frac{DkTcN}{2000\pi} \right)^{1/2} I(a) \tag{41}$$

Loeb, et al. (99) used the following values of the physical constants in eq. (41)

$$k = 1.38026 \times 10^{-16} \text{ ergs/deg.}$$

$$D = 78.54$$

$$N = 6.02380 \times 10^{23}$$

resulting in

$$\sigma(a) = 1.7603 \times 10^{4} \sqrt{c} \, I(a) \tag{42}$$

at 25° C.

## METHODS

### Numerical Solution of the Poisson-Boltzmann Equation

An iterative method for the solution of second-order differential equations of the same form as eq. (35) was developed by Cowell and Crommelin (100) and reviewed by Milne (101). The essential feature of the method is a one-step double integration instead of two consecutive integrations which give the first derivative and function value separately.

### Wiersema's method

The iterative method as used in the present study was described by Wiersema (102). Briefly, the method is as follows: the reduced electrostatic potentials $y_1$ and $y_2$ at two points far from the reference ion are calculated from the Debye-Hückel approximation, eq. (43), in Table 13. A value of the variable $S_n$ is then calculated from eq. (47). This is followed by an iterative process consisting of two steps: (1) the calculation of $y_n$ from eq. (49) using an estimated value of the second derivative $y''_n$ and (2) substitution of the result into eq. (44) to obtain an improved estimate of $y''_n$. The iterative process is continued until the difference between two successive estimates of $y''_n$ does not exceed a certain limit. Improved estimates of the reduced surface potential $y_o$, an integration constant Y, and a space charge distribution function $I_o$, are obtained on successive iterations. The iterative process is summarized in detail in Table 13 and Fig. 9.

TABLE 13

SUMMARY OF WIERSEMA'S ALGORITHM FOR NUMERICAL SOLUTION OF THE POISSON-BOLTZMANN EQUATION[a]

E Q U A T I O N S

$$y(DH) = Y(x/x_o)\exp(1/x_o - 1/x) \quad (43)$$

$$y''_n = (e^{y_n} - e^{-y_n})/2x_n^4 \quad (44)$$

$$S_1 = y_1/h^2 - y''_1/12 \quad (45)$$

$$S_2 = y_2/h^2 - y''_2/12 \quad (46)$$

$$S_n = 2\,S_{n-1} - S_{n-2} + y''_{n-1} \quad (47)$$

$$y''_k = 2y''_{k-1} - y''_{k-2} \quad (48)$$

$$y_n = h^2\,(S_n + y''_n/12 - \ldots) \quad (49)$$

SYMBOLS

$x$ = $1/\varkappa$ r, r = radial distance from center of reference ion

$x_o$ = $1/\varkappa$ a, a = radius of exclusion

$y$ = $e\psi/kT$

$y''_n$ = value of second derivative of y at nth value of x

$y''_k$ = kth estimate of $y''_n$

$y(DH)$ = Debye-Hückel approximation to y

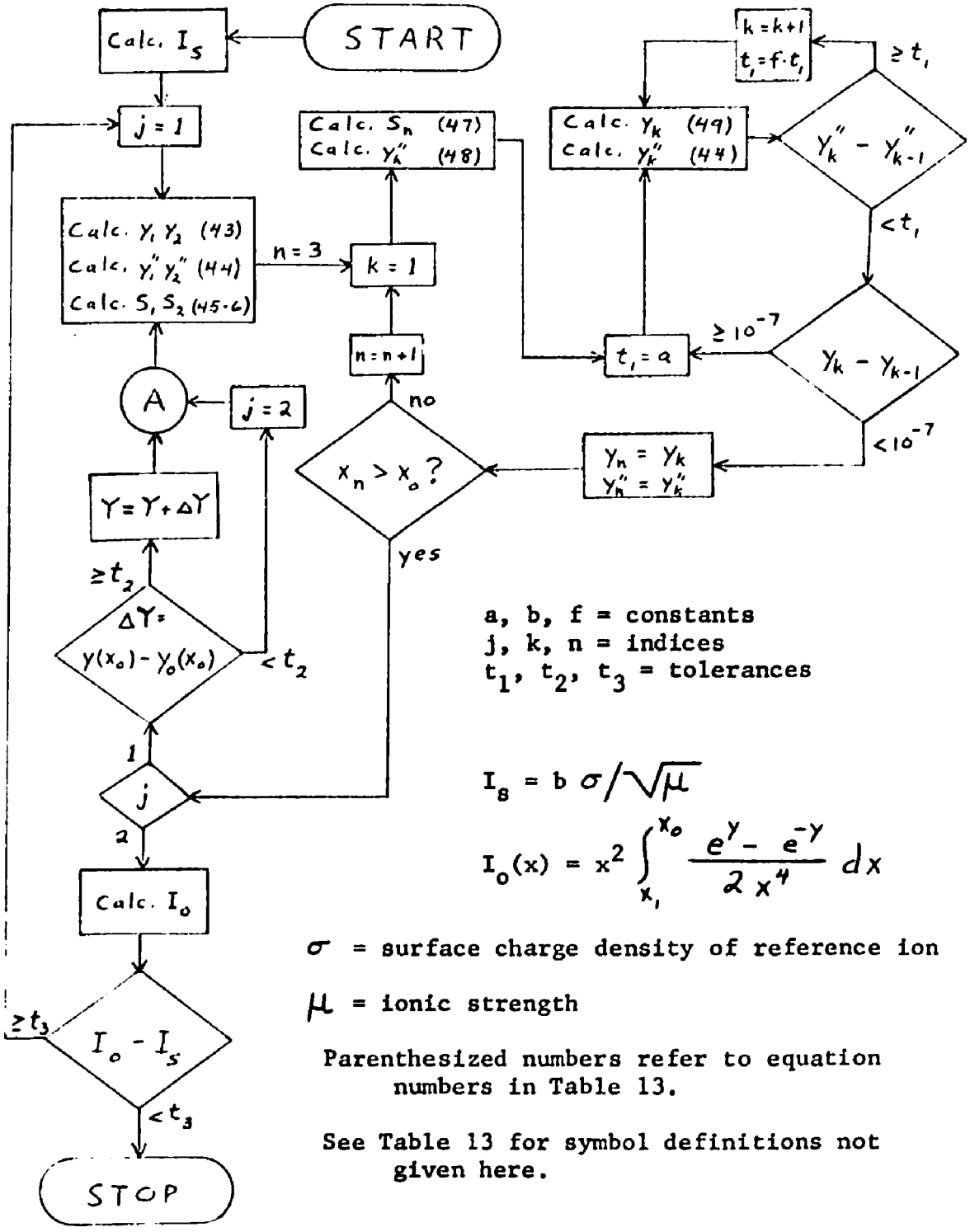
$Y$ = an integration constant

$h$ = integration interval

a. Ref. 102, pp. 66-71.

FIGURE 9

FLOW CHART OF WIERSEMA'S ALGORITHM FOR NUMERICAL SOLUTION OF THE POISSON-BOLTZMANN EQUATION




a, b, f = constants
j, k, n = indices
$t_1$, $t_2$, $t_3$ = tolerances

$$I_s = b\,\sigma/\sqrt{\mu}$$

$$I_o(x) = x^2 \int_{x_1}^{x_o} \frac{e^{Y} - e^{-Y}}{2x^4}\,dx$$

$\sigma$ = surface charge density of reference ion

$\mu$ = ionic strength

Parenthesized numbers refer to equation numbers in Table 13.

See Table 13 for symbol definitions not given here.

Truncation error

The computed values of y are subject to a truncation error because eq. (49) in Table 13 contains only two terms of the series given by Milne (101). The error is proportional to the second difference of the second derivative, $\Delta^2 y''$, which occurs in the first term deleted from the series. The second difference $\Delta^2 y''$ is proportional, in turn, to the square of the integration interval, $h^2$. Wiersema provided for an automatic reduction of the integration interval by a factor of 5 whenever the value of $\Delta^2 y''$ exceeded a certain limit (102). In the range of $x_o$ values encountered in the present study, Loeb, et al. (99) did not decrease the integration interval until the reduced surface potential $y_o$ attained a value of 6. All the values of $y_o$ encountered in the present study were less than 6. In the present study, the integration interval was held constant at a value such that there were at least 50 points between $x_1$ and $x_o$.

Calculation of Ion Distributions

Once the iterative procedure yielded a satisfactory set of potential values as a function of distance from the reference ion, the Boltzmann distribution law, eq. (29), was used to estimate the local concentrations of cations and anions.

Interpolation

Although the spacing between x-values in the present study was usually not altered for purposes of the iterative process, it did

prove expedient to interpolate after the iterative process was completed. As with most numerical procedures, the discrete nature of the solution may impose restrictions on certain applications of the results. In order to increase the ability to resolve small differences in concentration, 4 and sometimes 9 points were interpolated between consecutive points calculated from the iterative process. Whereas Wiersema employed a Lagrange interpolation when he decreased the integration interval (102), a finite difference interpolation was employed in the present study. The latter method has the advantage that less computing time is required when a large number of points must be interpolated with the same set of data (103). A difference table extending through the 4th order differences was constructed and stored in the computer. Newton's forward formula was used over the first interval of the table, Newton's backward formula over the last interval of the table, and the Gauss forward formula was employed over the interior intervals. A 3rd degree interpolating polynomial using 4 base points from the original set of data was employed. At the end of the table, where y changes most rapidly as a function of x, an estimate of the interpolation error was computed from the 4th order difference, i.e., the first term dropped from the interpolating polynomial.

## Integration

After additional points had been interpolated between the (x, y) values obtained from the iterative process, several numerical integrations were performed. A precoded program in the IBM

System 360 Scientific Subroutine Package (104) was used for this purpose. The specific subroutine used was DQSF which performs a numerical integration of an equidistantly tabulated function using Simpson's rule

$$\int_{x_1}^{x_3} y\,dx = \frac{h}{3}\left[y_1 + 4y_2 + y_3\right] \tag{50}$$

and Newton's 3/8 rule

$$\int_{x_1}^{x_4} y\,dx = \frac{3h}{8}\left[y_1 + 3y_2 + 3y_3 + y_4\right] \tag{51}$$

The local truncation error for both of these methods is on the order of $h^5$ (104, 105). In order to test the accuracy of subroutine DQSF, the descending exponential function $e^{-x}$ was integrated over the interval 0 to 1 with an integration sub-interval of 0.01538. This sub-interval is nearly identical to that used in most of the integrations of the (x, y) values. According to the above estimate the local truncation error is approximately $8.7 \times 10^{-10}$. Using double precision arithmetic, the numerical integration with subroutine DQSF gave 0.63212 05746 for the value of the integral and an analytical integration gave 0.63212 05588. The absolute error is $1.58 \times 10^{-8}$ or about 20 times larger than the estimated local truncation error. This indicates that there is some accumulation of local truncation errors but it appears that no more than the eighth significant figure of the result is affected. For a function whose integration properties are similar to

those of the descending exponential, the error involved in the integration with subroutine DQSF should be small compared to other sources of error.

## Calculation of Free Ion Concentrations

In the classical treatment of the Donnan equilibrium, it is assumed that the average concentration of ions is related to the average electrostatic potential (94). In studies of ion distribution around charged colloids (99, 102, 110) and in the present study, the local ion concentrations are related to the local potentials before any averages are taken. The following paragraphs describe a new method for averaging the local ion concentrations and for obtaining a unique estimate of the free ion concentration.

### Stoichiometric estimate

The definition of the protein component used in the present study is essentially that proposed by Scatchard and Bregman (106). The chemical formula corresponding to their definition is

$$Na_{\frac{\nu-h}{2}}\left(H_h P Cl_\nu\right) Cl_{\frac{h-\nu}{2}} \qquad (52)$$

where P represents the isoionic protein, h the number of bound H ions, and $\nu$ the number of bound Cl ions. A protein component of this composition might be formed from an $m_2$ molal isoionic albumin solution when NaCl and NaOH are added up to molalities of $m_3$ and $m_7$, respectively. The concentrations of free ions ($Na^+$) and ($Cl^-$)

were calculated from

$$(Na^+) = m_3 + m_7 + ((\nu - h)/2)m_2 \quad (53)$$

$$(Cl^-) = m_3 + ((h - \nu)/2) - \nu)m_2 \quad (54)$$

Estimation from ion distributions

Protein Model.--Equations (53, 54) provide a purely stoichiometric estimate of the free ion concentrations. In addition to this, values of the ion concentrations that are related to the volume and average charge of the protein molecule can be estimated. Since the shape, volume, and average charge of protein molecules are generally unknown, these properties must be calculated from a model. A simple yet apparently satisfactory model for globular proteins is a uniformly charged sphere (107). Specifically, a sphere with a radius of 30 Å appears to offer an adequate model of the serum albumin molecule (29). In solutions containing ions such as $Na^+$ and $Cl^-$, the exclusion radius is about 2.5 Å greater, or 32.5 Å. This value of the exclusion radius determines the upper limit $x_o$ of the reduced distance variable x. The lower limit $x_1$ of x is determined by the average distance between protein molecules. This distance can be estimated from the protein concentration and from a postulated distribution of protein molecules. In the present study, a distribution suggested by McMenamy (43) is used. The postulated distribution is derived from the closest-packed configuration of uniform spheres in which each sphere has

twelve nearest neighbors (ref. 108, p. 673). It is assumed that an exploded form of this configuration offers a reasonable approximation to the average distribution of protein molecules in solution. The average distance d between protein molecules was calculated from

$$d = \left( \frac{1000 \times 1.4}{N c_2} \right)^{1/3} \tag{55}$$

where N is Avogadro's number and $c_2$ is the protein concentration in moles per $cm^3$. The factor 1.4 in eq. (55) is the factor by which the radius of a sphere with the same volume as a given cube must be increased in order for the sphere to circumscribe the cube.

Averaging Procedure.--The procedure for estimating an average free $Cl^-$ concentration from the $Cl^-$ distribution is illustrated in Fig. 10. The projection of the $Cl^-$ distribution on the vertical line AB is treated as a one-dimensional mass with non-uniform density (109). The y-coordinate C of the one-dimensional center of mass is calculated from

$$C = \int_A^B y \rho \, dy \Big/ \int_A^B \rho \, dy \tag{56}$$

where y is the local $Cl^-$ concentration in equivalents per 1000 $cm.^3$ and $\rho$ is the one-dimensional mass density. The estimate of the average free $Cl^-$ concentration is equated to C. This procedure weights the $Cl^-$ in the space between the protein molecules more heavily than the $Cl^-$ close to the protein molecules. In this

FIGURE 10

METHOD FOR ESTIMATION OF FREE ION CONCENTRATIONS

FROM ION DISTRIBUTIONS

Abscissa - distance in Ångstroms from center of reference ion

Ordinate - local ion concentrations in $\mu$eq./cc. calculated from Boltzmann equation

A = maximum value of $Cl^-$ concentration

B = minimum value of $Cl^-$ concentration

C = one-dimensional center of mass of line AB calculated from eq. (56) using abscissa as variable 'density'.

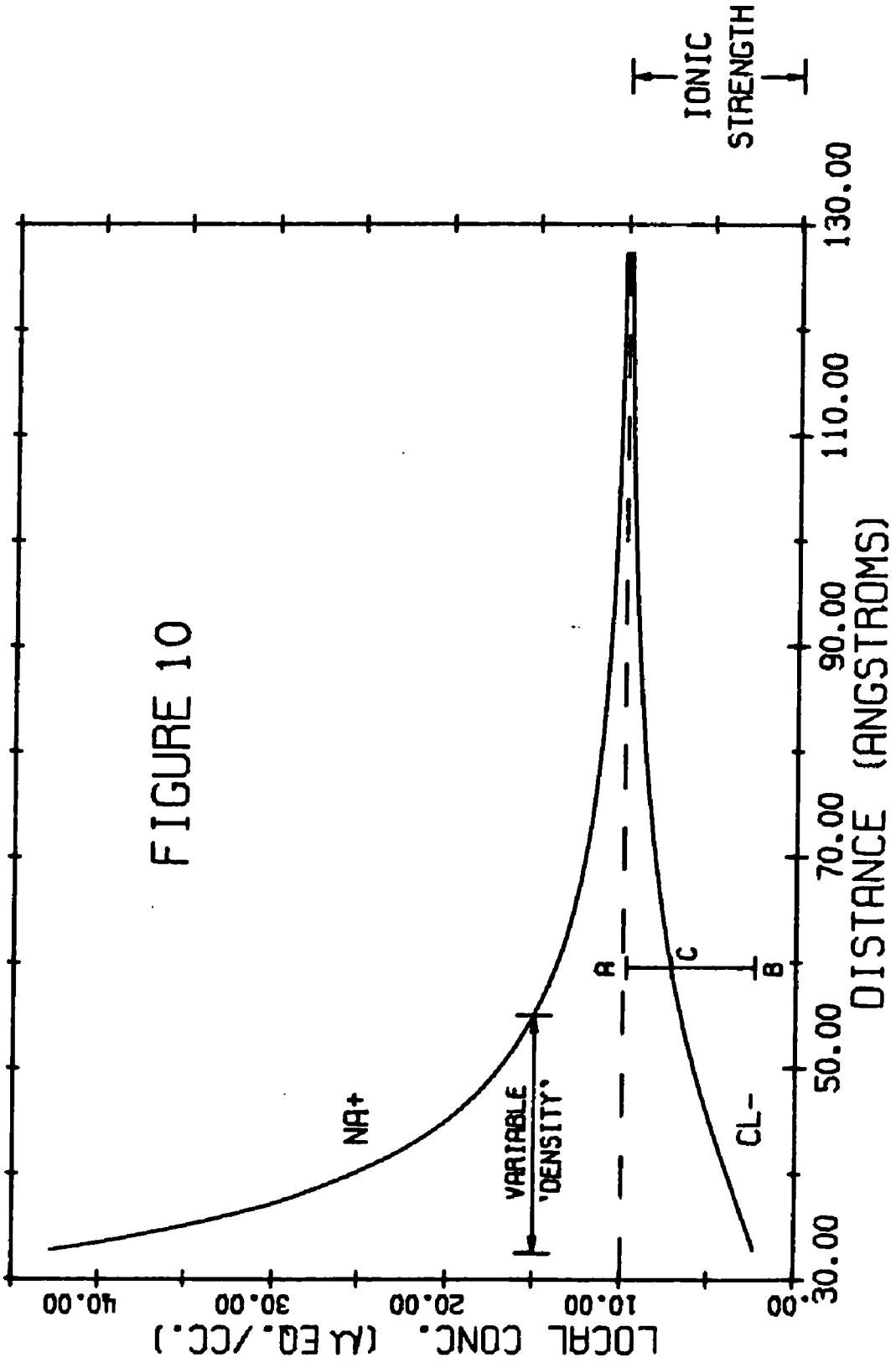

IONIC STRENGTH
130.00
110.00
90.00
70.00
50.00
30.00
DISTANCE (ANGSTROMS)
LOCAL CONC. (M EQ./CC.)
40.00
30.00
20.00
10.00
.00
NA+
CL-
VARIABLE 'DENSITY'
A
B
C

FIGURE 10

respect, it reflects the physical restriction between the globular protein molecule and the planar electrode surface postulated by McMenamy (43).

Assumptions

Equations (53, 54) and the method illustrated in Fig. 10 provide two ways of estimating the free ion concentrations. Both procedures were applied to several albumin solutions prepared by Scatchard, et al. (5) to determine if there exists a unique value of $\nu$ that is consistent with both criteria. Since these solutions contained either HCl or NaOH as well as NaCl, several simplifications were necessary before calculating the free ion concentrations. It was assumed that $Na^+$ and $OH^-$ are not bound to albumin (see p. 6). The local $Cl^-$ concentrations were obtained by multiplying the local anion concentrations by the ratio $(Cl^-)/(Cl^- + OH^-)$ where $(Cl^-)$ was calculated from eq. (54) and $(OH^-)$ was calculated from the pOH. The value of $(Cl^-)$ was usually so much greater than $(OH^-)$ that the value of the ratio $(Cl^-)/(Cl^- + OH^-)$ was very close to one.

## RESULTS

### Computer Solution of Poisson-Boltzmann Equation

Wiersema has programmed the numerical solution of the Poisson-Boltzmann equation for a digital computer (102). His program was written in the SAP (Share Assembly Programming) language for execution on an IBM 704. In the present study the method of numerical solution was coded in FORTRAN IV for execution on an IBM 360/67. The numerical results of the two programs for the same set of input parameters are shown in Table 14. For the indicated combination of input parameters, the values of the integration constant calculated by the two programs agree to within 1 part in 10,000 and the reduced potential values agree to within 4 parts in 100,000.

### Application to Albumin Solutions

The detailed results for one albumin solution are shown in Table 15 and Fig. 11. The points on line SB in Fig. 11 were calculated from the Scatchard-Bregman definition of the protein component. The points on line PB were calculated from the solution of the Poisson-Boltzmann equation and from the averaging procedure described above. Both sets of points were fitted with linear regression models of the form $y = A + Bx$. Curve PB was also fitted with an exponential model of the form $y = A \exp(-Bx)$, but the value of the residual variance ratio relative to the linear model was not significant. The value of $\nu$ which appears to satisfy both linear equations simultaneously is 3.16. Scatchard et al. reported a

TABLE 14

COMPARISON OF THE RESULTS OF TWO COMPUTER PROGRAMS FOR THE NUMERICAL SOLUTION OF THE POISSON-BOLTZMANN EQUATION

Input parameters[a]: $q_o = 1.0$, $y_o = 4.0$, $h = 0.025$

| | RESULTS[b] | |
|---|---|---|
| | LOW[c] Y = 3.4910 | This study Y = 3.4907 |
| x | y | y |
| 0.2 | 0.0127878 | 0.0127873 |
| 0.3 | 0.101572 | 0.101574 |
| 0.4 | 0.311975 | 0.311980 |
| 0.5 | 0.645373 | 0.645383 |
| 0.6 | 1.08976 | 1.08978 |
| 0.7 | 1.63673 | 1.63676 |
| 0.8 | 2.28787 | 2.28791 |
| 0.9 | 3.06022 | 3.06027 |
| 1.0 | 4.00001 | 4.00009 |

a. $q_o = \kappa a$ = reduced distance at exclusion radius a
$y_o$ = reduced potential at exclusion radius a
h = integration interval on same scale as x

b. Y = integration constant in equation (43)
y = $e\Psi/kT$ = reduced electrostatic potential

c. Loeb, Overbeek, and Wiersema, ref. 99 , p. 119.

TABLE 15

FREE $Cl^-$ CONCENTRATION AS A FUNCTION OF $\nu$ CALCULATED FROM PROTEIN COMPONENT AND FROM ION DISTRIBUTION

Solution composition[a]: pH = 7.24, $m_2$ = 0.0001429, $m_3$ = 0.008590, $m_7$ = 0.001406, h = -9.84

| $\nu$[b] | R[c] | $(Cl^-)_{SB} \times 1000$[d] | $(Cl^-)_{PB} \times 1000$[e] |
|---|---|---|---|
| 0.0 | 0.15131 | 7.8590 | 7.5556 |
| 0.5 | 0.15961 | 7.7522 | 7.4960 |
| 1.0 | 0.16798 | 7.6455 | 7.4278 |
| 1.5 | 0.17641 | 7.5387 | 7.3630 |
| 2.0 | 0.18490 | 7.4319 | 7.3010 |
| 2.5 | 0.19346 | 7.3252 | 7.2418 |
| 3.0 | 0.20209 | 7.2184 | 7.1852 |
| 3.5 | 0.21079 | 7.1116 | 7.1312 |
| 4.0 | 0.21955 | 7.0048 | 7.0795 |
| 4.5 | 0.22839 | 6.8981 | 7.0301 |
| 5.0 | 0.23729 | 6.7913 | 6.9828 |
| 5.5 | 0.24627 | 6.6845 | 6.9375 |
| 6.0 | 0.25532 | 6.5777 | 6.8941 |

a. Composition reported by Scatchard, et al. (5). Molalities of albumin, NaCl, and NaOH are denoted by $m_2$, $m_3$, and $m_7$, respectively. Number of bound H ions is denoted by h.

b. $\nu$ = number of bound Cl ions

c. R = ratio of difference between $Na^+$ concentration and unbound $Cl^-$ concentration to their sum.

d. $(Cl^-)_{SB}$ = free $Cl^-$ concentration calculated from Scatchard-Bregman component, eq. (54).

e. $(Cl^-)_{PB}$ = free $Cl^-$ concentration calculated as shown in Fig. 10 from numerical solution of Poisson-Boltzmann eq. (35).

FIGURE 11

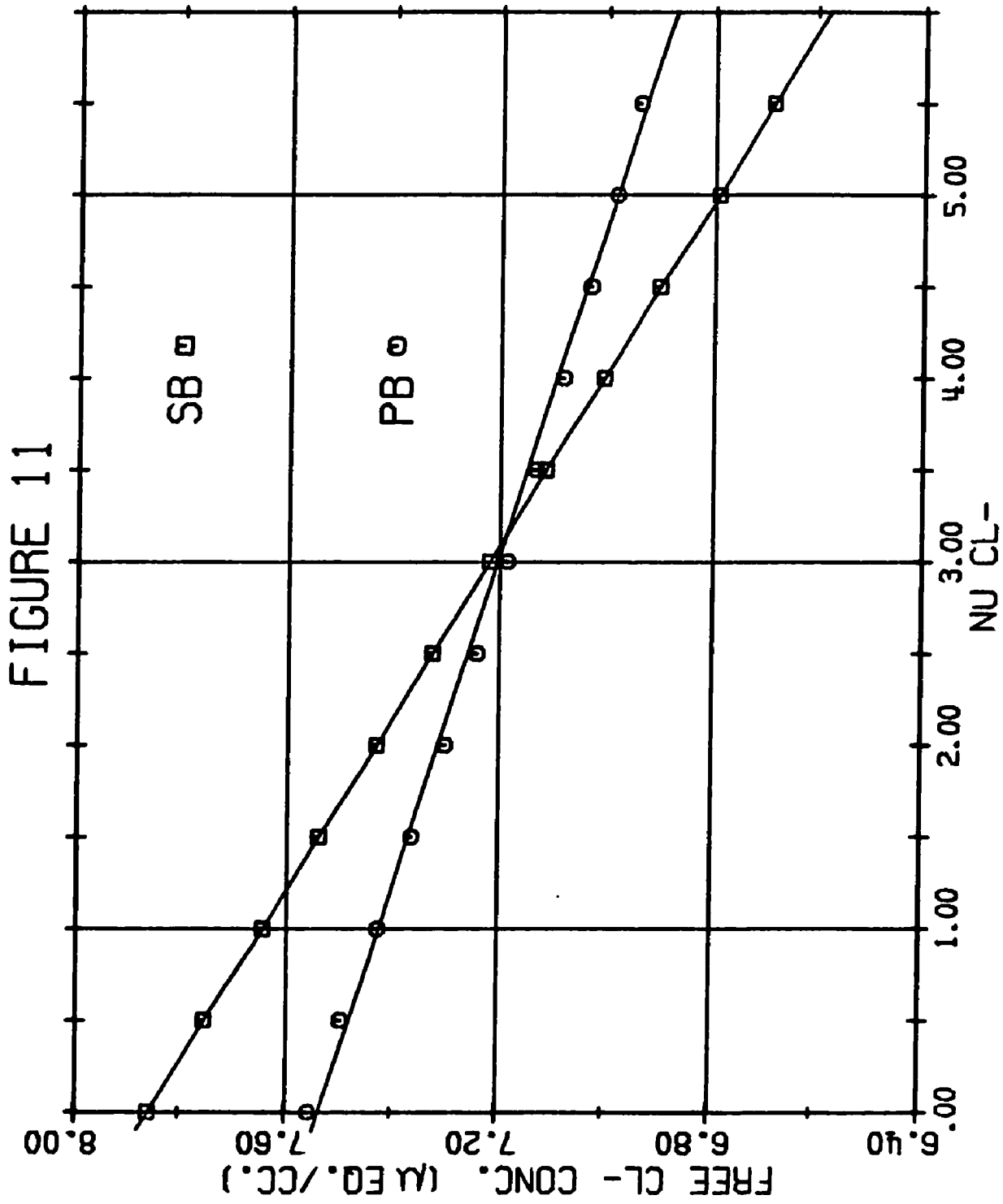
CALCULATION OF FREE $Cl^-$ CONCENTRATIONS FROM PROTEIN COMPONENT AND FROM ION DISTRIBUTION AS FUNCTIONS OF $\nu$

Abscissa - number of bound $Cl^-$ per mole of protein component

Ordinate - free $Cl^-$ concentration in $\mu$eq./cc. calculated in two different ways:

SB - from Scatchard-Bregman definition of the protein component, eq. (54)

PB - from ion distributions resulting from numerical solution of Poisson-Boltzmann eq. (35)


FIGURE 11
SB
PB
NU CL-
FREE CL- CONC. (μ EQ./CC.)
6.40
6.80
7.20
7.60
8.00
.00
1.00
2.00
3.00
4.00
5.00

$\nu$ value of 2.59 for this solution (5). When the process illustrated in Fig. 11 was applied to several other albumin solutions the results shown in Table 16 were obtained.

Scatchard and Bregman (106) indicated that their definition of the protein component is not satisfactory unless the value of the ratio

$$R = (Na^+ - Cl^-)/(Na^+ + Cl^-) \qquad (57)$$

is very small. In eq. (57), $(Na^+)$ represents the $Na^+$ concentration in the protein solution and $(Cl^-)$ represents the unbound $Cl^-$ concentration. In the present study, the value of R was calculated for each albumin solution for which the numerical computations were performed. The minimum values of R, i.e., the values corresponding to $\nu = 0$, are shown in Table 17. The value of R at the optimum $\nu$ value of 3.16 for the albumin solution of pH 7.24 was 0.205. Positive values of $\nu$ could not be obtained by the process illustrated in Fig. 11 if R was much larger than 0.20.

Hunter (51) has employed a series approximation for the free ion concentrations in a solution of protein concentration $m_2$, protein charge Z, and salt concentration $m_3$.

$$(Na^+) = m_3 - Zm_2/2 + (Zm_2)^2/8m_3 - (Zm_2)^4/128m_3^3 + \ldots \qquad (58)$$

$$(Cl^-) = m_3 + Zm_2/2 + (Zm_2)^2/8m_3 + (Zm_2)^4/128m_3^3 + \ldots \qquad (59)$$

TABLE 16

COMPARISON OF $\nu$ VALUES ESTIMATED FROM EMF MEASUREMENTS AND FROM NUMERICAL SOLUTION OF POISSON-BOLTZMANN EQUATION

| | | VALUE OF $\nu$ ESTIMATED FROM: | |
|---|---|---|---|
| pH[a] | h[a] | EMF measurement[a] | Numerical method[b] |
| 4.59 | 8.02 | 5.64 | 4.22 |
| 4.75 | 3.62 | 1.61 | 0.79 |
| 4.97 | 1.75 | 1.42 | 0.63 |
| 5.07 | 0.67 | 1.40 | 0.26 |
| 7.24 | -9.84 | 2.59 | 3.16 |

a. Data of Scatchard, Coleman, and Shen (5). h = number of $H^+$ ions bound to albumin.

b. Value of $\nu$ calculated as described in text and as illustrated in Fig. 11.

TABLE 17

MINIMUM VALUES OF THE RATIO $(Na^+ - Cl^-)/(Na^+ + Cl^-)$ for NINE ALBUMIN - NaCl - NaOH SOLUTIONS[a]

| pH | h | $m_3$ | $m_3 + m_7$ | $-hm_2$ | $(Na^+)$[b] | $(Cl^-)$[b] | R[c] |
|---|---|---|---|---|---|---|---|
| 5.51 | -0.82 | 0.0008790 | 0.0009998 | 0.0001205 | 0.001062 | 0.0008209 | 0.1280 |
| 5.60 | -1.75 | .0007499 | .0009988 | .0002483 | .001131 | .0006359 | .2800 |
| 5.91 | -3.46 | .0005058 | .001000 | .0004944 | .001277 | .0003158 | .6036 |
| 7.24 | -9.84 | .008590 | .009996 | .001406 | .01072 | .007916 | .1506 |
| 8.08 | -16.60 | .007464 | .009988 | .002524 | .01133 | .006308 | .2847 |
| 10.31 | -32.20 | .004932 | .009990 | .004829 | .01269 | .003077 | .6098 |
| 5.51 | -3.82 | .003890 | .005020 | .001130 | .005617 | .003366 | .2505 |
| 6.65 | -10.02 | .003784 | .006797 | .003010 | .008467 | .002568 | .5346 |
| 7.15 | -13.47 | .003776 | .007639 | .003858 | .009808 | .002311 | .6186 |

a. Data in columns 1 - 5 from Scatchard, et al. (5, 27). h = number of bound H ions, $m_3$ = NaCl molality, $m_7$ = NaOH molality.

b. Calculated from: $(Na^+)^2 + (Na^+)hm_2 - (m_3 + m_7)^2 = 0$

$$(Cl^-)^2 - (Cl^-)hm_2 - (m_3)^2 = 0$$

assuming number of bound $Cl^-$, $\nu = 0$ and mean ionic activity coefficient ratio = 1.0.

c. $R = (Na^+ - Cl^-)/(Na^+ + Cl^-)$.

The free ion concentrations calculated with the first 2 and 3 terms, respectively, were compared as functions of pH. The albumin titration data of Tanford, et al. (111), were used and it was assumed that there is no $Cl^-$ binding. The results for 1 per cent albumin at ionic strengths of 0.05 and 0.005 are shown in Table 18.

TABLE 18

CHLORIDE CONCENTRATIONS AND DONNAN RATIOS IN A 1 PER CENT ALBUMIN SOLUTION CALCULATED FROM TWO DIFFERENT SERIES APPROXIMATIONS

| IONIC STRENGTH = 0.05 | | | 2-term approximation[c] | | 3-term approximation[d] | |
|---|---|---|---|---|---|---|
| pH | h[a] | $hm_2/m_3$[b] | $Cl_i \times 10^3$ | $Cl_o/Cl_i$[e] | $Cl_i \times 10^3$ | $Cl_o/Cl_i$ |
| 5.0 | 5.7 | 0.342 | 50.43 | 0.9915 | 50.43 | 0.9915 |
| 6.0 | -3.6 | -0.216 | 49.73 | 1.005 | 49.73 | 1.005 |
| 7.0 | -8.7 | -0.522 | 49.35 | 1.013 | 49.35 | 1.013 |
| 8.0 | -15.6 | -0.936 | 48.83 | 1.024 | 48.84 | 1.024 |
| 9.0 | -21.2 | -1.272 | 48.41 | 1.033 | 48.44 | 1.032 |
| IONIC STRENGTH = 0.005 | | | | | | |
| 5.0 | 5.7 | 34.20 | 5.428 | 0.9212 | 5.446 | 0.9181 |
| 6.0 | -3.6 | -21.60 | 4.730 | 1.057 | 4.737 | 1.056 |
| 7.0 | -8.7 | -52.20 | 4.348 | 1.150 | 4.390 | 1.139 |
| 8.0 | -15.6 | -93.53 | 3.830 | 1.306 | 3.967 | 1.260 |
| 9.0 | -21.2 | -126.88 | 3.410 | 1.466 | 3.663 | 1.365 |

a. h = number of bound $H^+$ ions from albumin titration data of Tanford, et al. (111).

b. $m_2$ = protein molality, $m_3$ = salt molality

c. Calculated with first 2 terms of eq. (59).

d. Calculated with first 3 terms of eq. (59).

e. In a hypothetical equilibrium dialysis, $Cl_i$ is the inside $Cl^-$ concentration and $Cl_o$ is the outside $Cl^-$ concentration which was held constant for these calculations.

## DISCUSSION

Application of the computer method to albumin solutions with various values of pH and ionic strength led to two general results. In the case of the solutions shown in Table 16, small positive values of $\nu$ were obtained. These values agreed reasonably well with the $\nu$ values calculated from EMF measurements. In other cases, negative or unreasonably large $\nu$ values were obtained. There are several possible explanations for the anomalous results of the computer calculations under certain conditions of pH and ionic strength.

### Definition of the Protein Component

The definition of a protein component which minimizes the electrolyte concentration dependence of the properties of protein-electrolyte solutions is a difficult problem. Various definitions have been proposed by Scatchard (121), by Scatchard and Bregman (106), and by Casassa and Eisenberg (112). The value of the free $Cl^-$ concentration calculated with the first 2 terms on the right side of eq. (59) corresponds to the Scatchard definition (121). The validity of this definition over a range of pH values can be tested with the results of Table 18. At an ionic strength of 0.05, the free $Cl^-$ concentrations calculated from the 2 and 3-term approximations differed by less than 0.1 per cent over the pH range 5.0 to 9.0. At an ionic strength of 0.005, the two estimates differed by less than 1 per cent up to pH 7.0. At pH values of 8.0 and 9.0, the two estimates differed by 3 and 7 per cent, respectively. This

demonstrates that the validity of the free $Cl^-$ concentration calculated from the Scatchard definition is compromised as the ionic strength is decreased and as the pH is progressively removed from the isoionic point.

The deficiency of the Scatchard definition at low ionic strength and high pH is a plausible explanation for the anomalous results obtained with the computer method. The discrepancy between the 2 and 3-term approximations in Table 18 was especially pronounced at pH values greater than 7.5 where anomalous results were obtained. The discrepancy could also contribute to the anomalous results at ionic strengths of 0.001 between pH 5.0 and 6.0. The Scatchard-Bregman definition (106) was proposed with the stipulation that it would be satisfactory only when the value of $R = (Na^+ - Cl^-)/(Na^+ + Cl^-)$ is very small. From Table 17, it can be seen that this condition did not hold for many of the albumin solutions studied.

$Cl^-$ Binding

In the numerical computations, the number of bound $H^+$ ions, h, was held constant and the number of bound $Cl^-$ ions, $\nu$, was varied. Anomalous results were obtained for isoionic albumin solutions, i.e., for solutions in which the value of h was extremely low. If the protein charge $Z = h - \nu$ is too low, the ion distribution curves will be relatively shallow. Under these conditions, there is probably a loss in the physical significance of the Poisson-Boltzmann calculations and of the averaging procedure illustrated

in Fig. 10. On the alkaline side of the isoionic point, the effect of $Cl^-$ binding would be to increase the protein charge Z resulting in an even larger discrepancy between the 2 and 3-term approximations. On the acid side of the isoionic point, the effect of $Cl^-$ binding would be to decrease the charge Z resulting in a smaller difference between the two estimates. This might help to explain why the computer method appeared to be more successful on the acid side than on the alkaline side of the isoionic point.

## Conformational Changes

Another factor which could have contributed to the anomalous results below pH 4.5 and above pH 7.5 is the pH-dependent expansion of the albumin molecule. A conformational change in acid solution has been characterized in some detail (69, 70, 71). Much less is known about the conformational change in alkaline solution (113). Any appreciable expansion of the albumin molecule would invalidate the assumption of a constant exclusion radius of 32.5 Å.

## Implications for EMF Measurements

The averaging process illustrated in Fig. 10 weights the $Cl^-$ in the space between the protein molecules somewhat more heavily than the $Cl^-$ close to the protein molecules. This is one way of taking into account the physical restriction between a globular protein molecule and a planar electrode surface. The values of $\nu$ in Table 16 estimated from the numerical method are similar to those estimated from EMF measurements. This suggests that the

microscopic Donnan effect postulated by McMenamy (see p. 10) is not large for these particular solution compositions. Under different conditions of pH, ionic strength, and equivalent protein concentration ($Zm_2$), the postulated Donnan effect may be larger.

# IV. ULTRAFILTRATION STUDY

## INTRODUCTION

Ultrafiltration is a separation process in which a solution containing a solute whose molecular dimensions are greater than those of the solvent is depleted of solute by being forced to flow through a semipermeable membrane under a pressure gradient. As Michaels (114) has pointed out, the molecular dimensions of the solute in an ultrafiltration experiment can be arbitrarily specified as being greater than ten solvent diameters but less than the limit of resolution of the optical microscope (about 0.5 microns). Separations involving smaller solute particles are called reverse osmosis and those involving larger solute particles are called ordinary filtration. Ultrafiltration has been employed previously in binding studies with proteins (115-117).

In order for the ultrafiltration method to be useful in the study of interactions between proteins and electrolytes, there are at least two requirements which must be met. First, the ultrafiltration membrane must be freely permeable to the solvent and to the electrolyte. The membrane should also be equally permeable to ions of opposite charge. Second, the membrane must be practically impermeable to the dissolved protein. The impermeability of the membrane to the protein must be sufficiently independent of pressure and protein concentration that the chemical analysis of the ultrafiltered solution is not compromised.

## METHODS

### Ultrafiltration

Ultrafiltration experiments were performed with an ultrafiltration cell and membranes supplied by Amicon Corporation, Lexington, Mass. The cylindrical cell (Model 50) was made of Lucite and had a volume of 65 ml. The ultrafiltration membranes (PM-10) were 43 mm. in diameter and had a nominal solute molecular weight cutoff of 10,000.

Extensive pretreatment of the ultrafiltration membranes was necessary because they appeared to contain residual chemicals from their manufacture and because they were shipped in glycerol. New membranes were washed in a beaker with several changes of 0.1 M KCl for several hours before use. This was followed by exhaustive rinsing of the membrane in the cell with 0.1 M KCl at low pressure. The rinsing was continued until the absorbance of the filtrate in the wavelength range 350 to 200 nm. was less than 0.01. Between experiments the membranes were stored individually in 0.1 M KCl at $4^{\circ}$ C.

The cell was filled through a curved funnel made from a disposable pipette. The solution was agitated by a magnetic stirrer and pressure was applied to the cell from a tank of compressed $N_2$ gas. The Neoprene gasket had been leached with methanol to remove substances which could absorb ultraviolet light. The cell was emptied with a disposable pipette tipped with polyethylene tubing to avoid injury to the membrane surface. Following experiments with protein solutions, the top surface of the membrane was exhaustively

rinsed in the cell with successive aliquots of dilute KCl before dismantling, washing, and drying the cell.

Permeability Studies

The permeability of the membrane to water and to KCl was examined by ultrafiltering a KCl solution until its volume was about half the initial value. The concentrations of triplicate aliquots of the ultrafiltrate and retentate were then determined by dry weight measurement.

KCl dry weight measurements

Several clean, dry, glass-stoppered weighing bottles were removed from the drying oven and cooled to room temperature in a desiccator. The bottles were wiped with lens paper, placed in a Mettler M5 Microbalance (20 g. capacity, $\pm$ $10^{-6}$ g. sensitivity), and left to stand for about 30 min. to equilibrate. After weighing the empty bottles, aliquots of aqueous KCl solutions were pipetted into the bottles and they were reweighed. Two bottles were left empty to serve as tares. The stoppers were placed at right angles on top of the bottles and the bottles were placed in an air oven. The solutions were evaporated at 110° C for 40 hours. The tares and the bottles containing the dry solute were cooled, equilibrated, and weighed in the same order as before. The weights of the tares changed by small amounts between different sets of weighings, presumably due to the effects of changing atmospheric conditions. These weight changes were averaged and subtracted from the weights

of the sample bottles. In addition, the wet bulb and dry bulb temperatures and the barometric pressure were recorded. The sample weights were subsequently corrected for the buoyant effect of moist air.

The values of the estimated error in the salt concentrations were derived from a consideration of the propagation of experimental errors in the dry weight measurements. The uncertainty in reading the vernier scale on the balance was arbitrarily set equal to $\pm$0.000001 g. The remaining uncertainty was attributed to fluctuations in the zero-point setting of the balance. Ninety-nine per cent confidence limits $\lambda$ on the sample mean weights were calculated from the sample size, the sample standard deviation, and the t-distribution (ref. 67, p. 540), assuming that the sample weights were normally distributed. If this assumption is valid, the probability that the error in the sample weight will fall outside the interval $(-\lambda, \lambda)$ is approximately 1 per cent. The errors in the various weights were combined as suggested by Shoemaker and Garland (118).

Estimation of protein concentration

The permeability of the membrane to protein was examined by ultrafiltering a 1 to 3 per cent solution of BPA in 0.1 M KCl to about half its initial volume. The absorbance of the ultrafiltrate was measured against a KCl blank over the wavelength range 350 to 200 nm. in a Cary 15 recording spectrophotometer. The protein concentration was estimated assuming that the hypothetical absorbance

of a 1 per cent BPA solution in a 1 cm. cuvette is 6.67 at 279 nm. (52). When the absorbance at 279 nm. was less than 0.02, the protein concentration was usually estimated from the absorbance at 210 nm. Absorbance measurements with a series of BPA concentrations indicated that the absorbance at 210 nm. was approximately linear with respect to BPA concentration up to 0.004 per cent. In one case the absorbance at 279 nm. was measured in a Gilford spectrophotometer which had been modified so as to improve the signal-to-noise ratio.

In some cases several ultrafiltrates were pooled, freeze-dried, redissolved in a small volume of water and analyzed by means of a modified biuret reaction. The method of differential absorbance measurements at 290 and 390 nm. described by Janatova, et al. (52) was used. The BPA concentration was estimated from a 4-point calibration curve. The calibration curve was linear over the BPA concentration range 0.009 to 0.033 g. per 100 ml.

## RESULTS

### Permeability to Water and KCl

In order to test the permeability of the ultrafiltration membranes to water and electrolyte, several KCl solutions were ultrafiltered. The differences between the mean concentrations of the ultrafiltrates and retentates from dry weight measurement (Table 19) were less than the estimated experimental error. In another set of experiments, the concentrations of the ultrafiltrate and retentate were determined by conductivity measurement. This method yielded concentrations of 0.74209 and 0.74258 g. of solute per 100 g. of solution for the ultrafiltrate and retentate, respectively. On the basis of these experiments, it appears that the ultrafiltration membrane is sufficiently permeable to water and KCl to be useful for the study of protein salt interactions.

### Permeability to Albumin

The permeability of the membranes to albumin was examined in a similar manner. In a preliminary experiment, a 2 per cent solution of BPA in 0.1 M KCl was ultrafiltered through a membrane from lot no. 8. When 10 per cent TCA was added to the ultrafiltrate, there was no visible change. The absorbance of the ultrafiltrate relative to 0.1 M KCl in a Gilford spectrophotometer was 0.0058. This corresponds to a BPA concentration of less than 0.001 per cent.

The permeability of the membranes to BPA was further examined in a number of different ways. When BPA-KCl solutions were ultrafiltered through untreated membranes, the ultrafiltrate had a small

TABLE 19

CONCENTRATIONS OF KCl ULTRAFILTRATES AND RETENTATES AS DETERMINED BY DRY WEIGHT MEASUREMENT[a]

Concentrations in g. of solute per 100 g. of solution[b]

| Set | Ultrafiltrates | | Retentates |
|---|---|---|---|
| 1 | 0.87315 | | 0.87202 |
| | 0.86981 | | 0.87185 |
| | 0.87000 | | 0.87123 |
| Means | 0.87099 | | 0.87170 |
| Difference | | 0.00071 | |
| Calculated error[c] | | ±0.00090 | |
| 2 | 0.53396 | | 0.53410 |
| | 0.53447 | | 0.53352 |
| | 0.53395 | | 0.53366 |
| Means | 0.53413 | | 0.53376 |
| Difference | | -0.00037 | |
| Calculated error | | ±0.00086 | |

a. Ultrafiltrate is solution which passes through membrane under excess pressure (approximately 5 lbs./sq. in. for these experiments). Retentate is solution which remains in cell.

b. Solutions were evaporated in an air oven at 100° C for 40 hours. Weights of solutions and solutes were corrected for buoyant effect of air.

c. Derived from propagation-of-error analysis as described in ref. 118.

absorbance at 280 nm. and a larger absorbance at 210 nm. The absorbance of ultrafiltrates of some membranes could be decreased by imbedding a high molecular weight blue dextran in the surface of the membrane. With other membranes, the dextran treatment did not appreciably decrease the absorbance of the ultrafiltrate. The retention efficiency of ultrafiltration membranes can sometimes be improved by increasing the flow rate (114). A five-fold increase in the ultrafiltration pressure did not appear to alter either the flow rate or the absorbance of the ultrafiltrate. Combination of the membranes in stacks of two and three did not result in ultrafiltrates with significantly lower absorbance values. The results of the absorbance measurements are summarized in Table 20.

Some of the ultrafiltrates of BPA solutions gave a white precipitate on addition of 10 per cent TCA and many of them frothed at the air-solution interface when shaken. The results of a biuret analysis of several pooled ultrafiltrates are shown in Table 21. The positive results of the biuret analysis indicate that a substance containing multiple peptide bonds was present in the ultrafiltrates. Efforts to isolate peptides from the original albumin preparation led to negative results (51). This is strong circumstantial evidence for the presence of BPA in the ultrafiltrates.

TABLE 20

ULTRAVIOLET ABSORBANCE OF ALBUMIN-KCl SOLUTIONS
ULTRAFILTERED THROUGH PM-10 MEMBRANES

| Lot. no. | Membrane number | Imbedded blue dextran[a] | Initial BPA conc. (g./100 g. soln.) | Ultrafiltration pressure (lbs./sq.in.) | Absorbance[b] 280 nm. | Absorbance[b] 210 nm. |
|---|---|---|---|---|---|---|
| 8 | 1 | 0 | 2.0 | 10 | 0.0058[c] | |
| 12 | 1 | 0 | 1.0 | | 0.04 | 0.85 |
| 12 | 1 | 1 | 2.0 | 14 | 0.08 | >1.0 |
| 12 | 3 | 0 | 1.5 | | 0.02 | |
| 12 | 3 | 1 | 1.8 | | 0.00 | 0.04 |
| 18 | 3 | 1 | 2.0 | | 0.01 | 0.18 |
| 18 | 3 | 1 | 1.8 | | 0.00 | 0.06 |
| 18 | 3 | 1 | 1.8 | 10 | 0.03 | 0.51 |
| 18 | 4 | 0 | 2.2 | | 0.03 | 0.57 |
| 18 | 5 | 0 | 2.2 | | 0.03 | 0.77 |
| 18 | 4,5 | 0,0 | 2.0 | 6 | 0.01 | 0.16 |
| 18 | 6 | 0 | 2.0 | 8 | 0.01 | 0.16 |
| 18 | 6 | 0 | 2.0 | 40 | 0.01 | 0.21 |
| 18 | 5,4,6 | 0,1,0 | 2.0 | | 0.01 | 0.17 |
| 18 | 5,4,6 | 0,1,0 | 2.0 | 14 | 0.05 | >1.0 |

a. "0" indicates that membrane had not been treated with blue dextran.
"1" indicates that membrane had been treated with blue dextran.
b. Absorbance values have been corrected for absorbance of cell blank.
c. Measured in a modified Gilford spectrophotometer with improved signal-to-noise ratio.
All other values were measured in a Cary 15 spectrophotometer.

TABLE 21

ANALYSIS OF FREEZE-DRIED ULTRAFILTRATES BY MODIFIED BIURET METHOD[a]

| Solutions | ABSORBANCE[b] 290 nm. | 390 nm. | Difference | Albumin concentration (g./100 ml.) |
|---|---|---|---|---|
| Sample 1[c] | 0.192 | 0.012 | | |
| Blank 1 | 0.122 | 0.012 | | |
| Difference | 0.070 | 0.000 | 0.070 | < 0.0010[d] |
| Sample 2 | 0.464 | 0.021 | | |
| Blank 2 | 0.313 | 0.015 | | |
| Difference | 0.151 | 0.006 | 0.145 | 0.0066 |
| Sample 3 | 0.501 | 0.033 | | |
| Blank 3 | 0.190 | 0.021 | | |
| Difference | 0.311 | 0.012 | 0.299 | 0.0195 |

a. Method of Janatova, Fuller, and Hunter (52).

b. Absorbance of solutions was measured with a Zeiss PMQ II spectrophotometer.

c. Sample solutions 1, 2, and 3 consisted of miscellaneous pooled ultrafiltrates which had been freeze-dried and redissolved in a small volume of water.

d. Albumin concentrations estimated from calibration curve with 4 points. Calibration curve was linear over concentration range 0.009 to 0.033 g./100 ml.

DISCUSSION

It is evident that the amount of albumin escaping into the ultrafiltrate could have been reduced by using lower albumin concentrations. However, the uncertainty in the protein-electrolyte interaction parameter becomes increasingly unfavorable at albumin concentrations less than about 1 per cent. This is shown by the following calculation.

From eq. (1), p. 5 and ref. (118), the limit of error $\lambda(\nu)$ is, in general, given by

$$\lambda(\nu) = \left|\frac{\partial \nu}{\partial m_3}\right| \lambda(m_3) + \left|\frac{\partial \nu}{\partial X^-}\right| \lambda(X^-) + \left|\frac{\partial \nu}{\partial m_2}\right| \lambda(m_2) \qquad (60)$$

Differentiation of eq. (1), and substitution into eq. (60) gives

$$\lambda(\nu) = \frac{1}{m_2}\left[\lambda(m_3) + \lambda(X^-) + \frac{m_3 - X^-}{m_2}\lambda(m_2)\right] \qquad (61)$$

When $(m_3 - X^-)$ and $\lambda(m_2)$ are sufficiently small, the value of the third term in eq. (61) is several orders of magnitude smaller than the sum of the first two terms. Under these conditions, an approximate minimum limit of error $\lambda'(\nu)$ is given by

$$\lambda'(\nu) = \frac{\lambda(m_3) + \lambda(X^-)}{m_2} \qquad (62)$$

Consideration of the propagation of errors in the KCl dry weight measurements yielded a limit of error in the salt concentration of about 0.1 per cent. If this limit of error is assumed for a salt

concentration of 0.1 m, the sample calculations in Table 22 are obtained. Scatchard, et al. (5), reported $\nu$ values ranging from 5 to 9 in isoionic albumin solutions in this range of salt concentration. At albumin concentrations below 1 per cent, the limit of error in the interaction parameter approaches the magnitude of the parameter itself.

From the results of Table 20, there appears to be some variation in membrane permeability to albumin between different lot numbers. Ultrafiltrates of albumin solutions from many of the membranes had absorbance values at 279 nm. of 0.02 or more. These absorbance values correspond to albumin concentrations in the ultrafiltrates of 0.003 per cent and higher. Albumin concentrations of this magnitude could discredit the analysis and interpretation of a quantitative ultrafiltration study of albumin-electrolyte interactions.

TABLE 22

CALCULATED UNCERTAINTY IN ION-BINDING PARAMETER $\nu$ AS A FUNCTION OF ALBUMIN CONCENTRATION AT 0.1 MOLAL SALT CONCENTRATION[a]

| Albumin concentration | | |
|---|---|---|
| Weight % | Molality[b] | $\lambda_{.01}(\nu)$[c] |
| 0.1 | 0.000030 | 6.6 |
| 0.5 | 0.000075 | 2.7 |
| 1.0 | 0.00015 | 1.3 |
| 2.0 | 0.00030 | 0.66[d] |
| 3.0 | 0.00045 | 0.44 |

a. $\nu = (m_t - m_f)/m_p$ where $m_t$ = total salt concentration, $m_f$ = "free" salt concentration, and $m_p$ = protein concentration.

b. Molecular weight of albumin was assumed to be 67,000.

c. $\lambda_{.01}(\nu)$ is a 99% confidence limit for $\nu$ as defined in eq. (1). $\lambda_{.01}(\nu)$ was calculated from $\lambda(\nu) = (\lambda(m_t) + \lambda(m_f))/m_p$, assuming $\lambda(m_t) = \lambda(m_f) = 0.0001$

d. Scatchard, et al. (5, 27) report $\nu$ values ranging from 5 to 9 in the range of albumin concentration 0.00034 to 0.00077 molal.

# V. IMPLICATIONS FOR THE DESIGN OF BINDING STUDIES

## COMPOSITION VARIABLES

Ion binding in protein solutions is a complicated function of the relative amounts of the protein, acid or base, and salt components that are present. In general, the concentrations of each of the components can be varied independently but their activities cannot. An important difference between binding studies with $H^+$ and $Cl^-$ is evident from a comparison of their relative association constants with proteins. The weakest binding sites for $H^+$ in proteins are the carboxyl groups with association constants on the order of 10,000 (29). The strongest binding site for $Cl^-$ in albumin has an association constant of 2400 (5). One consequence of this difference in association constants is that the concentration of ligand must be raised to higher values in the case of $Cl^-$ than in the case of $H^+$ before the corresponding binding sites are 50 per cent occupied. As a consequence, the effect of varying the concentration of $Cl^-$ in the region of its "pK" has a larger effect on the ionic strength than the corresponding variation of the $H^+$ concentration in the region of its pK.

It has been shown that the activity coefficient of each component of an electrolyte mixture is primarily a function of the total ionic strength (ref. 45, p. 586). Similarly, the ratio of activity coefficients of two protein species with different valences depends on the ionic strength (106). The interpretation of a binding study is therefore made simpler if the total ionic strength

can be maintained constant, at least over small ranges of ligand concentration. The total ionic strength can be maintained constant with an electrolyte other than the one whose binding is under study. If the additional electrolyte is a salt, its effect on the binding of the ligand to the protein should be shown to be negligible (42). The buffer capacity of the added electrolyte should also be negligible in order to avoid the net transfer of $H^+$ to or from the protein (125). If the added electrolyte is an acid or base, the titration curve of the protein should be known so that the change in $H^+$ dissociation of the protein can be calculated (5, 25).

pH Range

The minimal pH range of a protein-ion binding study is suggested by the results of the computer calculations in the present study (Table 16, p. 107). The similarity of the $\nu$ values for albumin and $Cl^-$ calculated by the EMF method and by the numerical method indicates that the microscopic Donnan effect postulated by McMenamy (43) is not large. This conclusion applies if the equivalent albumin concentration is not much larger than 20 per cent of the ionic strength, i.e., within the approximate range of pH 4.5 to pH 7.5. The magnitude of the microscopic Donnan effect outside this pH range can be estimated by making certain refinements in the computer calculations. The first is to include the higher order terms of equations (58) and (59) in equations (53) and (54), respectively. At pH values appreciably removed from the isoionic point, addition of the higher order terms would lead to curvature

of the line "SB" in Fig. 11, resulting in a slightly different intersection with the line "PB". A second refinement is to treat the exclusion radius "a" as an adjustable parameter. In terms of the concentric spherical model, bound $H^+$ can penetrate beneath the surface of the protein sphere (124) while bound $Cl^-$ can approach no closer than the exclusion radius. Instead of holding the radius "a" constant at 32.5 Å, an average radius determined by the radii of the concentric spheres and the relative number of bound $H^+$ and $Cl^-$ ions could be used. This would alter the surface charge density, the surface potential, and the upper limit of integration in eq. (40).

Salt and Protein Concentration

The lower limit of protein concentration in a protein-ion binding study is determined by the maximum acceptable uncertainty in the molal binding ratio $\nu$. From a sample calculation analogous to that of Table 22, p. 127, the uncertainty in $\nu$ is approximately 0.7 for a 1 per cent albumin solution in 0.01 M KCl. This uncertainty decreases at higher protein concentration and lower salt concentration. The lower limit of salt concentration in a binding study is determined to a large extent by the electrode properties. Ag-AgCl electrodes, for example, have a lower threshold of approximately $10^{-5}$ M determined by the solubility of AgCl in water (119). In practice, the electrodes sometimes deviate from reversible behavior at concentrations approaching $10^{-3}$ M (60). The upper limits of the salt and protein concentration in an ion binding study are

related to the interactions between protein molecules. These interactions increase with increasing protein concentration but they can be reduced by the addition of salt. The addition of salt is postulated to reduce the electrostatic potential to zero at a distance less than the average separation between protein molecules (ref. 28, p. 469). As the salt concentration is increased, greater experimental precision is required to estimate $\nu$ since its value depends on the difference between the total and unbound salt concentration. Tanford has cited an extreme example of total and unbound salt concentrations on the order of 1 M which cannot be distinguished by the EMF method (ref. 28, p. 541).

## EXPERIMENTAL METHOD

### Cell Design

The reproducibility of the EMF measurements in the present study was marginal. It was concluded that inefficient solution agitation resulted in the formation of interfacial diffusion layers whose contribution to the EMF varied with time (see eq. (25), p. 78). Ideally, extrapolation of the EMF to zero time should yield the EMF corresponding to diffusion layers of infinitesimal thickness. The EMF cell should be redesigned to increase the turbulent flow of the solutions thereby reducing the diffusion layer thickness and improving the reproducibility of the extrapolation to zero time.

Stirred Solutions

The most important factors in the fluid regimen of a stirring vessel are the shapes of the compartment and of the impeller. The compartment should have baffles or some other kind of shape irregularity to break laminar flow. The rotating impeller could be either of two different kinds. A 3-blade marine-type propeller produces solution flow that is mostly parallel to the axis of rotation. In order to achieve the greatest turbulence from axial flow at the membrane-solution interface, the latter should be perpendicular to the axis of rotation and the propeller should be offset from the axis of the compartment. A flat-blade turbine impeller produces solution flow that is primarily radial or perpendicular to the axis of rotation (122). The radial flow produced by the turbine is confined to a smaller volume of solution than the axial flow of the propeller. The turbine would therefore lead to more efficient agitation at a membrane-solution interface parallel to the axis of rotation.

Flowing solutions

An alternative way of agitating solutions and minimizing the diffusion layer thickness is to direct a jet of solution at high velocity against the face of the membrane. The cells used by Scatchard and Helfferich (81) and by Lorimer (89) are examples of this design. It would be necessary to eliminate or at least to minimize the air-solution interface in order to minimize surface denaturation of the protein. Either a continuous flow design or a

circulating peristaltic flow design would be suitable. Volume flow rates on the order of 10 ml. per second can be attained readily with the former method (123).

## Electrodes

It was observed in the present study (pp. 30-31) that unprotected Ag-AgCl electrodes did not give stable EMF readings in the presence of dissolved albumin. The electrode stability can be improved in either of two ways. The electrode can be isolated from the protein solution via a saturated KCl bridge. This method introduces an additional liquid junction potential but it has the advantage that it can be used to determine the activity ratio of anions other than $Cl^-$ such as $F^-$ and trichloroacetate (5, 25). Alternatively, the AgCl electrode can be coated with collodion and immersed directly into the protein solution (4, 26). In this case, the EMF depends on the activity ratio of the anion whose sparingly soluble Ag salt is present in the electrode. The collodion should be dried in $N_2$ rather than in air to avoid oxidation of the collodion (46).

## The Transference Method

The measurement of electrolyte and solvent transference numbers in salt concentration cells is a viable alternative to the use of calibration curves of EMF vs. salt concentration. The latter method groups all the various sources of deviation into one term, the difference between the ideal and observed EMF. In the

transference method, the principal sources of deviation, i.e., irreversible electrolyte diffusion and solvent transport, correspond to the parameters $t_+$ and $t_w$, respectively, in equations (18), (19), and (21). The transference method does not require a constant concentration ratio as used in the construction of calibration curves (25), nor does it require a constant reference solution as does the use of counterion-reversible electrodes (see Table 4, p. 46). A final advantage of the transference method is that it is closely associated with processes occurring inside the membrane. The transference numbers are therefore less likely than activity coefficients to be strongly influenced by charged protein molecules in solution. The membrane transference numbers measured in the present study were $t_+ = 1.000 \pm 0.005$ and $t_w = 4.50 \pm 0.67$ moles per Faraday. These values were essentially constant up to an RMS molality of 0.10 and up to a molality ratio of 8.0. Within experimental error, the entire deviation of the observed EMF from the ideal EMF can be attributed to water transport in the cation exchange membrane. This relatively simple, predictable behavior of the cation exchange membranes should facilitate further investigation and solution of other design problems such as solution agitation and isolation of the electrodes from the protein solution.

Nagasawa and Holtzer (16) have called attention to the apparent scarcity of protein-ion binding information as a function of salt concentration at appreciable protein charge. This scarcity is due in part to the difficulty of varying component activities independently of each other. The relative invariance of the

transference numbers $t_+$ and $t_w$ with salt concentration may facilitate the measurement of protein-ion binding over wider ranges of salt concentration. A more complete knowledge of the salt concentration dependence of the molal binding ratio $\nu$ should help to distinguish between alternative binding models with heterogeneous binding sites (5, 25) and heterogeneous binding forces (36, 124).

# VI. SUMMARY AND CONCLUSIONS

## POTENTIOMETRIC STUDIES

There are two primary approaches to the use of concentration cells containing ion-exchange membranes in the study of protein-electrolyte interactions. The first involves the construction of empirical calibration curves of EMF vs. electrolyte concentration in the absence of protein. The assumptions and approximations involved in the use of such calibration curves were discussed. An alternative to the use of calibration curves is the independent measurement of electrolyte and solvent transference numbers. An equation was derived which facilitates the theoretical calculation of the EMF of an ion-exchange membrane cell from the ion and solvent transference numbers as functions of concentration.

Three different methods were employed for the measurement of transference numbers. The first method consisted of EMF measurements with electrodes reversible to the counterions of the ion-exchange membrane. This method was found to yield solvent transport correction curves of limited applicability. The second method was a modified Hittorf method consisting of the measurement of solution composition and volume changes accompanying the passage of electrical current through an ion-exchange membrane cell. For uncertain reasons, the changes in solution composition and volume did not appear to be related to the passage of current or to its direction. The final method was the estimation of transference numbers from EMF measurements of concentration cells. The

experimental data could be fitted by transference numbers close to the ideal, limiting values. Within the concentration range 0.005 to 0.10 m, the cation transference number did not appear to deviate significantly from 1.00 and the estimated water transference number (4.50) was close to the minimum hydration number of the $K^+$ ion.

The reproducibility of the EMF measurements was marginal. Membrane effects such as directional asymmetry, leaching, evaporation, heat dissipation, and pressure variation did not appear to be major sources of EMF variation. Ag-AgCl electrode effects such as surface strain and stripping of AgCl were identified as possible sources of EMF variation. It was concluded that the difficulty of maintaining uniform solution agitation throughout a series of experiments was a primary source of irreproducibility in the EMF measurements.

The effects of dissolved polysaccharides and macro-ions on the EMF between Ag-AgCl electrodes were studied. The effects of macro-ions on the EMF and on the activity ratio were qualitatively consistent with the theory of the Donnan equilibrium. The effect of colloidal silica on the EMF exhibited an exponential pH dependence. This dependence was qualitatively consistent with the expected degree of dissociation of the colloidal silica. The polysaccharide amylose dissolved in 0.27 M KCl had no observable effect on the EMF between Ag-AgCl electrodes.

## COMPUTER SIMULATION

A computer program for the numerical solution of the Poisson-Boltzmann equation was written. The results of the program were

used to simulate the distributions of salt ions around a charged protein molecule. The free $Cl^-$ concentration was estimated by an averaging process analogous to the calculation of a one-dimensional center of mass. Using the Scatchard-Bregman definition of the protein component, a value of the ion-binding parameter $\nu$ in a series of albumin solutions was estimated independently of experimental activity measurements. In five cases, the computer estimate of $\nu$ was in reasonable agreement with that from experimental EMF measurements. Anomalous results with the remaining albumin solutions were attributed to three causes: (1) diminished utility of the Scatchard-Bregman definition when the ratio of equivalent protein concentration to ionic strength is not small, (2) diminished physical significance of the Poisson-Boltzmann calculations when the ion distribution curves are too shallow, and (3) expansion of the albumin molecule below pH 4.5 and above pH 7.5. In the case of the albumin solutions for which similar values of $\nu$ were obtained by the computer method and by the EMF method, it was concluded that the microscopic Donnan effect postulated by McMenamy (43) was not large.

## ULTRAFILTRATION STUDY

The permeability of commercially available ultrafiltration membranes to water and KCl was examined. Dry weight measurements and conductivity measurements indicated that the composition of the KCl ultrafiltrate was identical to that of the KCl retentate within experimental error. When albumin solutions were ultra-

filtered, absorbance measurements indicated that appreciable amounts of albumin were escaping into the ultrafiltrate. The uncertainty in the measured ion-binding parameter $\nu$ was shown to approach the magnitude of the parameter itself as the protein concentration is decreased below 1 per cent. It was concluded that the permeability of the ultrafiltration membranes to albumin at concentrations greater than 1 per cent was too great for an accurate, quantitative study of protein-electrolyte interaction to be undertaken.

## REFERENCES


1. Scatchard, G., A.C. Batchelder, and A. Brown, J. Clinical Investigation, 23, 458, (1944).

2. White, A., P. Handler, and E.L. Smith, Principles of Biochemistry, 3rd ed., McGraw-Hill Book Company, New York, 1964, p. 679.

3. Carr, C.W., Arch. Biochem. Biophys., 46, 417, (1953).

4. Scatchard, G., I.H. Scheinberg, and S.H. Armstrong, J. Am. Chem. Soc., 72, 535, (1950).

5. Scatchard, G., J.S. Coleman, and A.L. Shen, J. Am. Chem. Soc., 79, 12, (1957).

6. Carr, C.W., Arch. Biochem. Biophys., 43, 147, (1953).

7. Carr, C.W., Arch. Biochem. Biophys., 55, 1, (1955).

8. Rosenberg, R.M., and I.M. Klotz, J. Am. Chem. Soc., 77, 2590, (1955).

9. Sandor, G., Bull. Soc. Chim. Biol., (Paris), 18, 877, (1936).

10. Scatchard, G., Ann. N.Y. Acad. Sci., 51, 660, (1949).

11. Sandor, G., Bull. Soc. Chim. Biol., (Paris), 19, 555, (1937).

12. Scatchard, G., and E.S. Black, J. Phys. Colloid Chem., 53, 88, (1949).

13. Ghosh, B.N., and E. Mihalyi, Arch. Biochem. Biophys., 41, 107, (1952).

14. Ho, C., and D. Waugh, J. Am. Chem. Soc., 87, 110, (1965).

15. Basch, J.J., and S.N. Timasheff, Arch. Biochem. Biophys., 118, 37, (1967).

16. Nagasawa, M., and A. Holtzer, J. Am. Chem. Soc., 86, 531, (1964).

17. Cassel, J.M., and J. Steinhardt, Biochemistry, 8, 2603, (1969).

18. Bugarszky, S., and L. Liebermann, Pflüger's Archiv. Ges. Physiol., 72, 51, (1898).

19. Simon, W., H.R. Wuhrmann, M. Vasak, A.R. Pioda, R. Dohner, and Z. Stefanac, Angew. Chem., Internat. Ed., 9, 445, (1970).

20. Teorell, T., J. Biol. Chem., 113, 735, (1936).

21. Meyer, K.H., and J.V. Sievers, Helv. Chem. Acta, 19, 649, (1936).

22. Ijsseling, F.P., and E. van Dalen, Analyt. Chim. Acta, 36, 166, (1966).

23. Botre, C., S. Borghi, and M. Marchetti, Biochim. Biophys. Acta, 135, 208, (1967).

24. Scatchard, G., J. Am. Chem. Soc., 75, 2883, (1953).

25. Scatchard, G., Y.V. Wu, and A.L. Shen, J. Am. Chem. Soc., 81, 6104, (1959).

26. Scatchard, G., I.H. Scheinberg, and S.H. Armstrong, J. Am. Chem. Soc., 72, 540, (1950).

27. Scatchard, G., and W.T. Yap, J. Am. Chem. Soc., 86, 3434, (1964).

28. Tanford, C., Physical Chemistry of Macromolecules, John Wiley and Sons, Inc., New York, 1961.

29. Edsall, J.T., and J. Wyman, Biophysical Chemistry, vol. I., Academic Press, Inc., New York, 1958.

30. Stewart, R.J., and W.F. Graydon, J. Am. Chem. Soc., 61, 164, (1957).

31. Rosenberg, N.W., J.H.B. George, and W.D. Potter, J. Electrochem. Soc., 104, 111, (1957).

32. Lakshminarayanaiah, N., J. Phys. Chem., 70, 1588, (1966).

33. Tombalakian, A.S., and W.F. Graydon, J. Phys. Chem., 70, 3711, (1966).

34. Saroff, H.A., J. Phys. Chem., 61, 1364, (1957).

35. Klotz, I.M., "Protein Interactions", in The Proteins, Neurath, H., and K. Bailey, eds., Academic Press, Inc., New York, 1953, vol. IB, p. 727.

36. Arvidsson, E.O., Small Molecule-Protein Interactions, Student-litteratur, Lund, Sweden, 1965.

37. Pallman, H., Kolloidchem. Beihefte, 30, 334, (1930).

38. Overbeek, J. Th. G., "Electrochemistry of the Double Layer", in Colloid Science, Kruyt, H., ed., Elsevier Publishing Company, Amsterdam, 1949, vol. 1, p. 191.

39. Sollner, K., J. Colloid Sci., 8, 179, (1953).

40. Bates, R.G., Electrometric pH Determinations, John Wiley and Sons, Inc., New York, 1954.

41. Jenny, H., T.R. Nielson, N.T. Coleman, and D.E. Williams, Science, 112, 164, (1950).

42. McMenamy, R.H., M.I. Madeja, and R. Watson, J. Biol. Chem., 243, 2328, (1968).

43. McMenamy, R.H., Personal communication.

44. Lewis, G.N., and M. Randall, Thermodynamics, 2nd ed., revised by K.S. Pitzer and L. Brewer, McGraw-Hill Book Company, Inc., New York, 1961, p. 362.

45. Harned, H.S., and B.B. Owen, The Physical Chemistry of Electrolytic Solutions, 3rd ed., Reinhold Publishing Corporation, New York, 1958.

46. Helfferich, F., Ion Exchange, McGraw-Hill Book Company, Inc., New York, 1962.

47. Hills, G.J., P.W.M. Jacobs, and N. Lakshminarayanaiah, Proc. Royal Soc., (London), A262, 246, (1961).

48. Lorimer, J.W., E.I. Boterenbrood, and J.J. Hermans, Disc. Faraday Soc., 21, 141, (1956).

49. Lakshminarayanaiah, N., and V. Subrahmanyan, J. Polymer Sci., A2, 4491, (1964).

50. Dintzis, H.M., Ph.D. Thesis, Harvard University, 1952.

51. Hunter, M.J., Personal communication.

52. Janatova, J., J.K. Fuller, and M.J. Hunter, J. Biol. Chem., 243, 3612, (1968).

53. Hunter, M.J., J. Phys. Chem., 70, 3285, (1966).

54. DuBois, M., K.A. Gilles, J.K. Hamilton, P.A. Rebers, and F. Smith, Analyt. Chem., 28, 350, (1956).

55. Greyson, J., J. Electrochem. Soc., 109, 745, (1962).

56. Blaedel, W.J., and V.W. Meloche, Elementary Quantitative Analysis, Theory and Practice, 2nd ed., Harper and Row, Publishers, New York, 1963.

57. Greyson, J., J. Phys. Chem., 71, 259, (1967).

58. Ionics, Inc., Technical Bulletin No. CR61, Watertown, Mass., (1966).

59. Hittorf, J.W., Pogg. Ann., 106, 337, (1859).

60. Brydges, T.G., Ph.D. Thesis, University of Western Ontario, London, Ontario, 1966.

61. McWilliams, J., Fischer and Porter Co., Personal communication.

62. Lakshminarayanaiah, N., and V. Subrahmanyan, J. Phys. Chem., 72, 1253, (1968).

63. Shalaby, R.A., K. Banerjee, and M.A. Lauffer, Biochemistry, 7, 955, (1968).

64. Floyd, B.F., and F. Friedberg, J. Biol. Chem., 241, 5533, (1966).

65. Jones, G., and G.M. Bollinger, J. Am. Chem. Soc., 53, 411, (1931).

66. Jones, G., and B.C. Bradshaw, J. Am. Chem. Soc., 55, 1780, (1933).

67. Hald, A., Statistical Theory with Engineering Applications, John Wiley and Sons, Inc., New York, 1952.

68. Hills, G.J., "Membrane Electrodes", in Reference Electrodes, Theory and Practice, Ives, D.J.G., and G.J. Janz, eds., Academic Press, Inc., New York, 1961, p. 411.

69. Yang, J.T., and J.F. Foster, J. Am. Chem. Soc., 76, 1588, (1954).

70. Kronman, M., and J.F. Foster, Arch. Biochem. Biophys., 72, 205, (1957).

71. Foster, J.F., "Plasma Albumin", in The Plasma Proteins, Putnam, F.W., ed., Academic Press, New York, 1960, vol. 1, p. 179.

72. National Bureau of Standards, (U.S.), Tech. News, 47, 175, (1963).

73. MacFarlane, A., and H. Hartley, Phil. Mag., 20, 611, (1935).

74. Noyes, A.A., and J.H. Ellis, J. Am. Chem. Soc., 39, 2532, (1917).

75. Janz, G.J., and H. Taniguchi, Chem. Rev., 53, 397, (1953).

76. Janz, G.J., and D.J.G. Ives, Ann. N.Y. Acad. Sci., 148, 210, (1968).

77. Gurd, F.R.N., and P.E. Wilcox, Advances in Protein Chemistry, 11, 312, (1956).

78. Brush, J.S., E.V. Jensen, and H.I. Jacobsen, Biochim. Biophys. Acta, 74, 688, (1963).

79. Strobel, H.A., Chemical Instrumentation, Addison-Wesley Publishing Company, Inc., Reading, Mass., 1960, p. 300.

80. Janz, G.J., "Silver-Silver Halide Electrodes", in Reference Electrodes, Theory and Practice, Ives, D.J.G., and G.J. Janz, eds., Academic Press, Inc., New York, 1961, p. 179.

81. Scatchard, G., and F. Helfferich, Disc. Faraday Soc., 21, 70, (1956).

82. Scatchard, G., and W.H. Orttung, J. Colloid Interface Sci., 22, 19, (1966).

83. Vielstich, W., Z. Elektrochem., 57, 646, (1953).

84. Levich, V.G., Physicochemical Hydrodynamics, Prentice-Hall, Inc., Englewood Cliffs, N.J., 1962, Chapter II.

85. Nernst, W., Z. physik. Chem., 47, 52, (1904).

86. Schlegelmilch, W., Z. physik. Chem., 214, 165, (1960).

87. Peers, A.M., Disc. Faraday Soc., 21, 124, (1956).

88. Glueckauf, E., and R.E. Watts, Proc. Royal Soc., (London), A268, 339, (1962).

89. Lorimer, J.W., Personal communication.

90. Gronwall, A., and B. Ingelman, Acta Physiol. Scand., 9, 1, (1945).

91. Rowe, D.S., Nature, 175, 554, (1955).

92. Ogston, A.G., and E.F. Woods, Nature, 171, 221, (1953).

93. Everett, W.W., and J.F. Foster, J. Am. Chem. Soc., 81, 3464, (1959).

94. Donnan, F.G., Z. Elektrochem., 17, 572, (1911).

95. Iler, R.K., The Colloid Chemistry of Silica and Silicates, Cornell University Press, Ithaca, New York, 1955.

96. Handbook of Chemistry and Physics, 43rd ed., The Chemical Rubber Publishing Co., Cleveland, Ohio, 1960.

97. "Ludox Colloidal Silica", Product Information Bulletin A-54022, E.I. duPont de Nemours and Co., Wilmington, Del.

98. Müller, H., Kolloidchem. Beihefte, 26, 257, (1928).

99. Loeb, A.L., J.Th.G. Overbeek, and P.H Wiersema, The Electrical Double Layer Around a Spherical Colloid Particle, M.I.T. Press, Cambridge, Mass., 1961.

100. Cowell, P.H., and A.D.C. Crommelin, "Essay on the Return of Halley's Comet", Greenwich Observations, 1909.

101. Milne, W.E., Numerical Solution of Differential Equations, John Wiley and Sons, Inc., New York, 1957.

102. Wiersema, P.H., Doctoral Thesis, University of Utrecht, The Netherlands, 1964.

103. Carnahan, B., H.A. Luther, and J.O. Wilkes, Applied Numerical Methods, John Wiley and Sons, Inc., New York, 1969.

104. System/360 Scientific Subroutine Package, (360A-CM-03X), Version II, Programmer's Manual, IBM Application Program H20-0205-2, IBM Corp., White Plains, New York, 1966.

105. Hildebrand, F.B., Introduction to Numerical Analysis, McGraw-Hill Book Company, Inc., New York, 1956.

106. Scatchard, G., and J. Bregman, J. Am. Chem. Soc., 81, 6095, (1959).

107. Linderstrom-Lang, K., Compt. rend. trav. lab. Carlsberg, Ser. chim., 15, no. 7, (1924).

108. Moore, W.J., Physical Chemistry, 3rd ed., Prentice-Hall, Inc., Englewood Cliffs, N.J., 1962.

109. Oakley, C.O., The Calculus, Barnes and Noble, Inc., New York, 1961.

110. Overbeek, J.Th.G., Progress in Biophysics and Biophysical Chemistry, 6, 58, (1958).

111. Tanford, C., S.A. Swanson, and W.S. Shore, J. Am. Chem. Soc., 77, 6414, (1955).

112. Casassa, E.F., and H. Eisenberg, Advances in Protein Chemistry, 19, 287, (1964).

113. Leonard, W.J., K.K. Vijai, and J.F. Foster, J. Biol. Chem., 238, 1984, (1963).

114. Michaels, A.S., Progress in Separation and Purfication, 1, 297, (1968).

115. Blatt, W.F., S.M. Robinson, and H.J. Bixler, Analyt. Biochem., 26, 151, (1968).

116. Loo, T.L., J.K. Luce, J.H. Jardine, and E. Frei, Cancer Res., 28, 2448, (1968).

117. Loo, T.L., J.K. Luce, M.P. Sullivan, and E. Frei, Clin. Pharmacol. Ther., 9, 180, (1968).

118. Shoemaker, D.P., and C.W. Garland, Experiments in Physical Chemistry, McGraw-Hill Book Company, Inc., New York, 1962, p. 32.

119. Covington, A.K., "Reference Electrodes", in Ion-Selective Electrodes, Durst, R.A., ed., National Bureau of Standards Special Publication 314, Washington, D.C., 1969, p. 107.

120. Bowker, A.H., and G.J. Lieberman, Handbook of Industrial Statistics, Prentice-Hall, Inc., Englewood Cliffs, N.J., 1955.

121. Scatchard, G., J. Am. Chem. Soc., 68, 2315, (1946).

122. Rushton, J.H., "Mixing", in Technique of Organic Chemistry, Weissberger, A., ed., Interscience Publishers, Inc., New York, 1950, vol. III, p. 99.

123. Borg, D.C., "Continuous Flow Methods Adapted for EPR Apparatus", in Rapid Mixing and Sampling Techniques in Biochemistry, Chance, B., Q.H. Gibson, R.H. Eisenhardt, and K.K. Lonberg-Holm, eds., Academic Press, New York, 1964, p. 135.

124. Tanford, C., and J.G. Kirkwood, J. Am. Chem. Soc., 79, 5333, 5340, (1957).

125. Scatchard, G., Amer. Scientist, 40, 61, (1952).